Unifying the Physical Understanding of CMEs Through Remote Sensing Observations in the PSP/SolO Era

Alessandro Liberatore

alessandro.liberatore@inaf.it

2nd Metis Science Meeting

January 27-29, 2025
Capodimonte Astronomical Observatory, Naples, Italy

Coronal Mass Ejections

➢ Observed for the first time only ~50y ago! [Howard et al., 2023]

Analysis of CME propagation at different dimensions:

- **1D:** in-situ
  [“precise” and geoeff., but single point]
- **2D:** remote sensing (single S/C)
  [less precise, general structure, models]
- **3D:** remote sensing (multi-viewpoint)

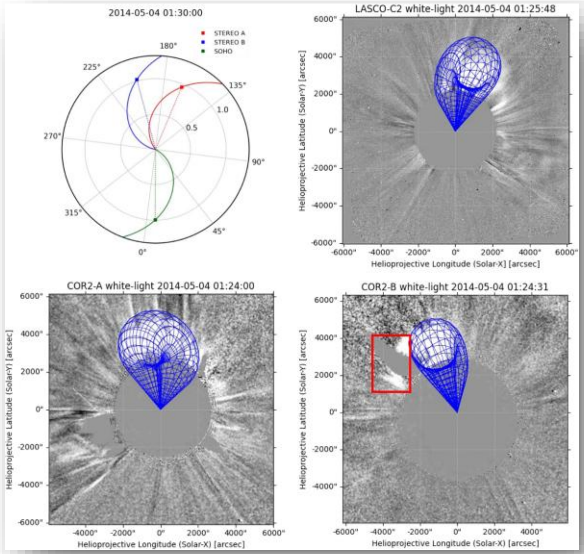

[Kansabanik et al., 2023]

[Thernisien, 2011]
Graduated Cylindrical Shell (GCS)

- Drag Based Model,
- WSA-Enlil,
- …

2006: STEREO A/B
first stereoscopic observations of CMEs (from 1 AU)
+
heliospheric imagers (CMEs propagation between the Sun and Earth)

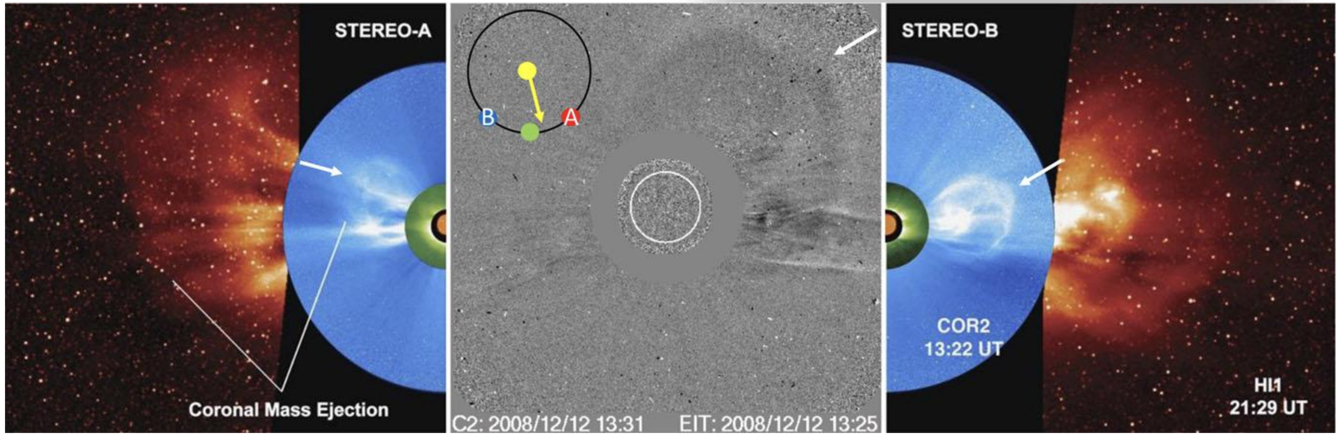

[Byrne, 2010, Temmer, 2021]

Heliophysics Fleet Chart (updated January 01, 2024)

Incoming: CODEX, PROBA-3, … (Vigil, PUNCH...)

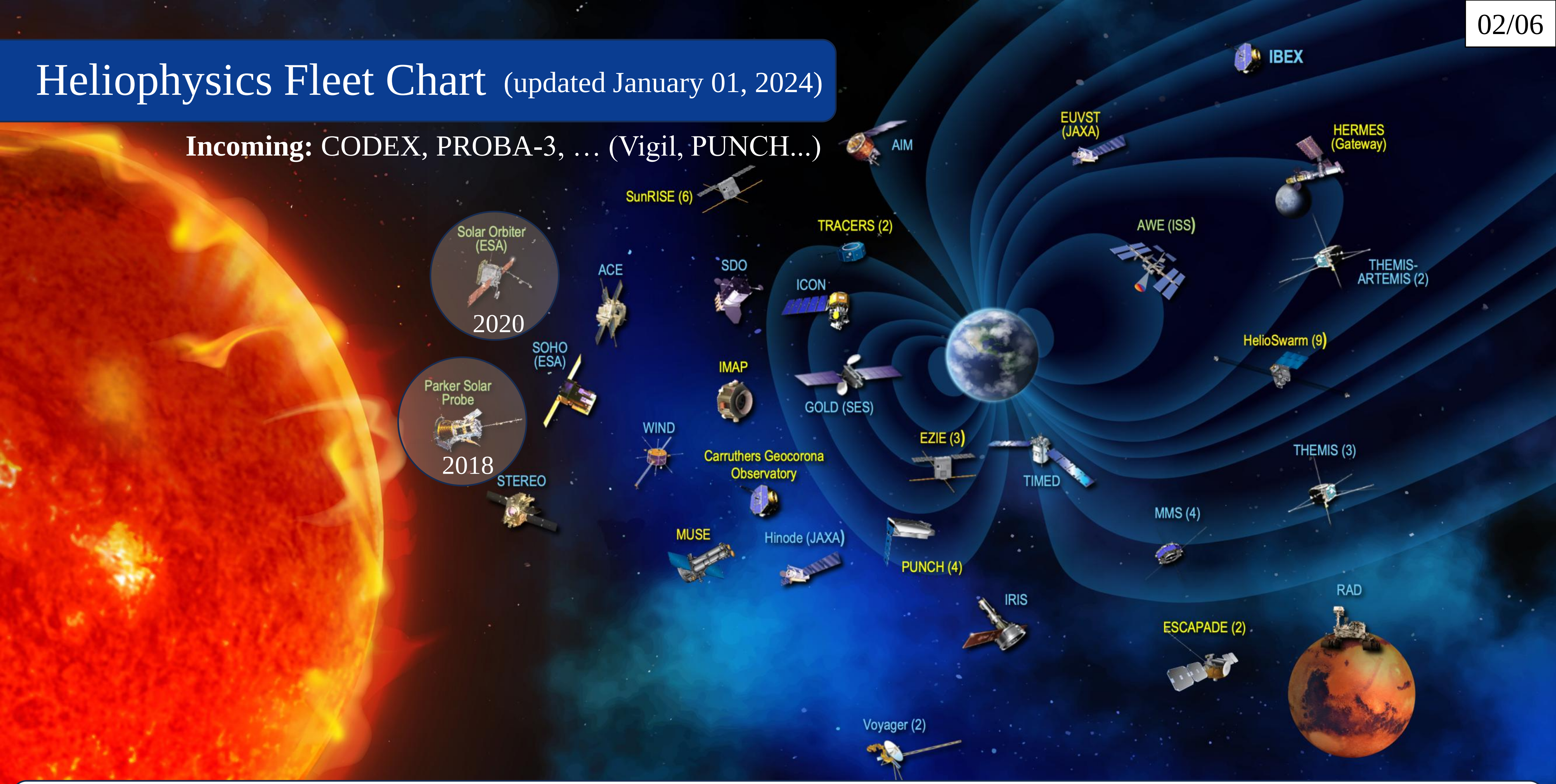

SolO & PSP remote sensing instruments

Spacecraft	Remote Sensing Instruments	Products
Solar Orbiter • Up to ≈ 60 $R_\odot$ = 0.28 AU • 33° outside the ecliptic	**EUI** [Extreme Ultraviolet Imager]	High-resolution (E)UV images of the solar chromosphere, transition region and corona.
	Metis [Coronagraph]	Simultaneous images of the corona in (polarized) visible and ultraviolet wavelengths stretching out from 1.7 to 4.1 solar radii.
	PHI [Polarimetric Helioseismic Imager]	High-resolution measurements of photospheric magnetic field, VL maps of its brightness, and photosphere velocity maps.
	SoloHI [SolO Heliospheric Imager]	VL images of the inner heliosphere over a wide FoV, observing photospheric light scattered by electrons in the solar wind and interplanetary dust.
	SPICE [Spectral Imaging of the Coronal Environment]	High-resolution imaging spectrometer operating at extreme ultraviolet wavelengths.
	STIX [Spectrometer/Telescope for Imaging in X-rays]	Hard X-ray imaging spectrometer in the energy range from 4 to 150 keV energy range.
Parker Solar Probe • Up to ≈ 9.86 $R_\odot$ = 0.046 AU • v_M ≈ 192 km/s (≈ 3 × SolO)	**WISPR** [Wide Field Imager for Solar Probe]	VL wide-field images of the solar corona and outflows.

PSP & SolO era: additional remote-sensing (and in-situ) viewpoints

- **New viewpoints inside 1 AU (i.e., different radial distances)**, very fast, different longitudes and latitudes, closest images of the Sun and wide-field (E)UV corona (SolO/EUI + Metis), high-resolution VL images of the corona/inner heliosphere at different longitudes by SoloHI & WISPR.

- Useful S/C configurations:

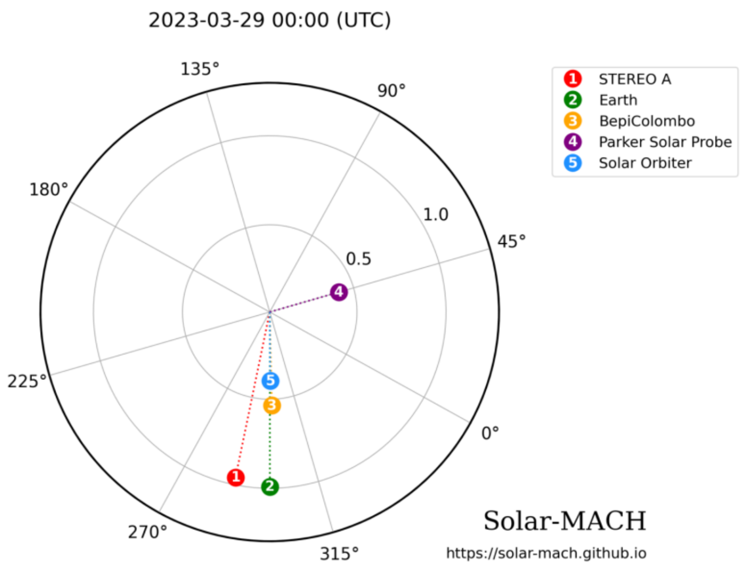

CME radial evolution
[e.g., Braga et al., 2021]

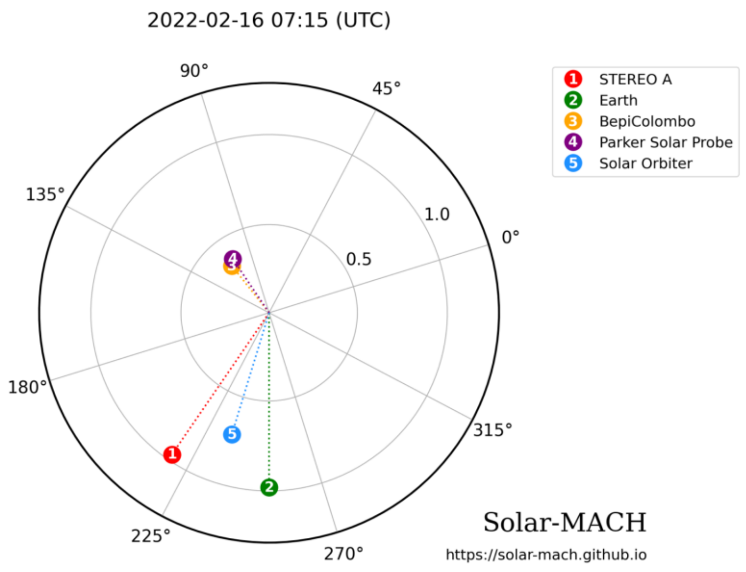

CME mesoscale structure and coherence length
[e.g., Lugaz et al., 2024; Palmiero et al., 2024]

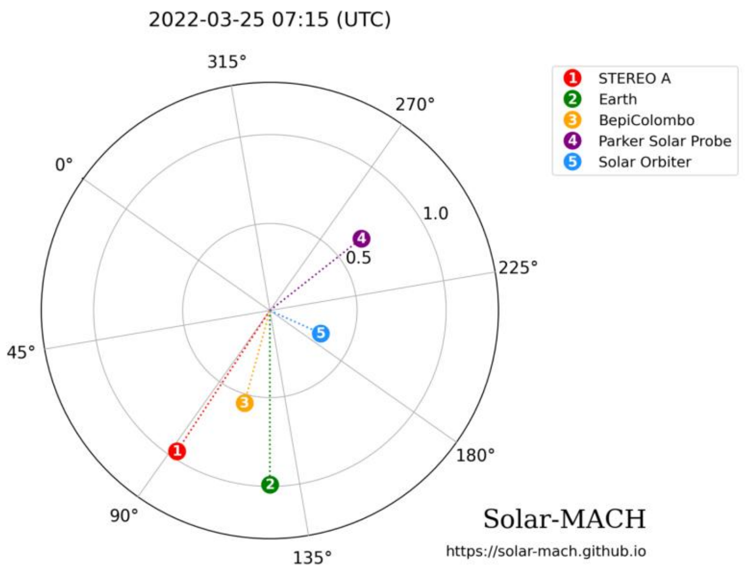

CME overall structure (and quadrature)
[e.g., Liberatore et al., 2023]

PSP (E13): flying through a CME in the corona

- *Simultaneous* remote-sensing imaging & in-situ detection of a CME!

- Sep.5, 2022 → huge event → Many papers
  [2400-2500 km/s at ~15 $R_\odot$] [e.g., Romeo et al., 2023]

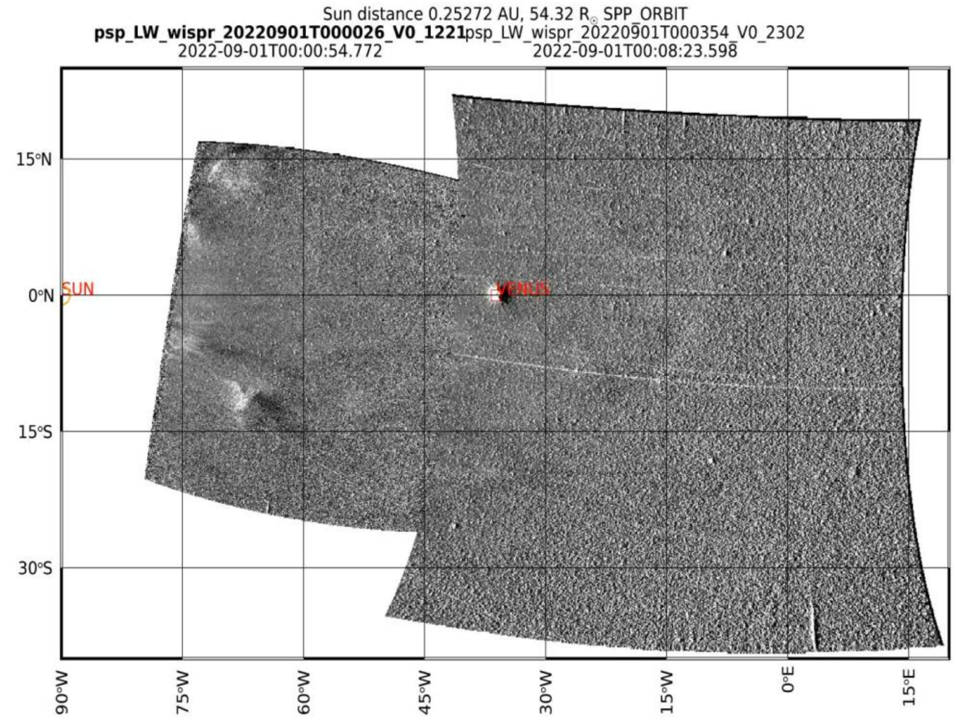

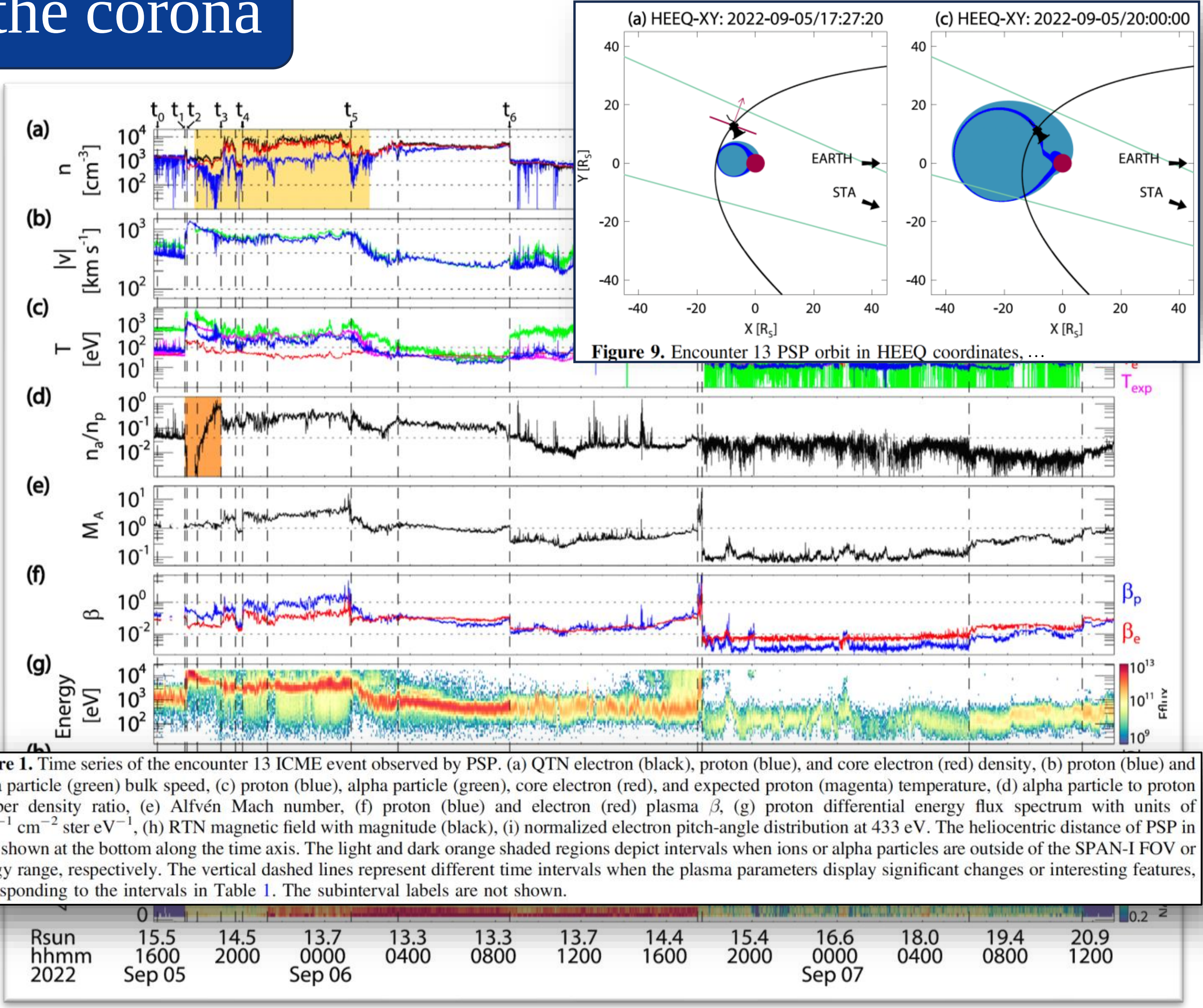

Figure 1. Time series of the encounter 13 ICME event observed by PSP. (a) QTN electron (black), proton (blue), and core electron (red) density, (b) proton (blue) and alpha particle (green) bulk speed, (c) proton (blue), alpha particle (green), core electron (red), and expected proton (magenta) temperature, (d) alpha particle to proton number density ratio, (e) Alfvén Mach number, (f) proton (blue) and electron (red) plasma β, (g) proton differential energy flux spectrum with units of eV s^{-1} cm^{-2} ster eV^{-1}, (h) RTN magnetic field with magnitude (black), (i) normalized electron pitch-angle distribution at 433 eV. The heliocentric distance of PSP in R_S is shown at the bottom along the time axis. The light and dark orange shaded regions depict intervals when ions or alpha particles are outside of the SPAN-I FOV or energy range, respectively. The vertical dashed lines represent different time intervals when the plasma parameters display significant changes or interesting features, corresponding to the intervals in Table 1. The subinterval labels are not shown.

Figure 9. Encounter 13 PSP orbit in HEEQ coordinates, …

PSP (E13): flying through a CME in the corona

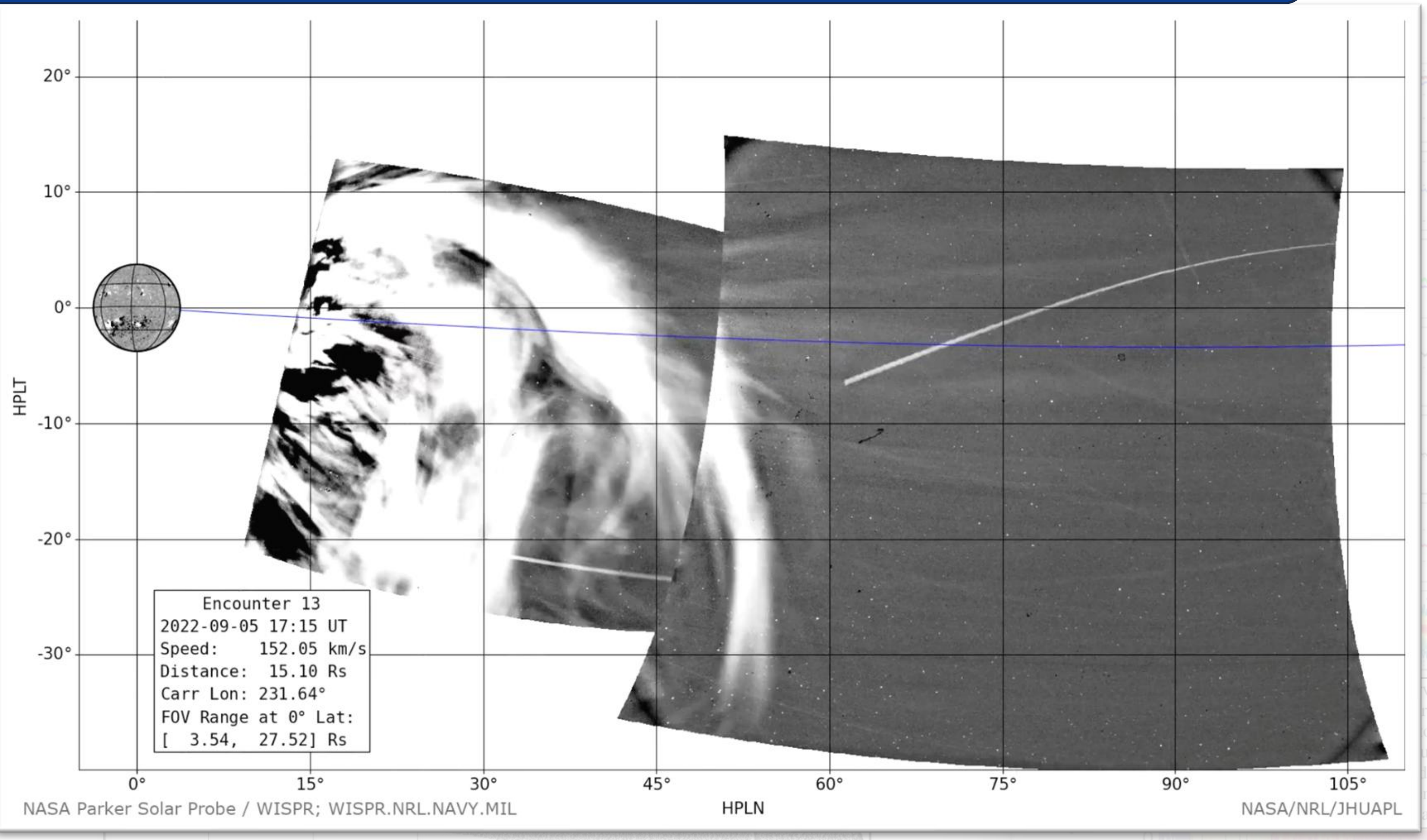

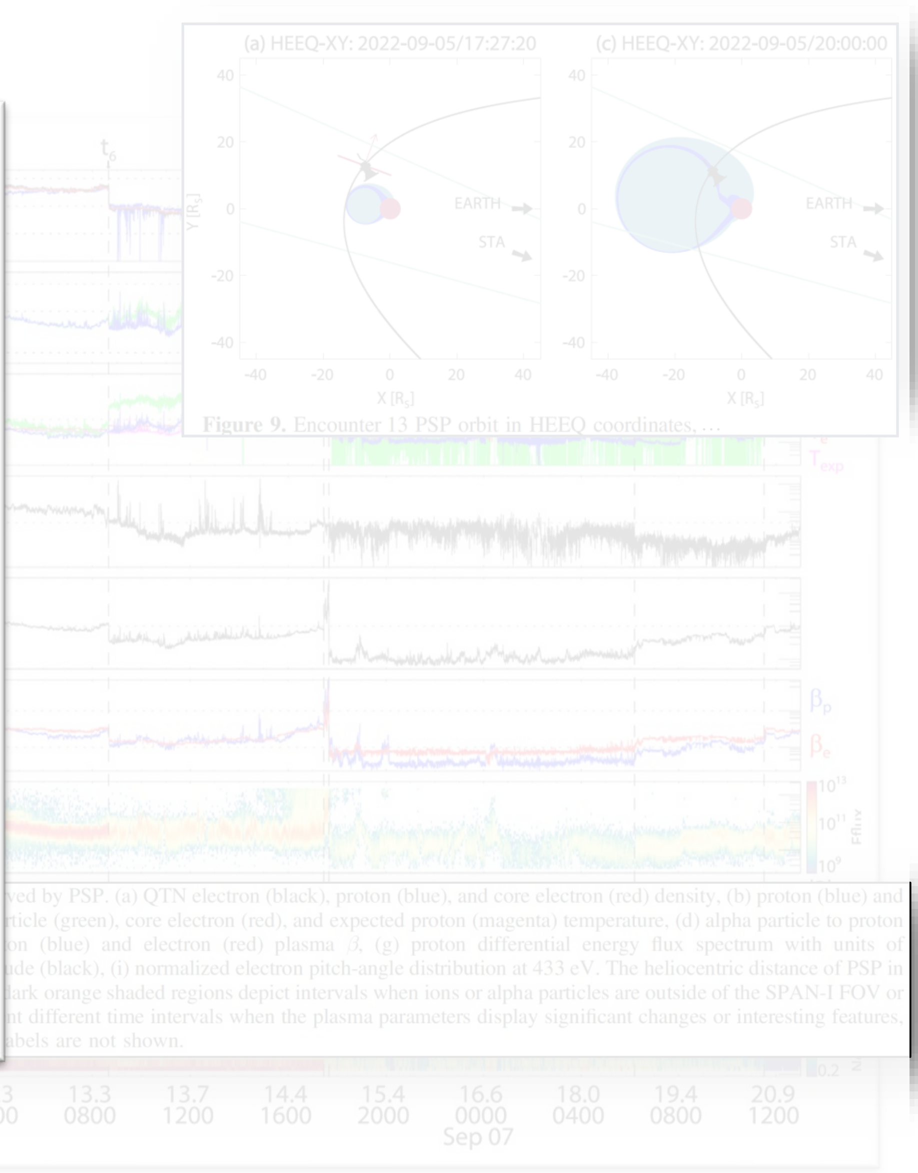

PSP (E13): flying through a CME in the corona

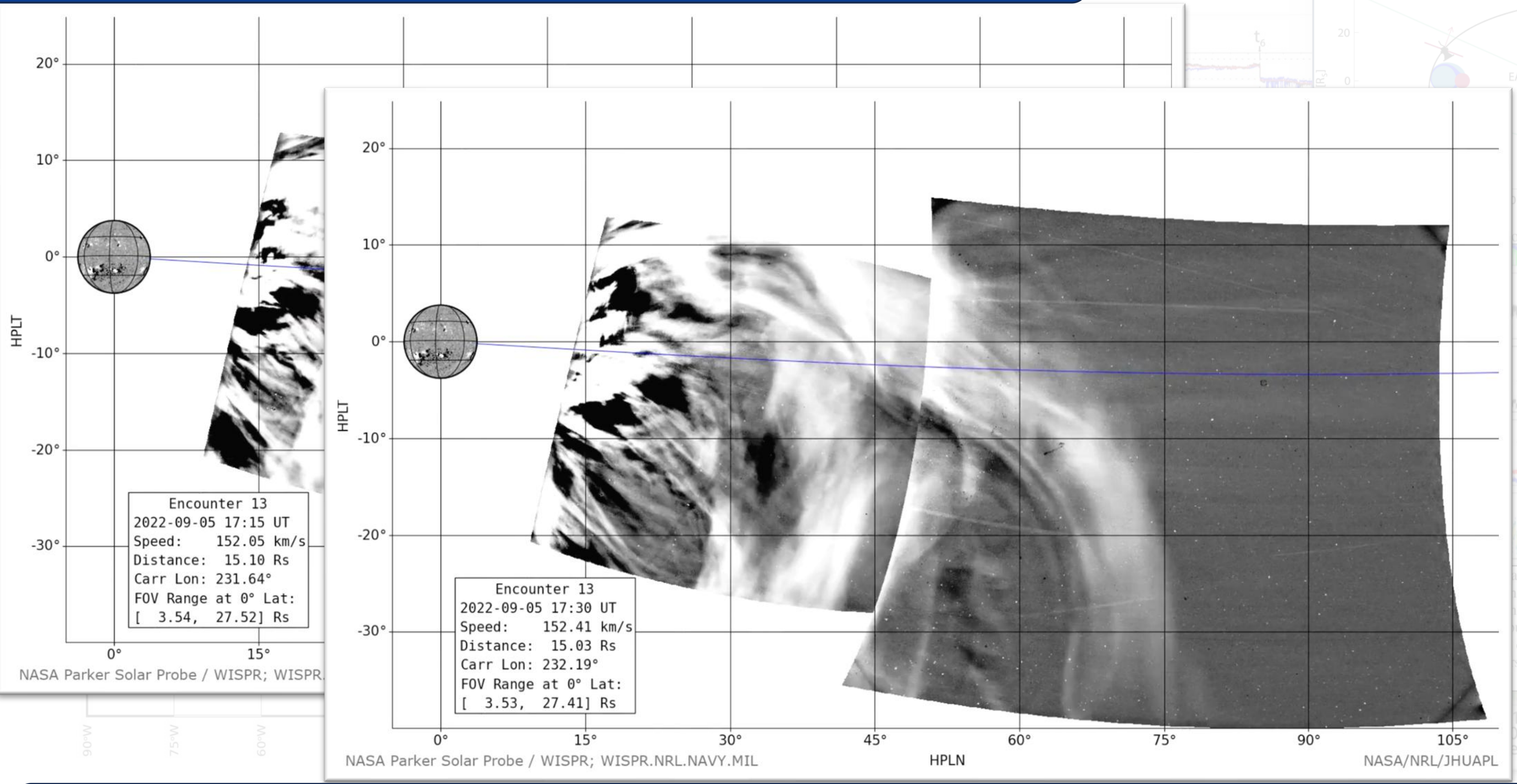

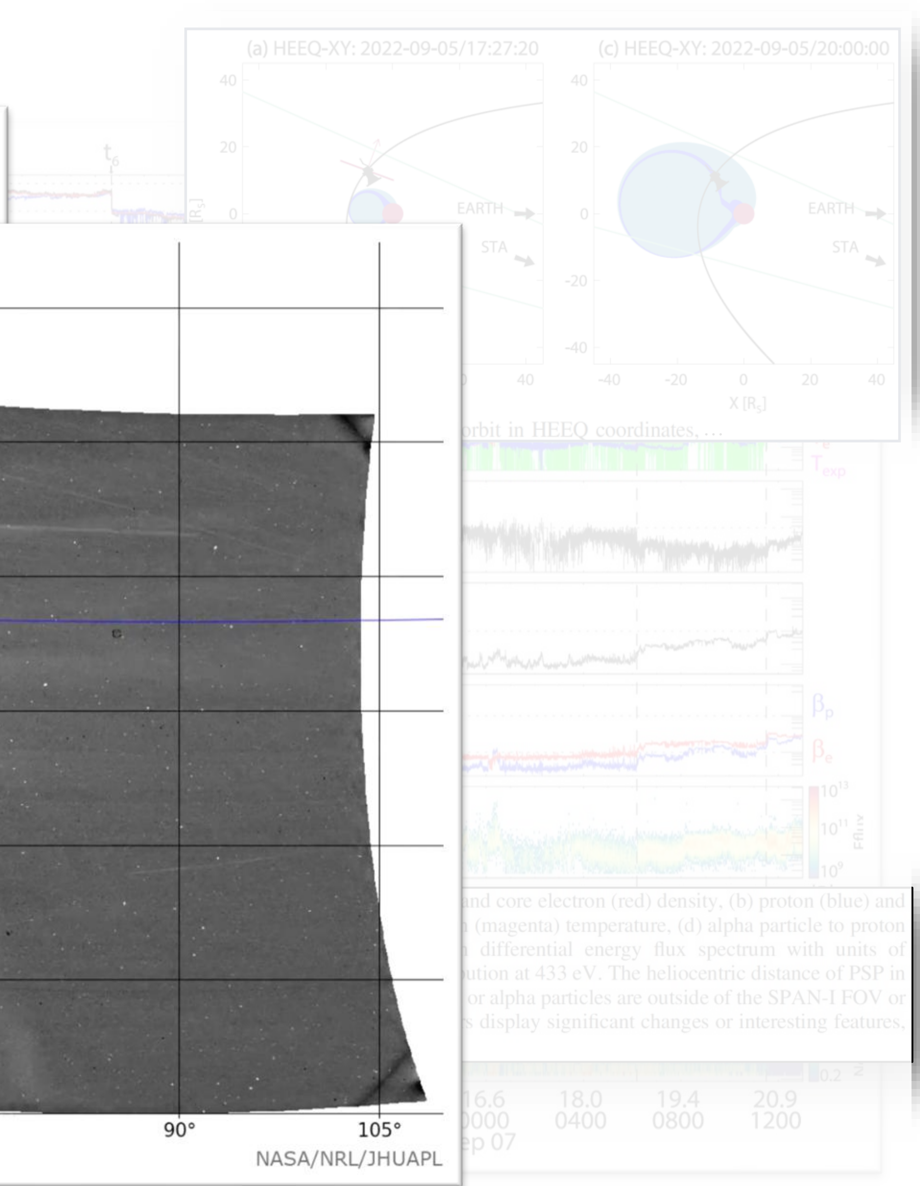

PSP (E13): flying through a CME in the corona

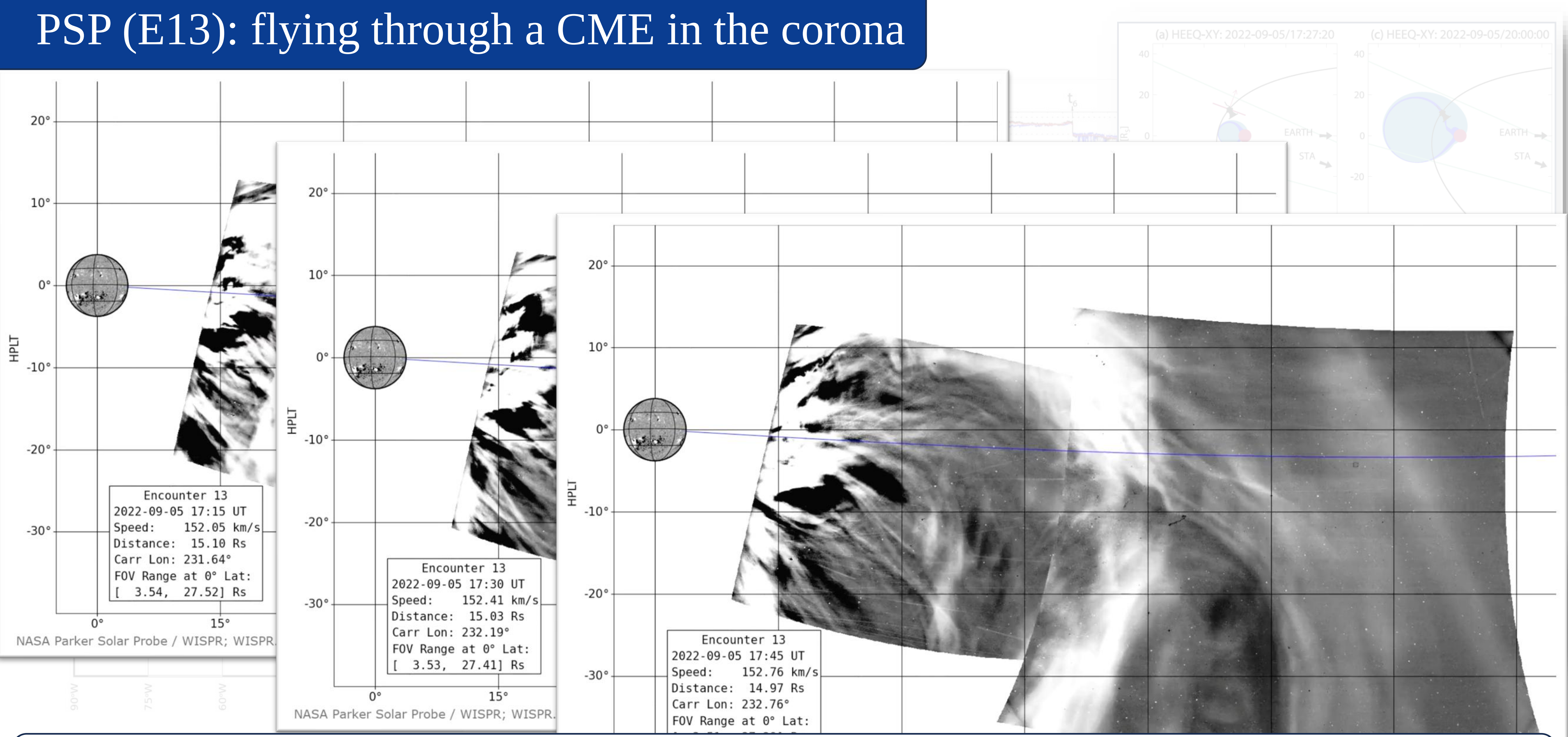

What is a Coronal Mass Ejection?

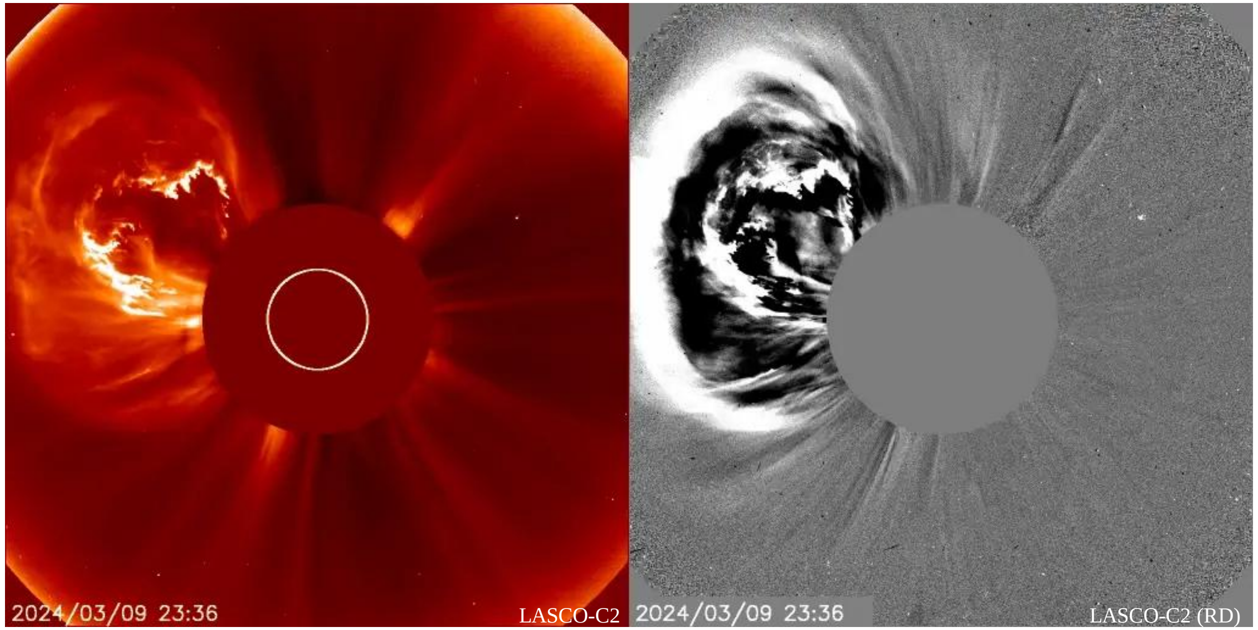

- **Rapid ejection of magnetic field and plasma from the Sun into the heliosphere**

- One of the major drivers of the most severe Space Weather disturbances
  (geoeffectiveness → north-south B component)
  [Temmer, 2021]

- CMEs eruption: loss of equilibrium,
  force imbalance,
  instability threshold

- Twisted magnetic fields
  → flux rope (complex magnetic field structures;
  main components: axial, helical)
  [Bothmer and Schwenn, 1998; Mulligan et al., 1998; Palmiero et al., 2018]

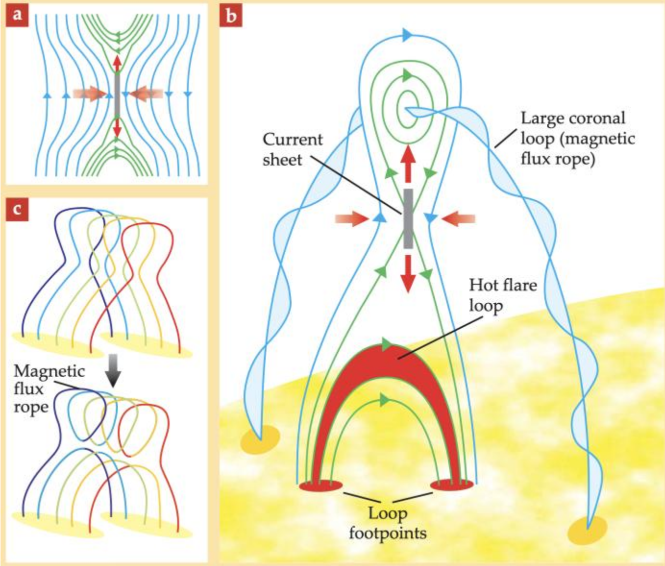

Figure 1. Magnetic reconnection and the standard model for solar eruptive events. **(a)** In magnetic reconnection, oppositely directed magnetic field lines (blue) flow inward and reconnect, releasing much of their magnetic energy to the ambient plasma. The reconnected field lines (green) flow outward, and their associated plasma is ejected in reconnection jets. In the reconnection region (gray), a sheet of current flows perpendicular to the plane of the page. **(b)** In a solar eruptive event, reconnection occurs in an arcade of loops rising above the visible surface of the Sun. **(c)** Because of shearing of the original arcade, the loops generally reconnect with their neighbors, not with themselves. A twisted magnetic flux rope forms and expands upward to become a coronal mass ejection.

CME structure… a global picture

CME structure

Classic 3-Part Structure

Halo CME

- Expanding shock wave front
- CME leading edge density enhancement

Plane of the sky

- Expanding shock wave front
- CME leading edge density enhancement
- Cavity due to the expanding magnetic ejecta
- Intensity enhancement

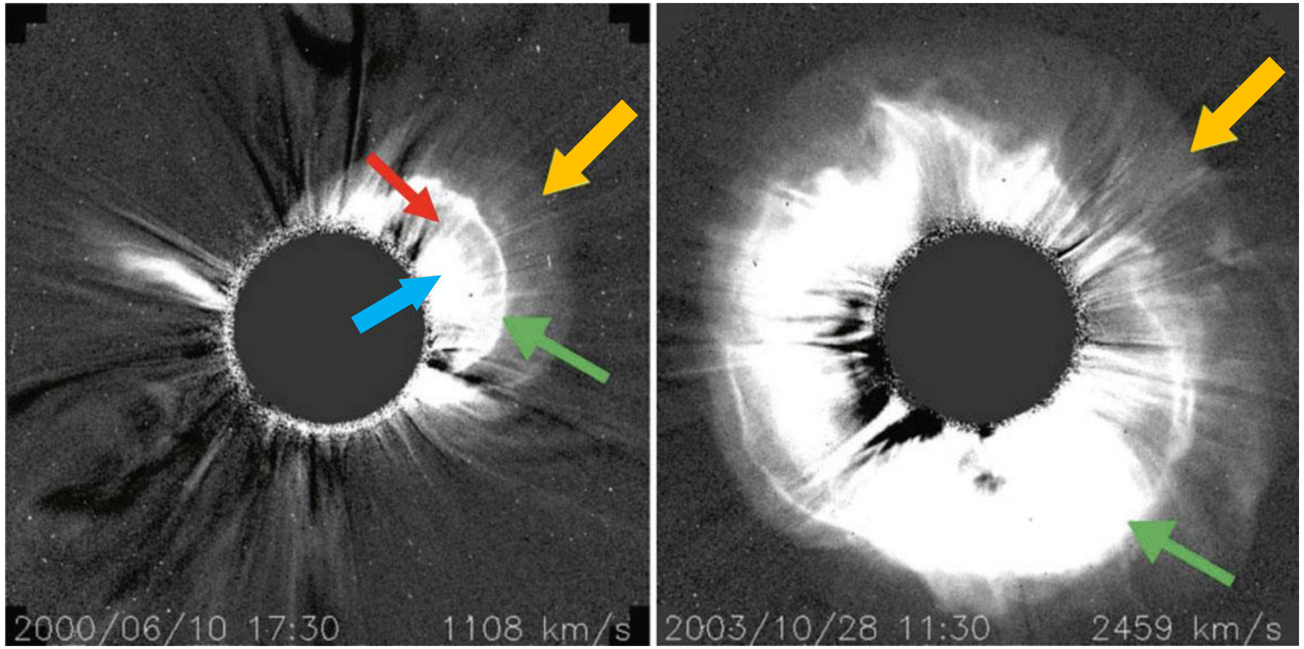

[Vourlidas et al., 2013; Temmer, 2021]

Solar Orbiter highly detailed observations

From EUI to Metis

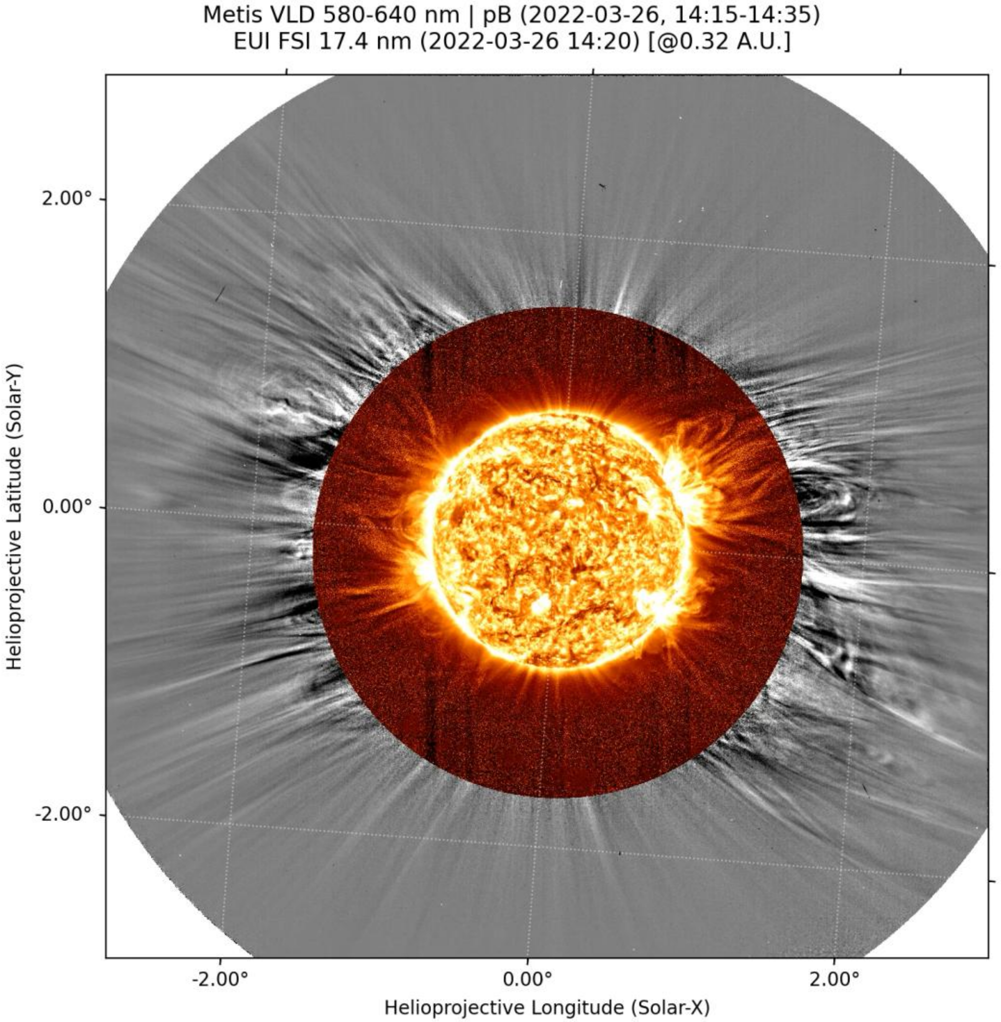

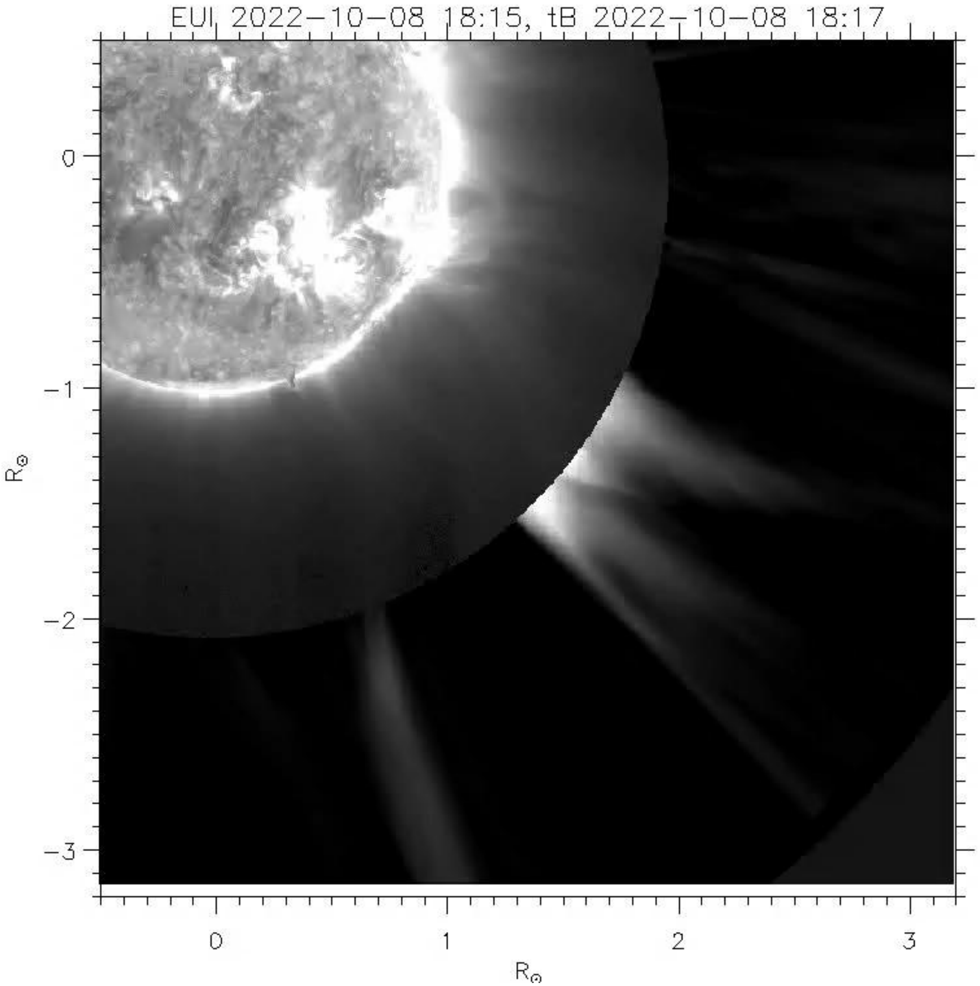

G. Russano & V. Andretta (Joint SolO, PSP, and DKIST Meeting, April 08-11, 2024)

Solar Orbiter highly detailed observations

From EUI to Metis

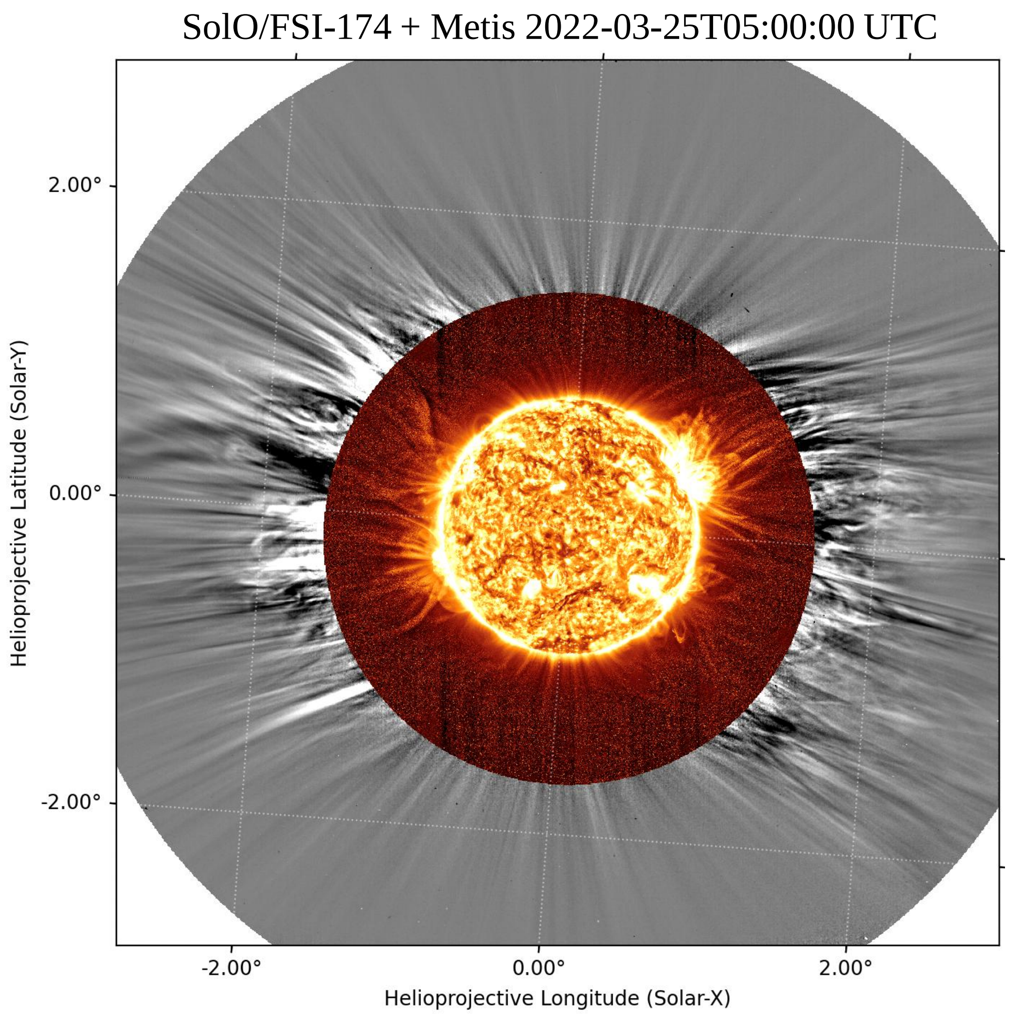

$T_{\text{change orientation}} < 1\text{s}$

T resolution:
- tB every 20sec
- pB every 1min

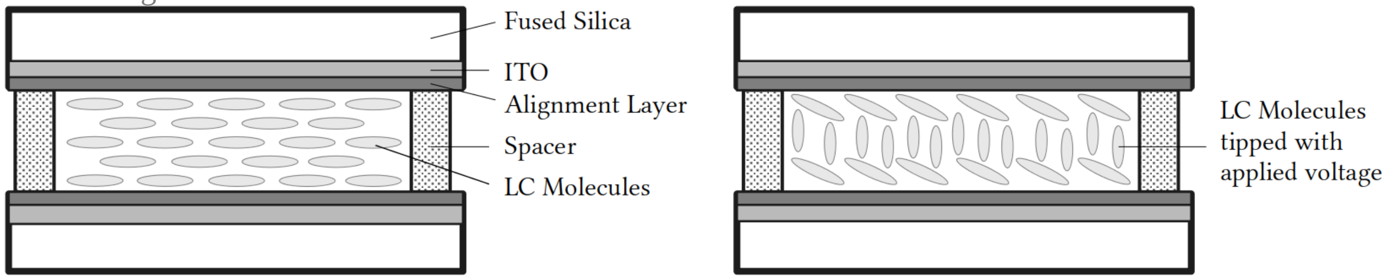

V = 0 (max. retardance)

V >> 0 (min. retardance)

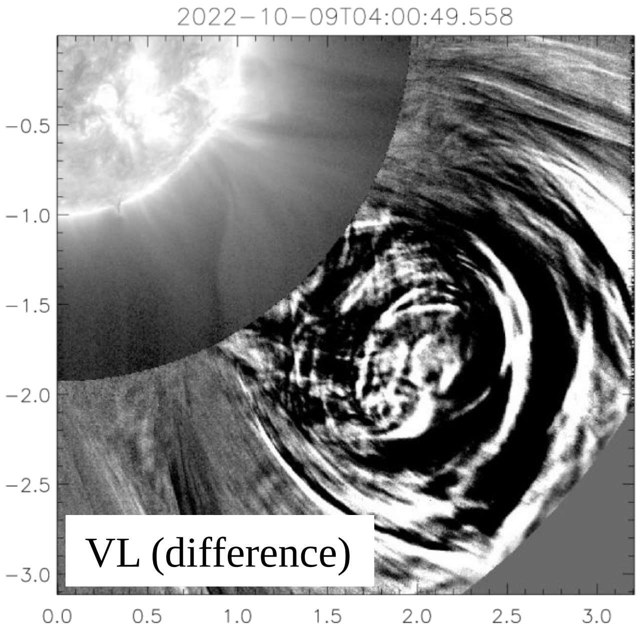

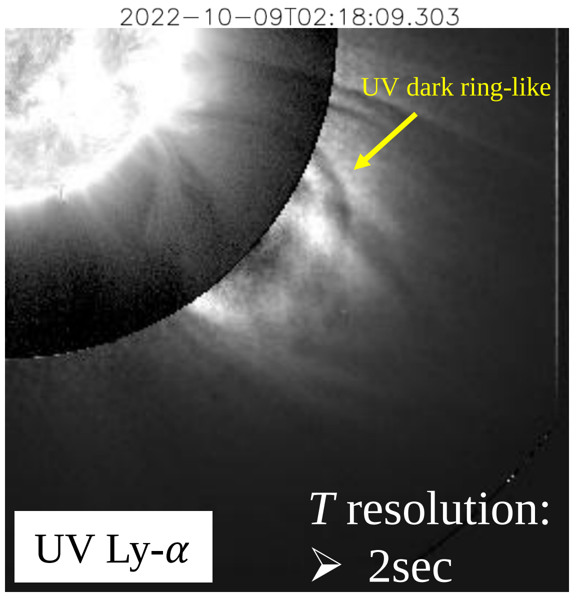

G. Russano & V. Andretta (Joint SolO, PSP, and DKIST Meeting, April 08-11, 2024)

Solar Orbiter highly detailed observations

SoloHI vs STA/HI-1

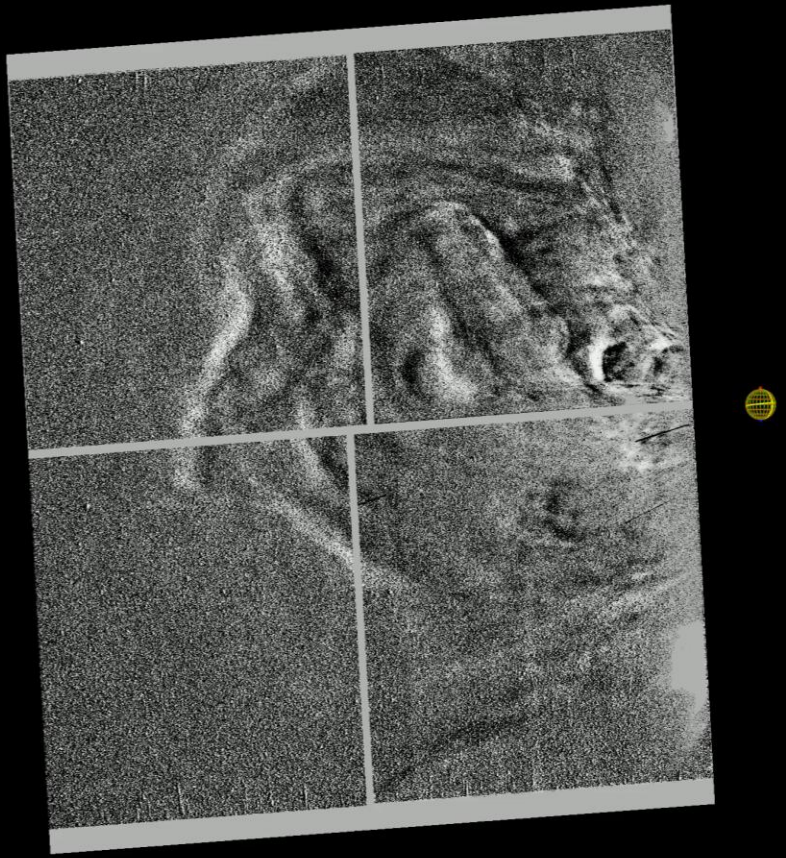

2022-03-31 T04:10:19.975

P. Hess, Solar Orbiter Meeting 10/25/2023

Solar Orbiter highly detailed observations

SoloHI *vs* **SECCHI** *vs* **LASCO**

2022/03/29 6-50 $R_\odot$

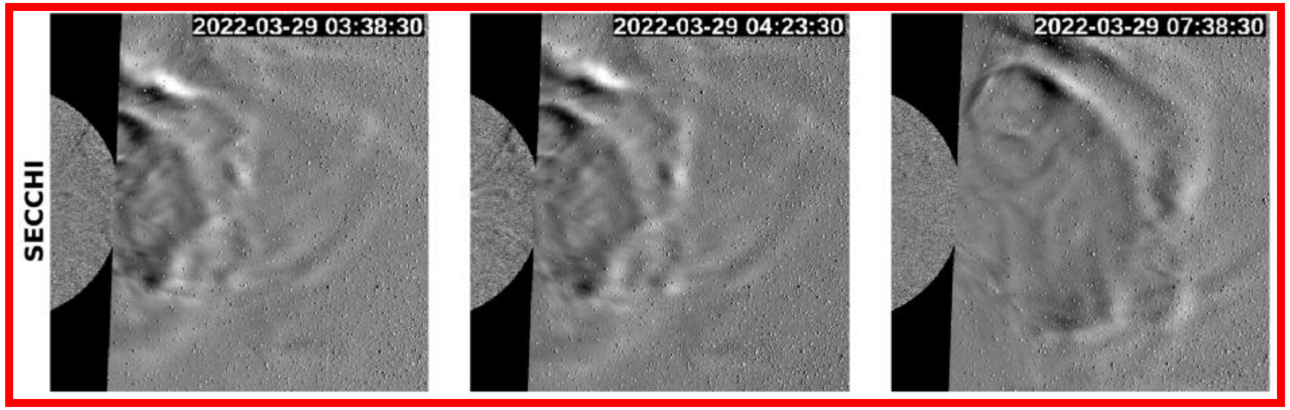

2022/04/02 6-30 $R_\odot$

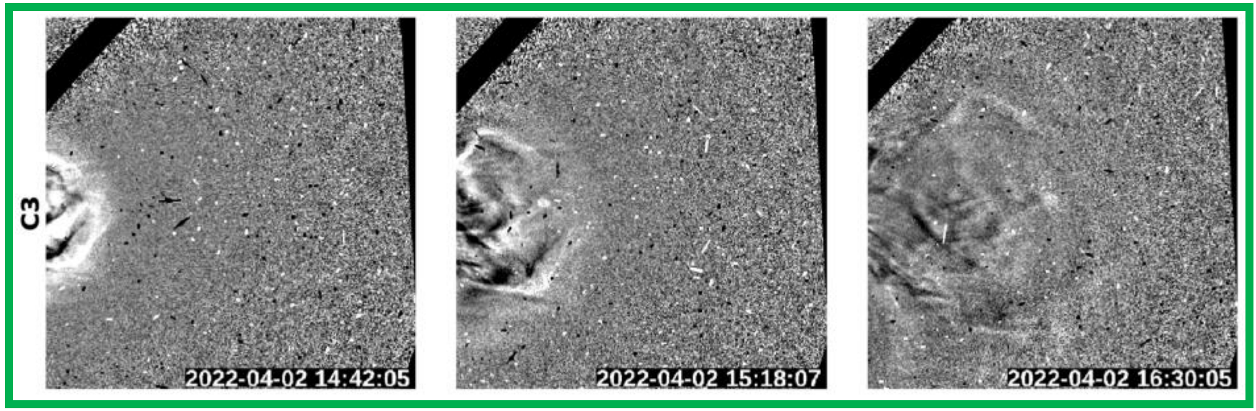

Adapted from P. Hess, Solar Orbiter Meeting 10/25/2023

Solar Orbiter highly detailed observations

SoloHI *vs* **SECCHI** *vs* **LASCO**

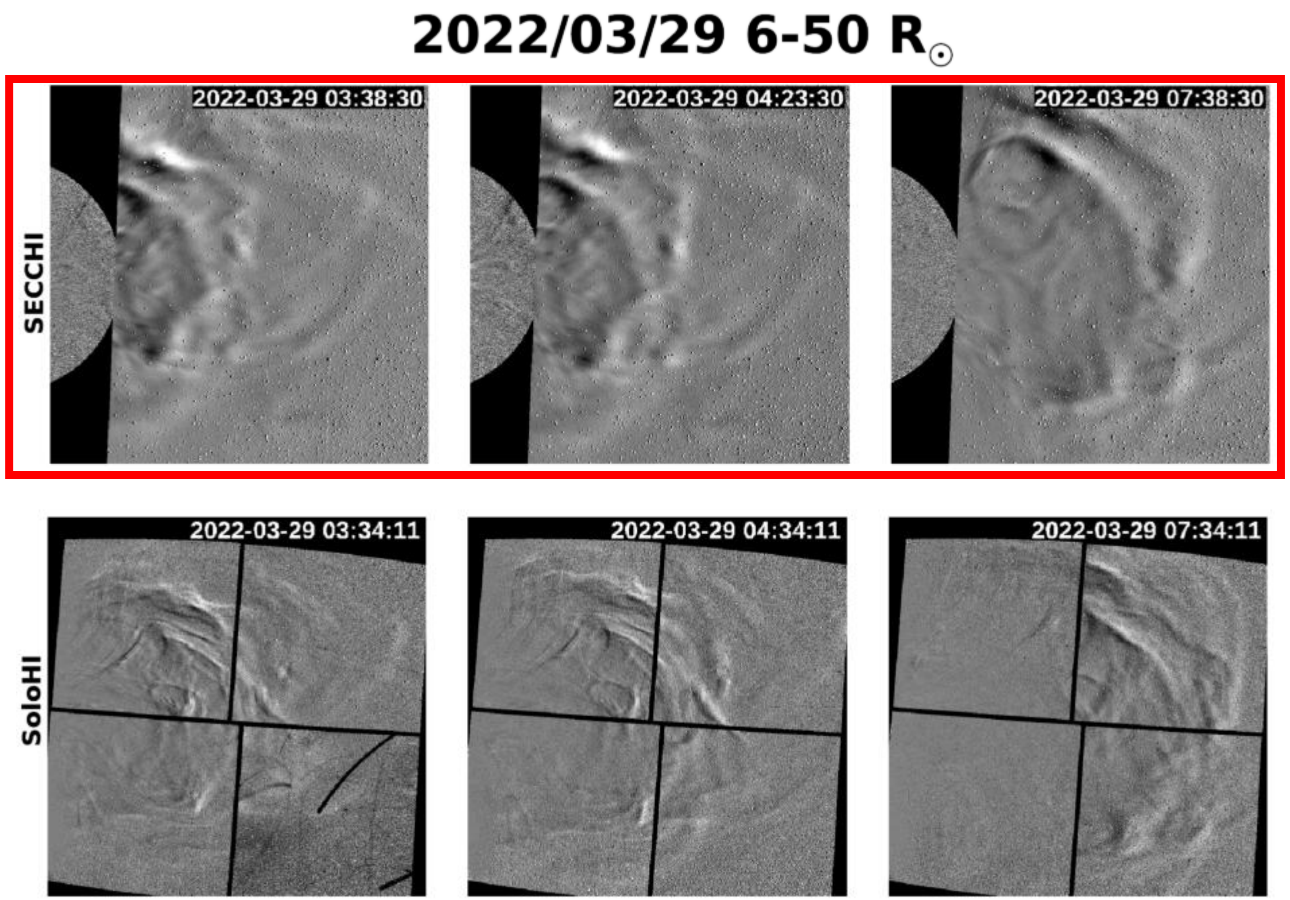

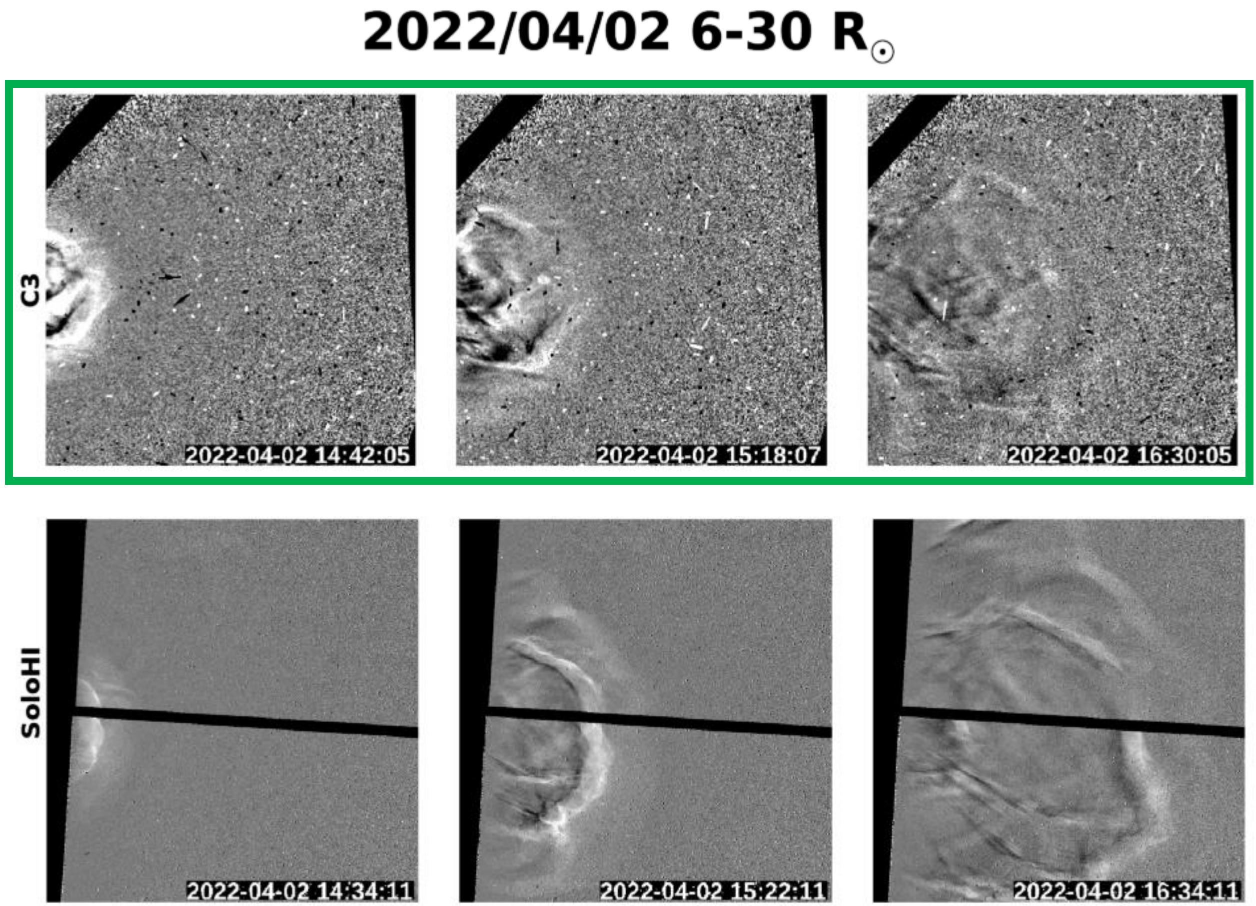

Adapted from P. Hess, Solar Orbiter Meeting 10/25/2023

- Highly detailed observations / interior structures (FoV ⇨ coronagraphs + HI)

PSP highly detailed observations

STA *vs* **WISPR**

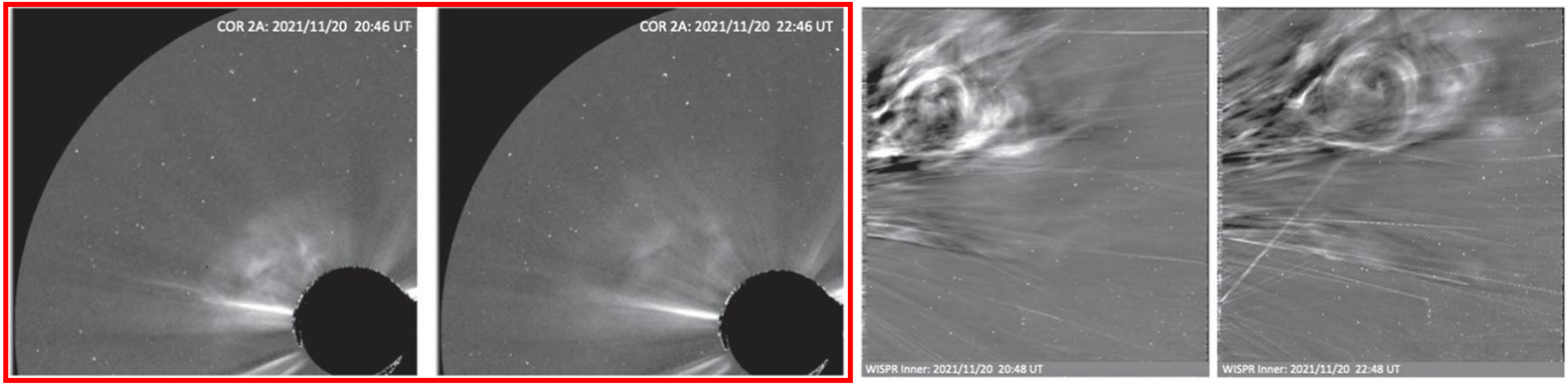

[Howard et al., 2022]

PSP highly detailed observations

STA *vs* **WISPR**

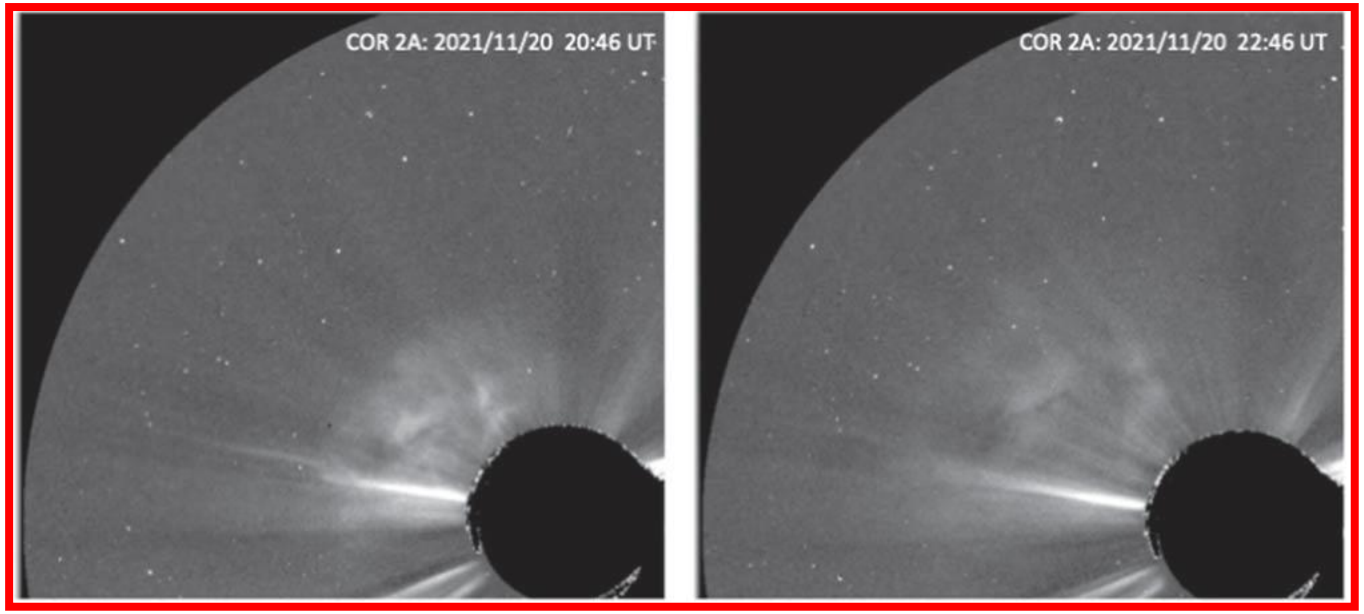

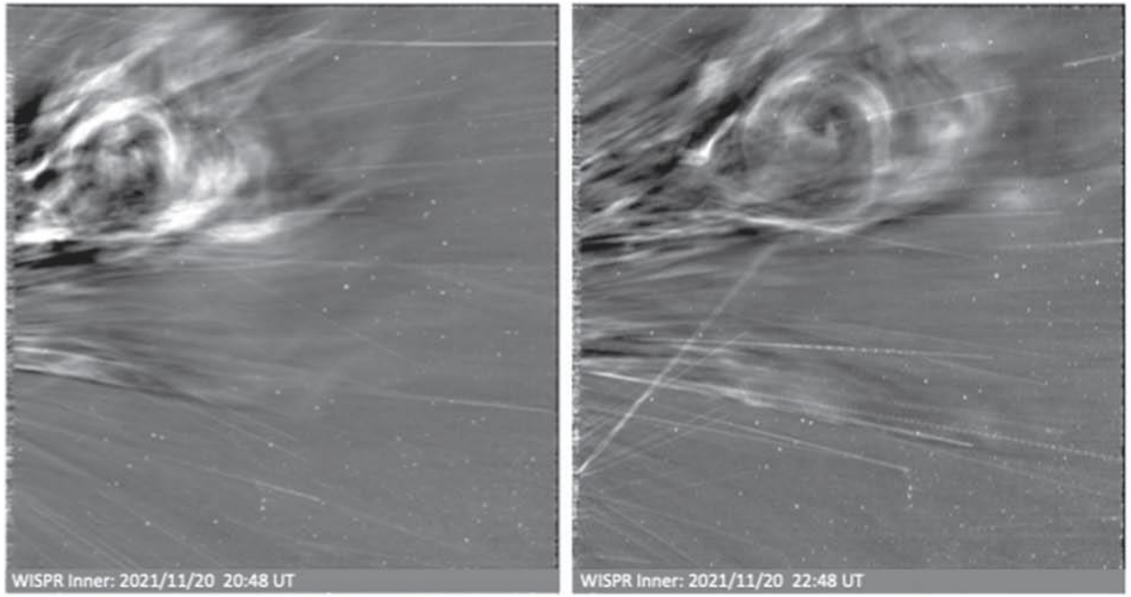

[Howard et al., 2022]

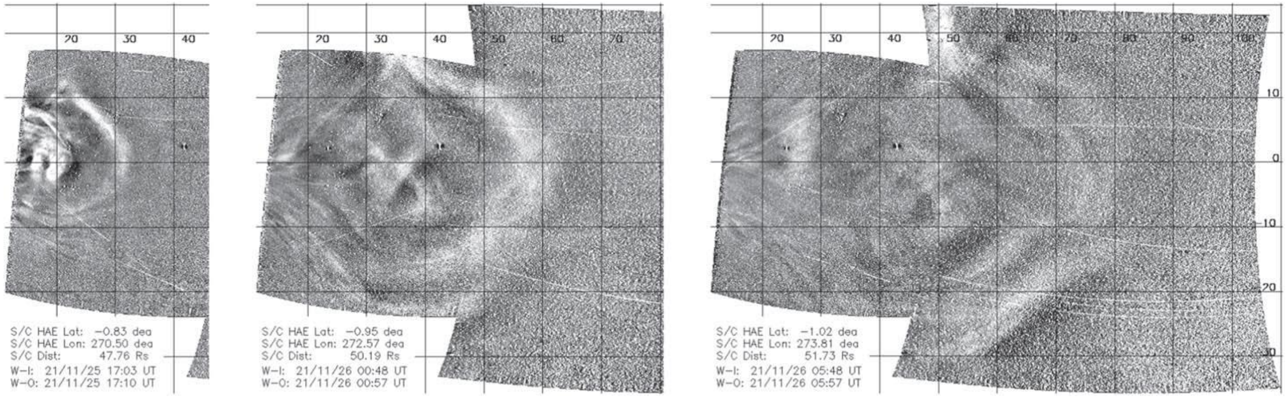

- Highly detailed observations / interior structures
- Multiple fronts

Is the 3-part structure too simplistic?

High complexity… some (of many) examples

PSP/WISPR [Howard et al., 2022]

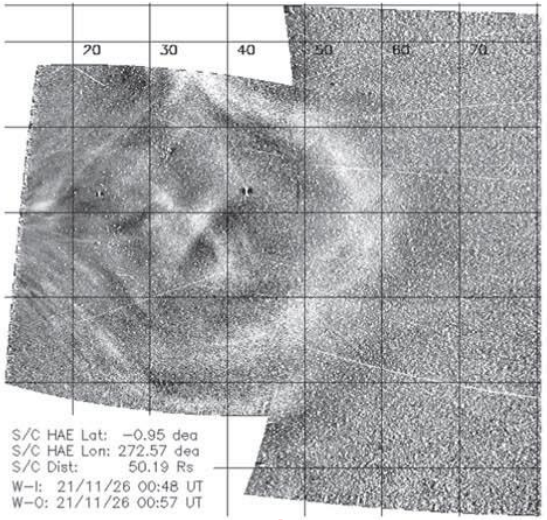

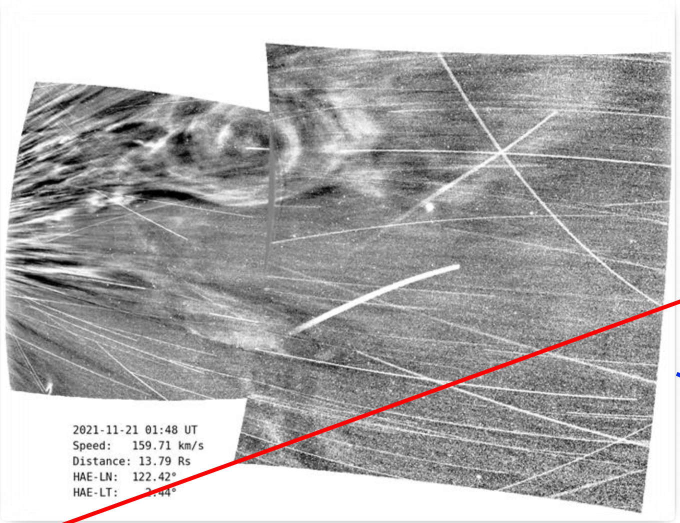

SO/SoloHI

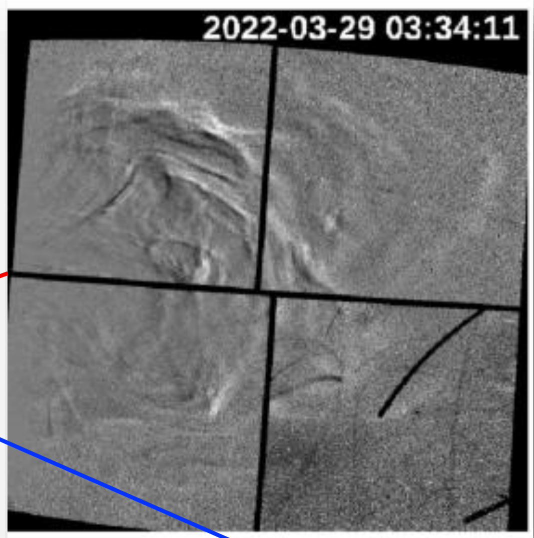

SO/EUI+Metis

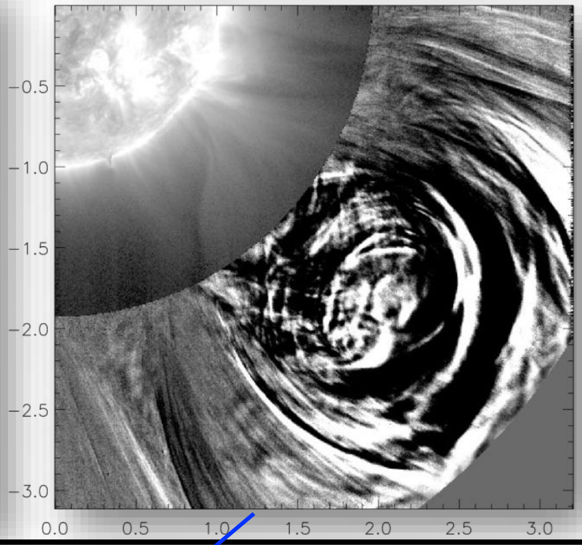

Multiple fronts?

…origin?

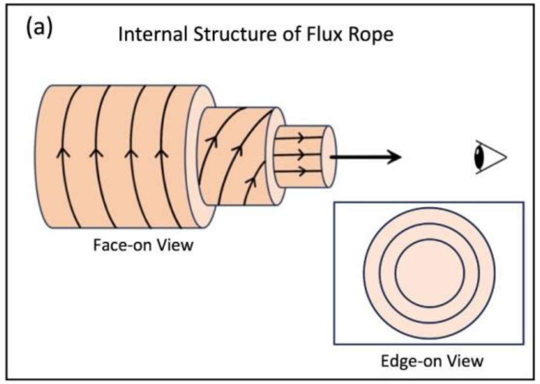

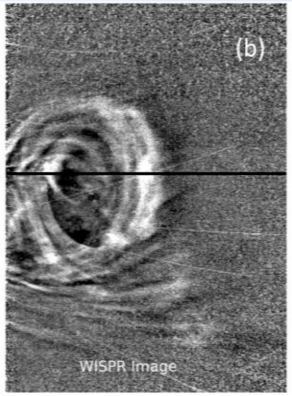

Nested-ring structure?

- Projection/Edge-on view of MFR?
- Superposition of the internal structures of MF?
- …

alessandro.liberatore@inaf.it

Is the 3-part structure too simplistic?

- Nested rings
- N-part structure
  (as variation of the 3-part structure)
- Complex structure but organized

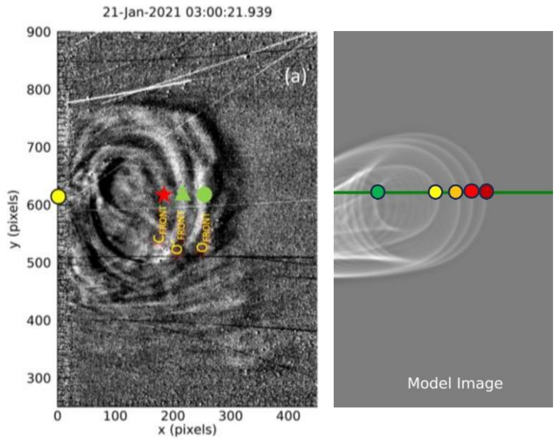

[Shaik et al., 2024]

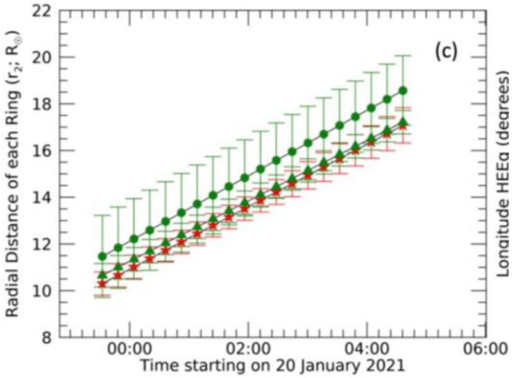

Coherence of the nested ring structure
- Systematic evolution of the fronts
- Rings propagate as a single structure (LN within error limits)

[Shaik et al., 2024 (in prep)]

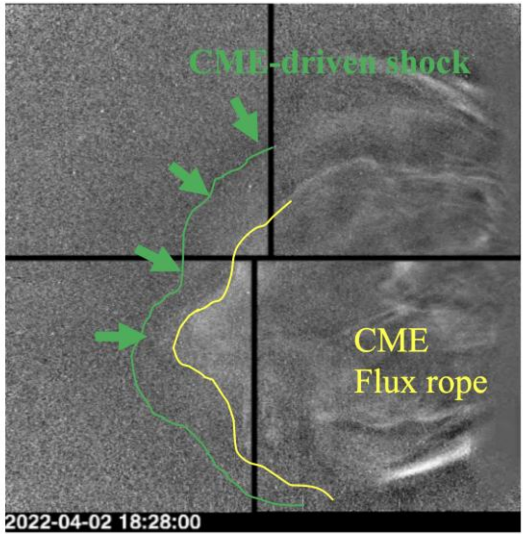

vs

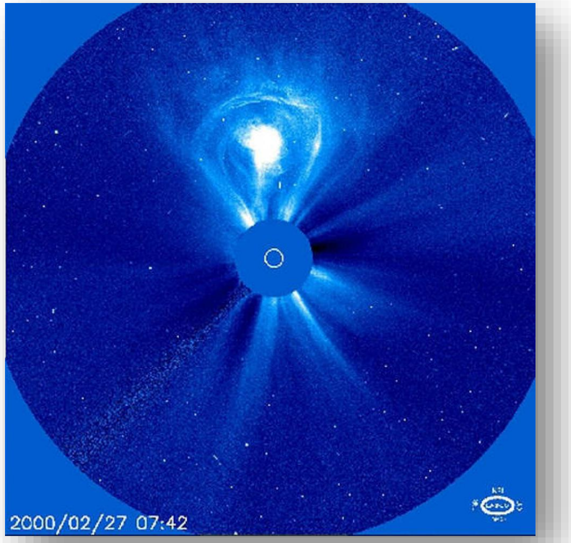

Anisotropic front
[corrugated observation of the front]

- Shocks in SoloHI can provide physical characteristics of shocks
- Density compression ratio (density jump) for shock strength

CME structure… a global picture

- Is the classic 3-part structure too simplistic? (What is erupting?)
- Many papers show CME with a clear 3-part structure. Is it really a so common or they are just beautiful and then studied? ("observational selection" effect)
- Nested-rings: origin? Coherence of the nested ring structure.
- Corrugated observation of the front (and shock).
- SHINE 2024: "Very high-resolution global simulations of CMEs reveal that CME structures exhibit a significant degree of variation within a small angular width!"

alessandro.liberatore@inaf.it

Internal magnetic field structures and flows

Solar Orbiter highly detailed observations

From EUI to Metis

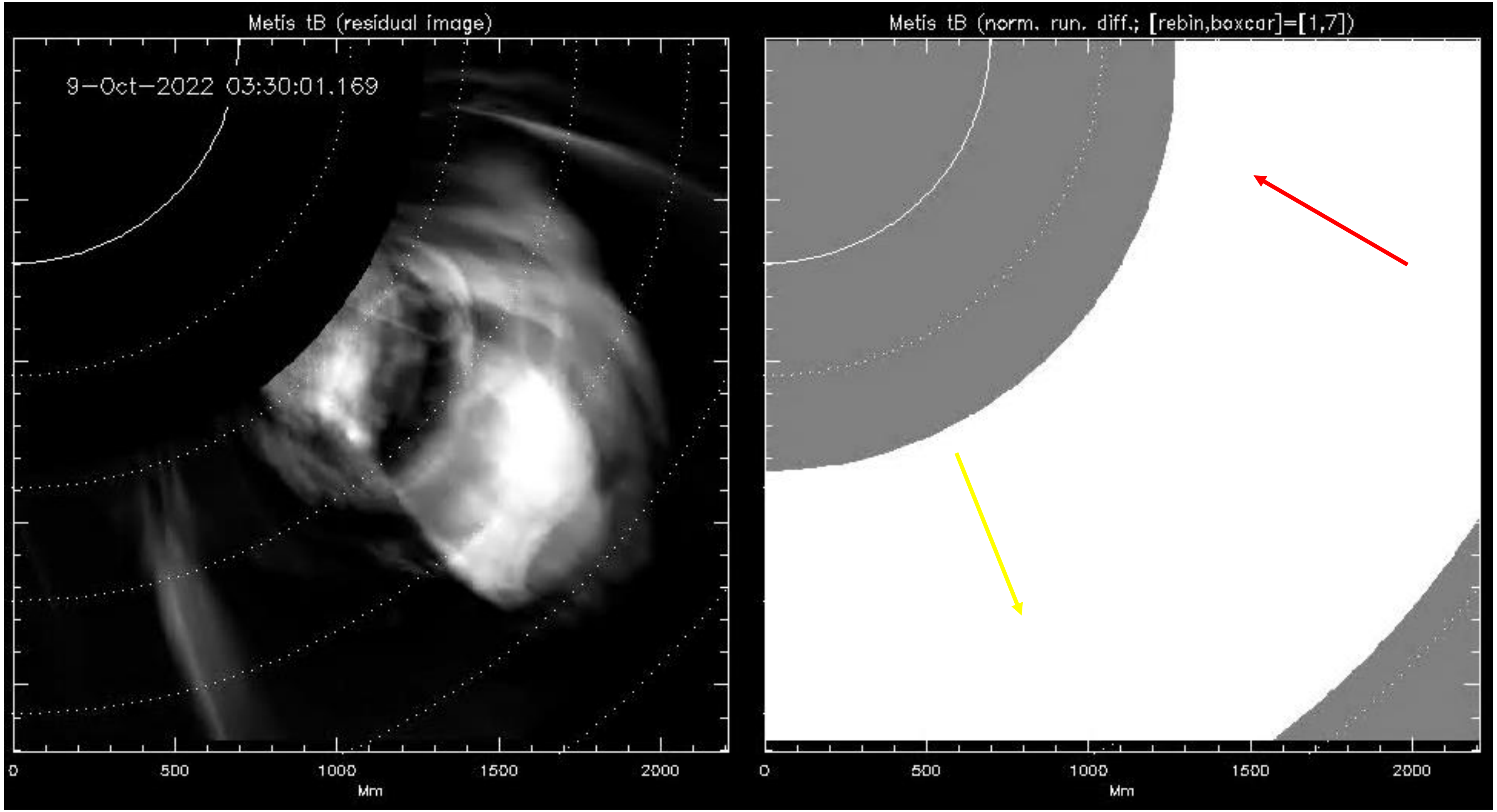

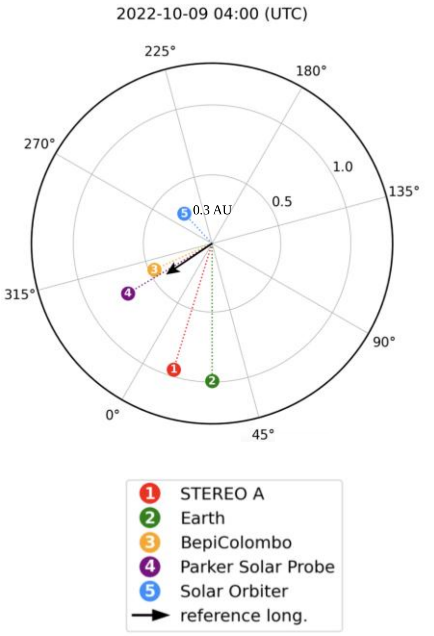

G. Russano (work in progress)

Parker Solar Probe highly detailed observations

WISPR *vs* STA/Cor2

PSP Encounter 10; Nov. 2021

CME 2021-11-20 T00

PSP at Car LN= 20°

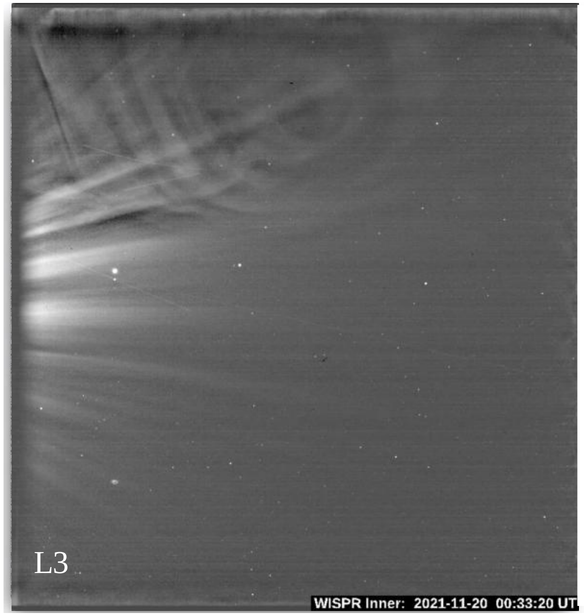

STA at Car LN = 55°

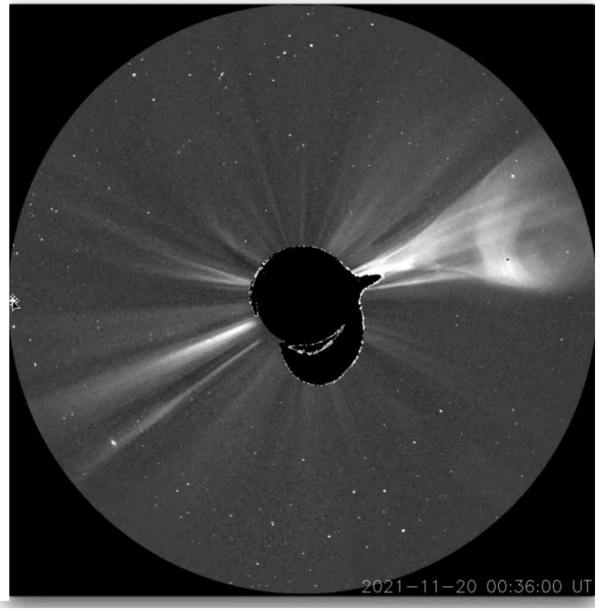

CME 2021-11-20 T23

PSP at Car LN = 7°

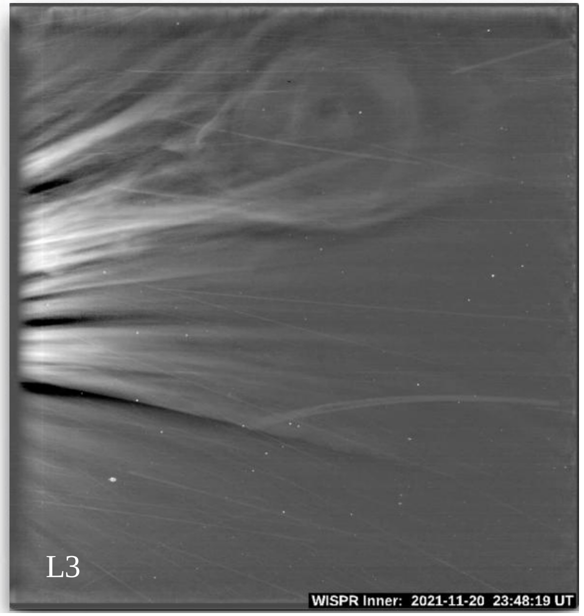

STA at Car LN = 42°

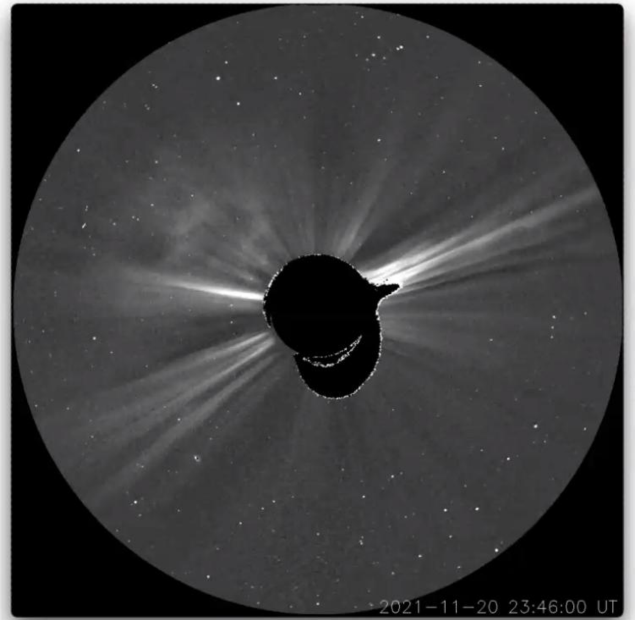

[Howard et al., 2022]

Parker Solar Probe highly detailed observations

WISPR *vs* STA/Cor2

PSP Encounter 10; Nov. 2021

CME 2021-11-20 T00

PSP at Car LN= 20°

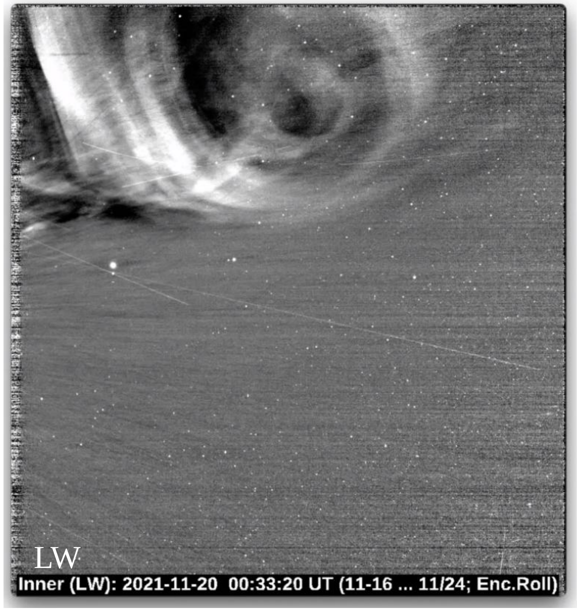

STA at Car LN = 55°

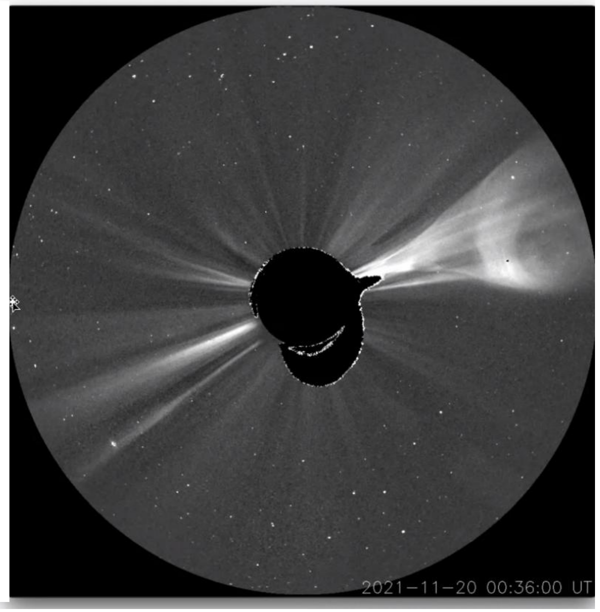

CME 2021-11-20 T23

PSP at Car LN = 7°

STA at Car LN = 42°

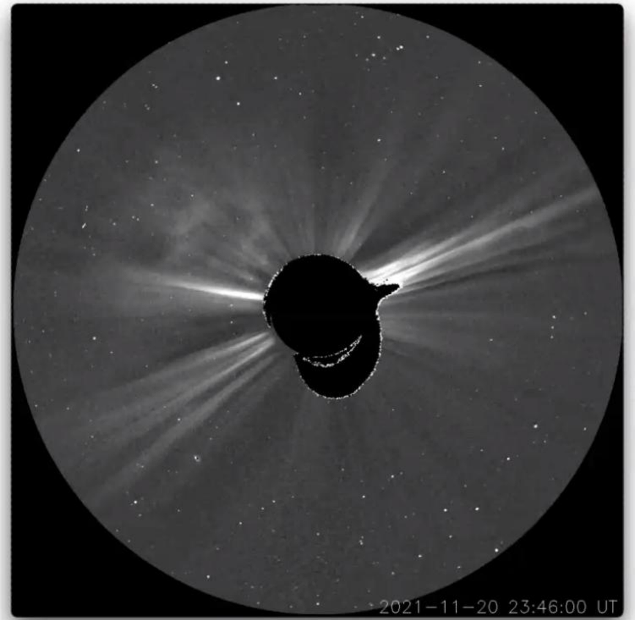

[Howard et al., 2022]

WISPR L3 vs LW

L3 (calibrated images) → streamers

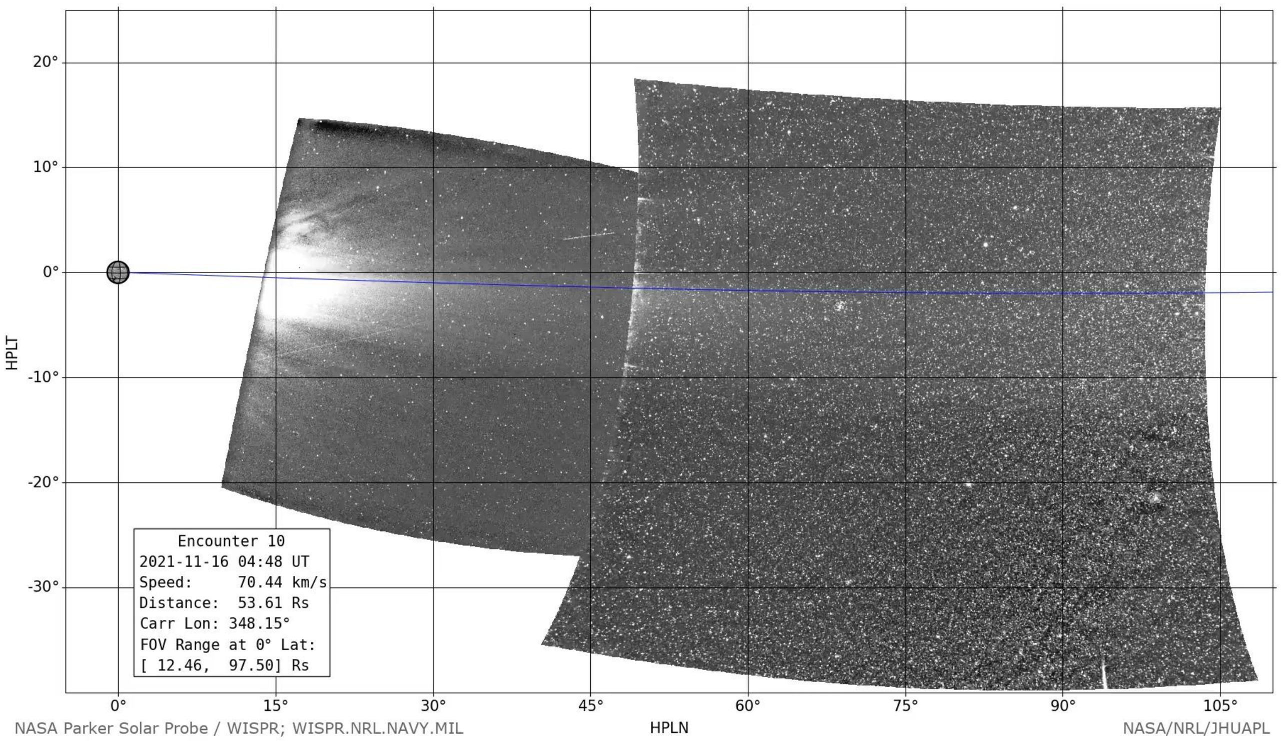

LW (difference) → post CME flows (flows with blobs)

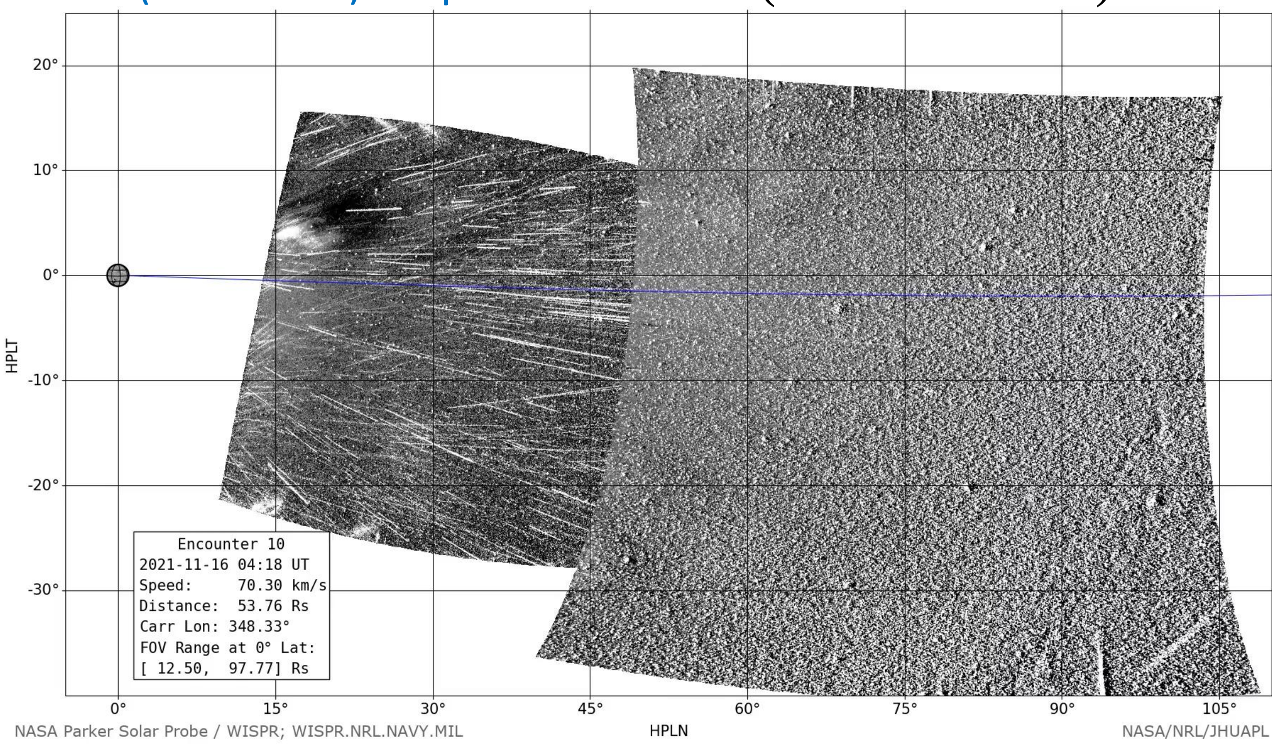

2021 Nov 21-22 WISPR observed flows with blobs

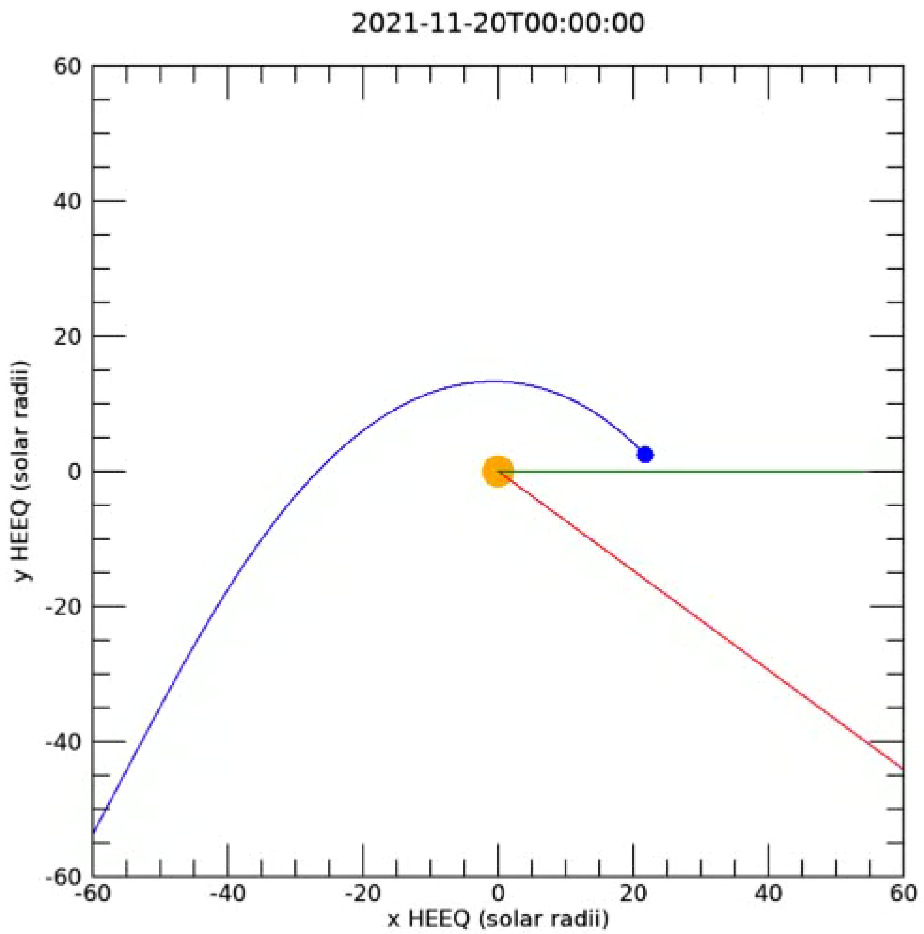

Origin of the pre-CME flow?

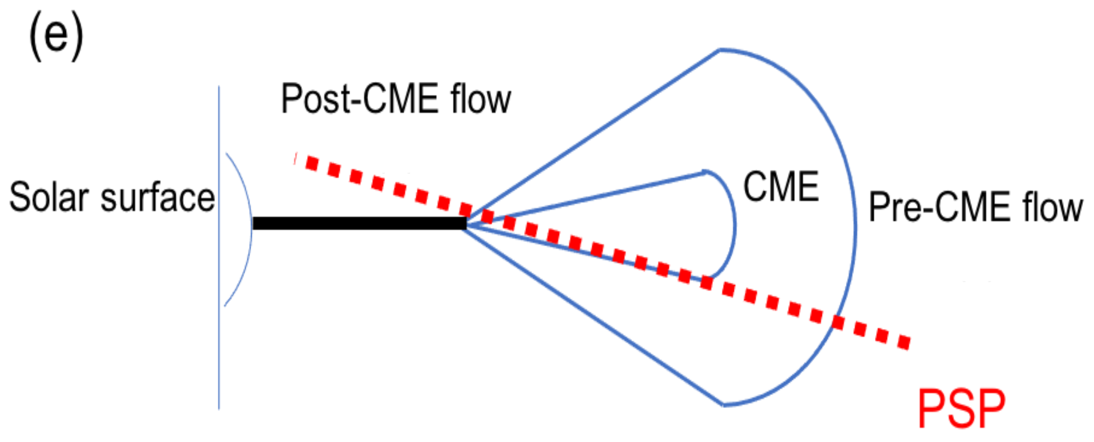

…comparison of PSP/WISPR *images* with *in-situ* data in progress!

- Determine when Parker is inside CMEs, or related flows
- Identify properties to understand processes that produce them

Adapted from C.Braga, COSPAR 2024

2021 Nov 21-22 WISPR observed flows with blobs

Origin of these blobs?

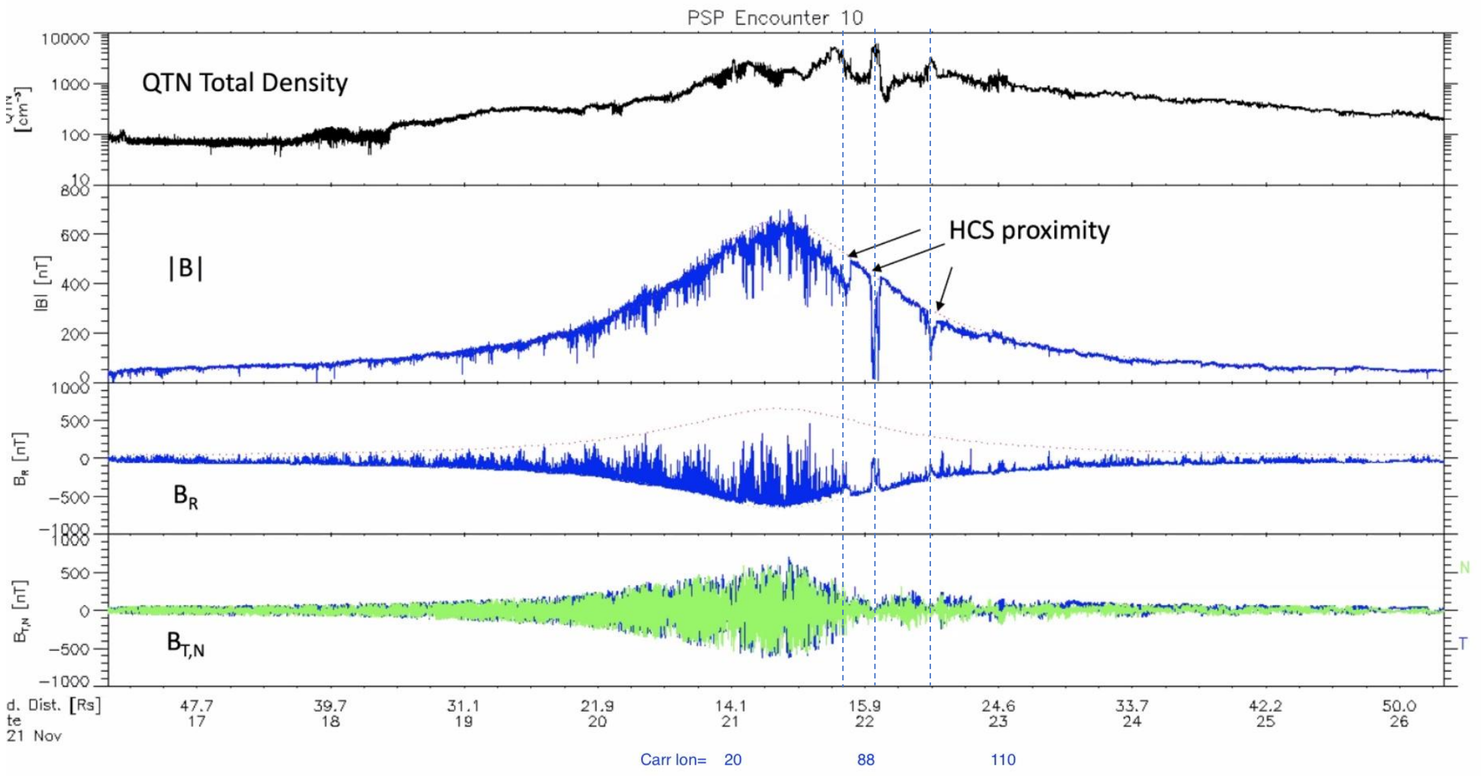

In situ data shows near HCS, but not crossing

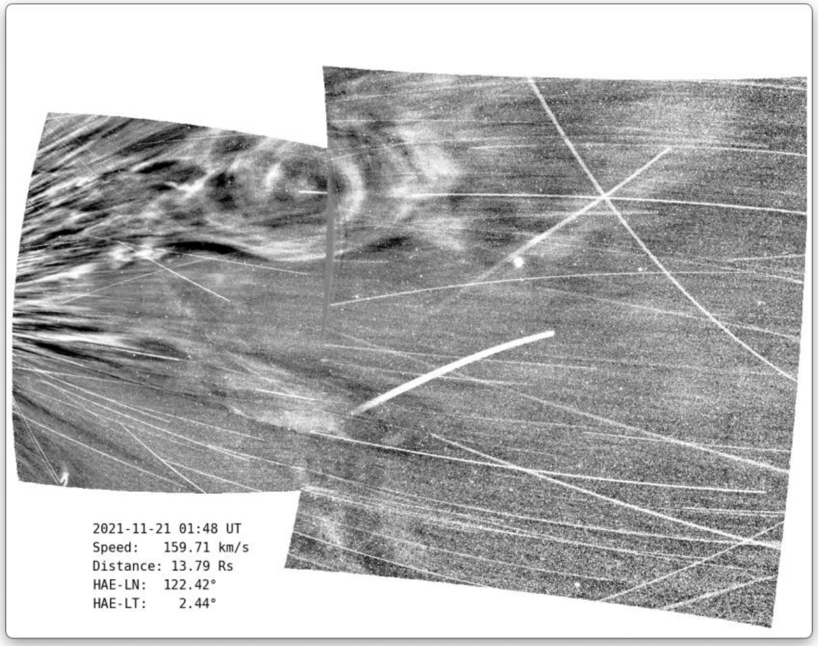

Parker intercepts the wake of a CME on Nov 21st and 22nd 2021

- Flow of blobs may be associated with HCS current sheet (Liewer et al., 2024), post-CME CS/flows?

(C.Braga, work in progress)

3D reconstruction with PSP

Cappello et al. 2024

PSP E14

2022-12-08 23:00:00

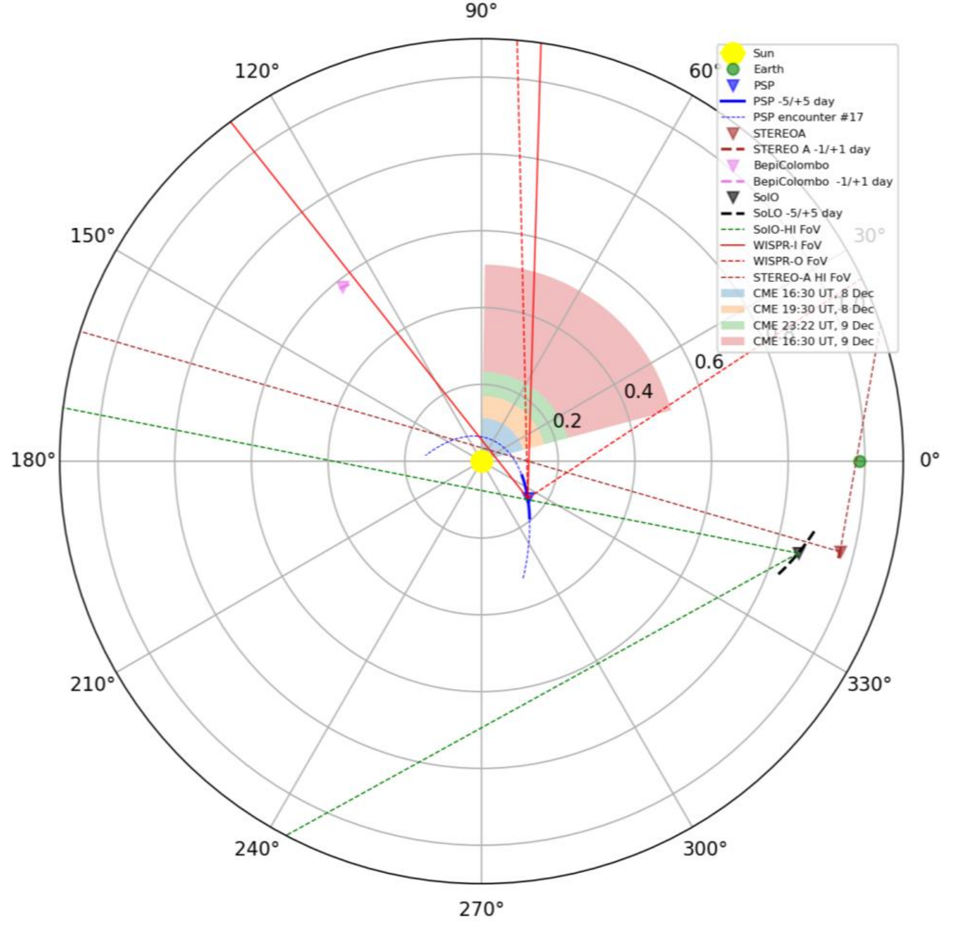

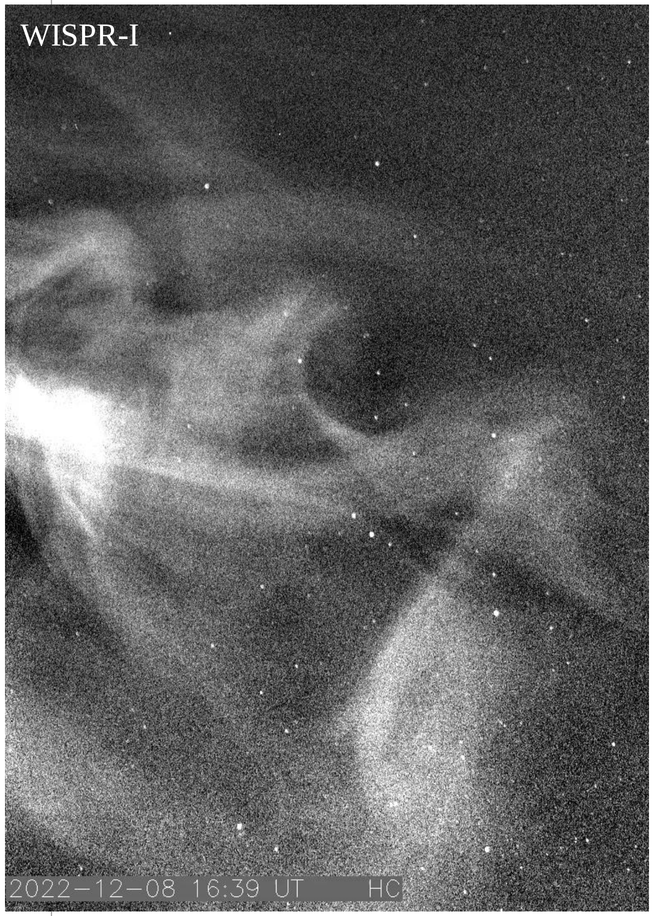

1) Twisted magnetic field structures with C- and J-shapes,

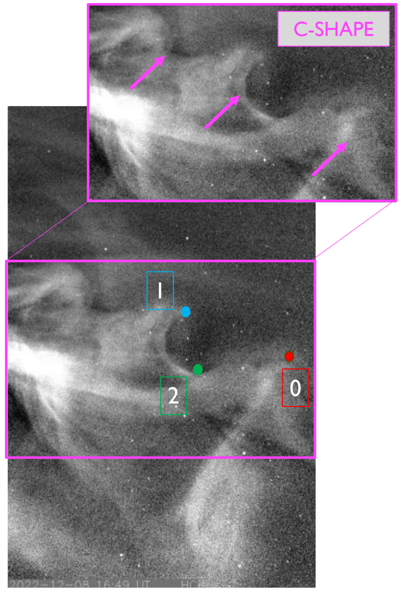

2) Thread-like patterns

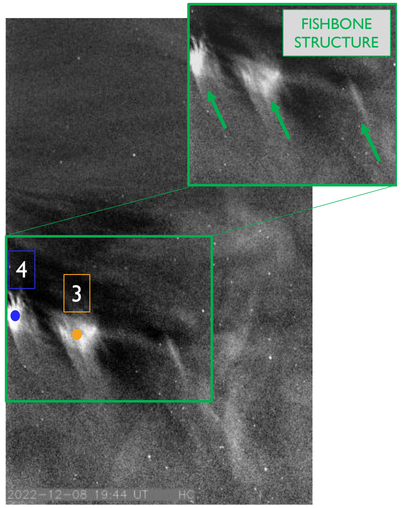

3) Blobs

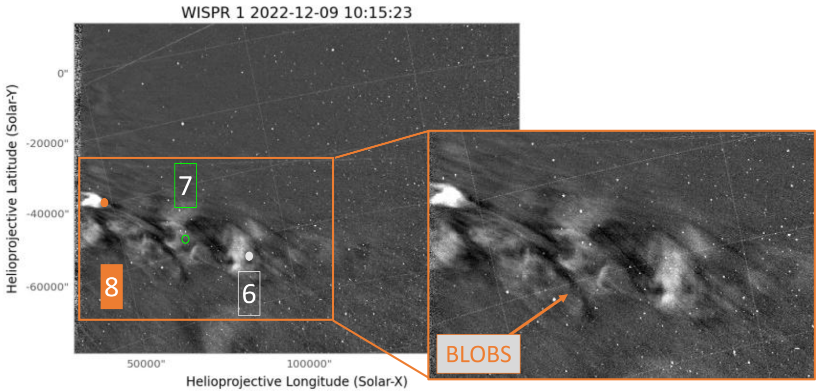

3D reconstruction with PSP

Cappello et al. 2024

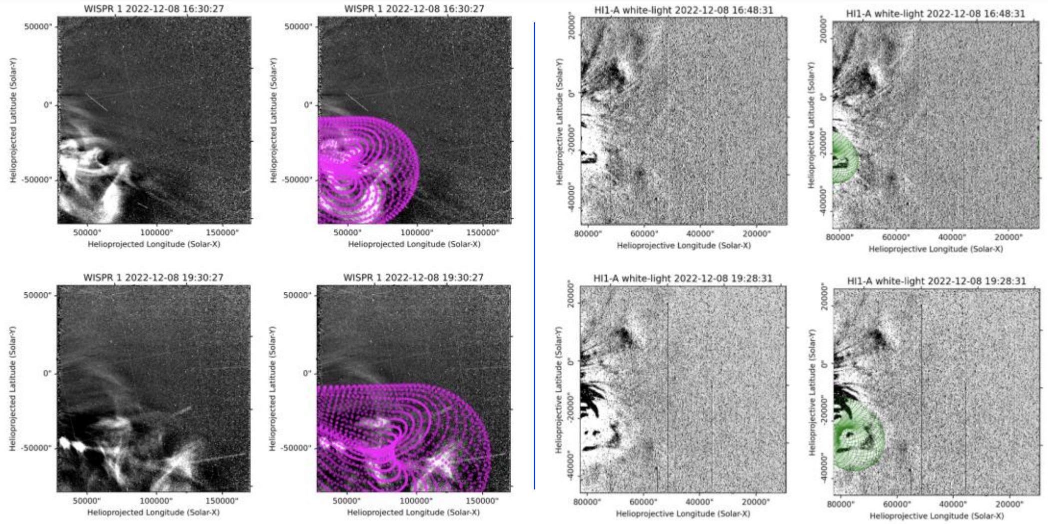

The global appearance of the CME can be very different in WISPR (0.11 - 0.16 AU) and instruments near 1 AU because of shorter line-of-sight integration of WISPR.

Single-spacecraft reconstruction - geometry

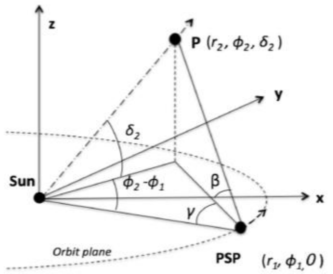

$$\beta(t) = \operatorname{atan}\left(\frac{\tan\delta_2 \sin(\gamma(t))}{\sin[\phi_2 - \phi_1(t)]}(1 - F\sin\epsilon)\right), \tag{A.3}$$

$$\cot(\gamma(t)) = \frac{r_1(t) - r_2(t)\cos\delta_2\cos([\phi_2 - \phi_1(t)])}{r_2(t)\cos\delta_2\sin([\phi_2 - \phi_1(t)])}(1 - G\sin\delta_2\sin\epsilon), \tag{A.4}$$

[Liewer et al. 2019; 2020; 2022]
[Braga et al. 2021; 2022]

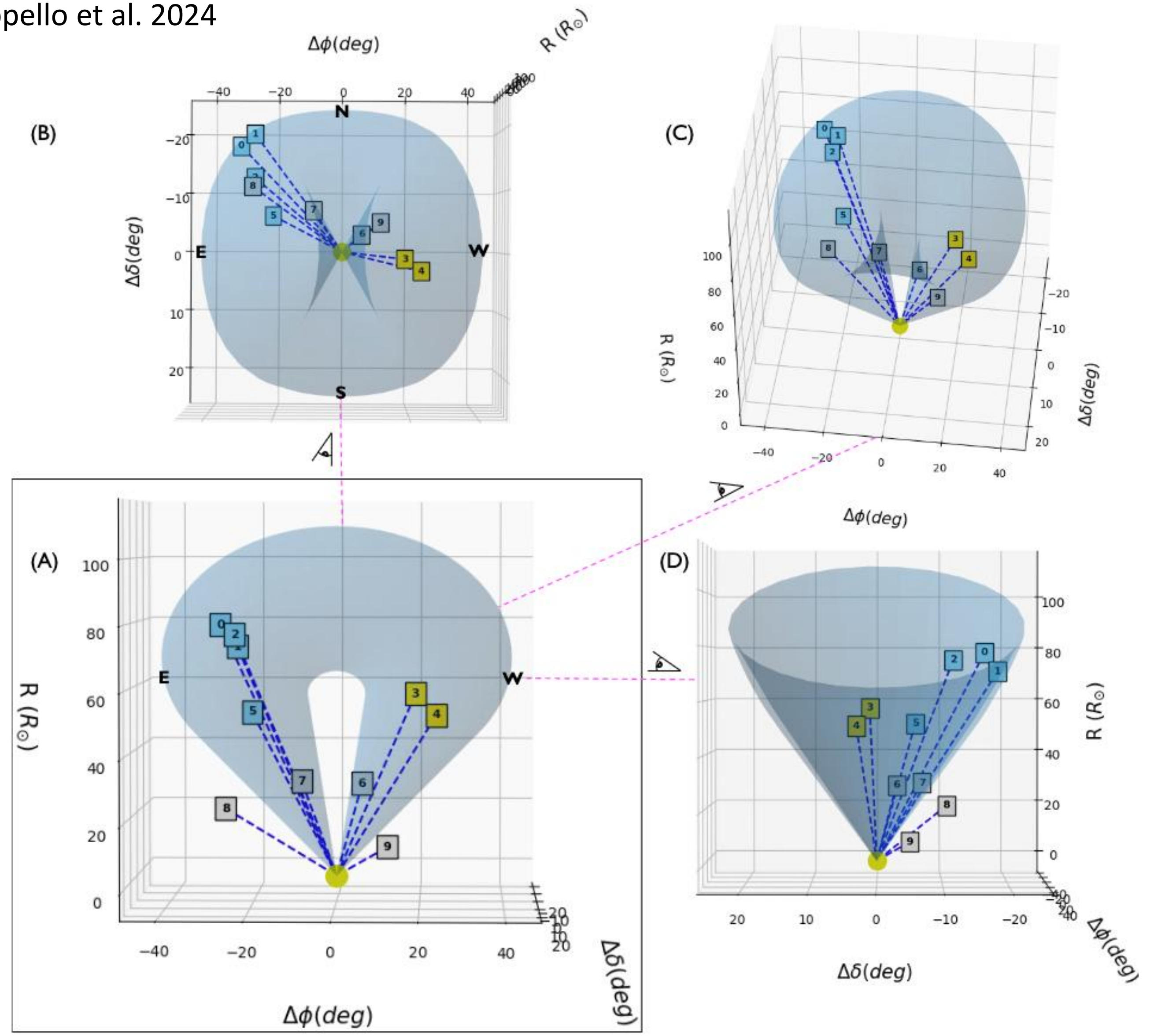

3D reconstruction with PSP

Why do these enhancements of density (blobs) in the wake of the CME have different longitudes?

- Multiple post-CME CS (?)
- Interchange reconnection (?)
- Solar wind interaction (?)
- Instabilities (?)

…any other ideas?

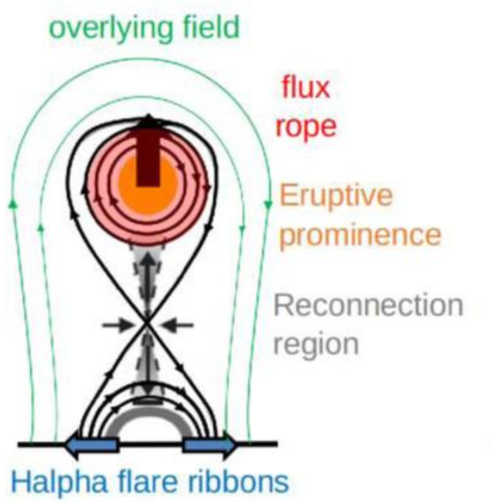

[Zhang et al., 2021]

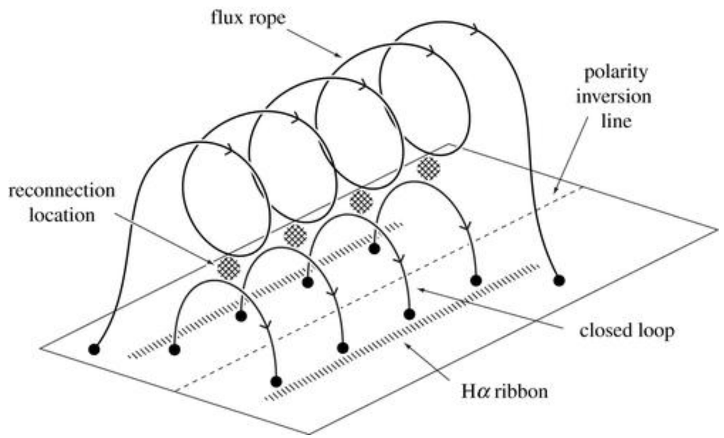

[Longcope et al., 2007]

-Basic elements of the CSHKP two-ribbon flare model in two (left) and three (right) dimensions-

Internal magnetic field structures and flows

- Are flows associated with HCS current sheet, post-CME CS/flows?
- "Organized" distribution of internal structures?
  Longitudinal distribution of blobs (Why no-thick post-CME CS?)
- Observation of downflows
- Pre-CME flows?

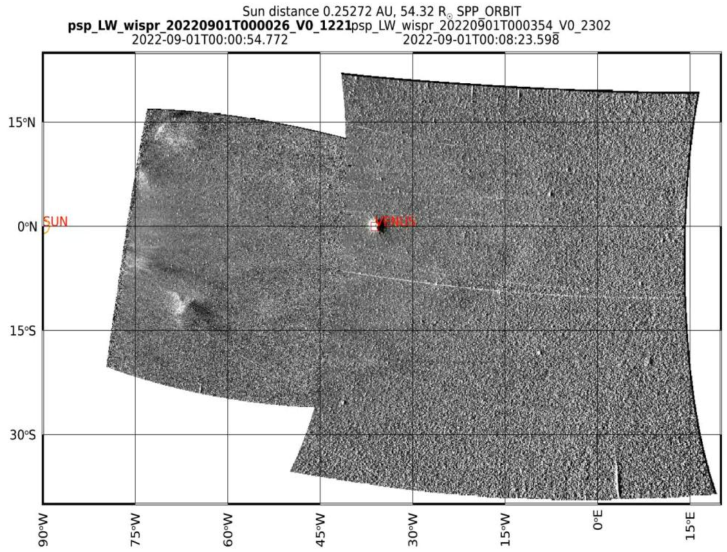

CME propagation

CME evolution in corona and heliosphere

What determines the evolution of the CMEs in corona and interplanetary space?

During the CME evolution in the solar corona and heliosphere, we observe:

- ➢ Deflected/non-radial propagating CMEs [Liu et al.,2010; Liewer et al., 2015; …]

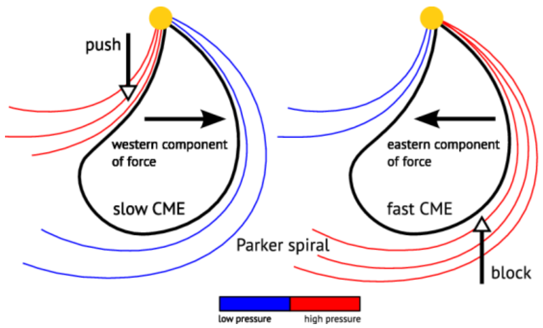

[Isavnin et al., 2013]

- ➢ Distorted CMEs [Braga et al., 2022; Liberatore et al., 2024; …]

- ➢ CME-CME interaction [Lugaz et al., 2012; Scolini et al.,2020; …]

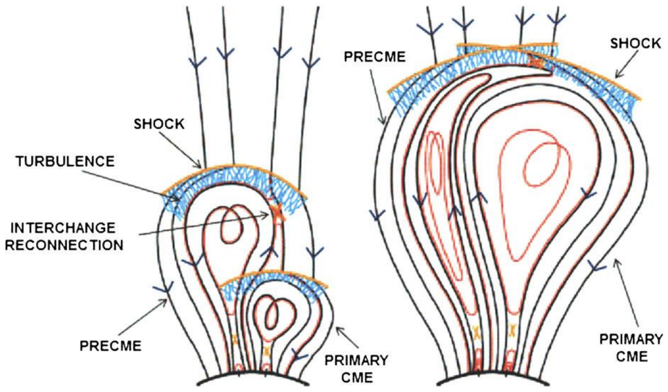

[Lugaz et al., 2017]

- ➢ CME-Solar Wind interaction [Heinemann et al., 2019; Kay et al., 2022…]

- ➢ …

Coronal Mass Ejection Deformation at 0.1 au Observed by WISPR

[Braga et al., 2022]

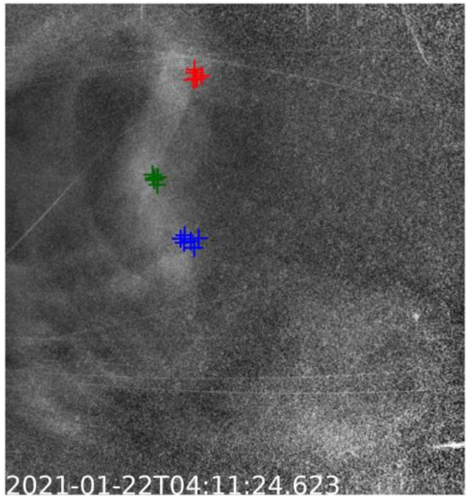

- The event was observed by multiple white-light imagers on 2021 January 20–22.
- CME becomes distorted at ~0.1 au → differences in the background solar wind speeds.
- The CME deformation seems to cause a time-of-arrival error of 16 hr at ~0.5 au.
- The deformation is evident only in WISPR observations → Such deformations may help explain the time-of-arrival errors in events where only coronagraph observations are available (8-10h)

Challenges in Forecasting the Evolution of a Distorted CME

[Liberatore et al., 2024]

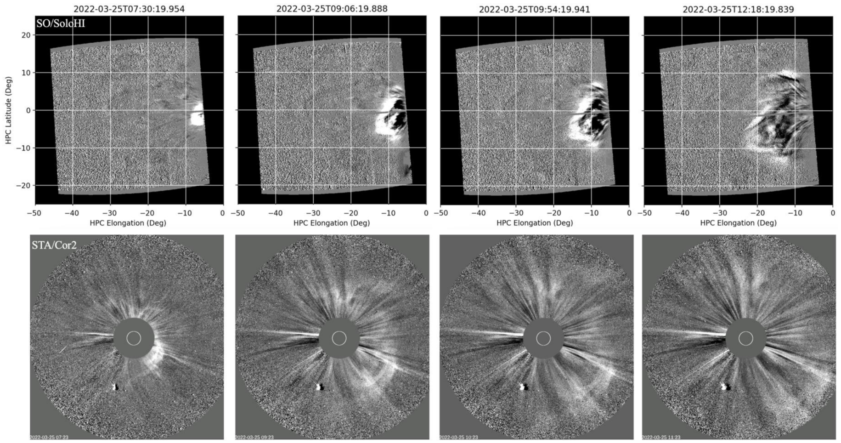

- The event was observed by multiple white-light imagers on 2022 March 25.
- Distortion of the CME in both latitude (thanks to SoloHI) and longitude.
- Strongly deformed CME; the GCS cannot fit the entire CME shape.
- Partial fit and fine-tuning with SoloHI → DBM → WSA-Enlil
  → 4 h error at 3 different S/C (BepiC at 0.5AU, STA and WIND at 1 AU with >30° LN diff)

CME/CME interaction – SOHO and STEREO coronagraphs

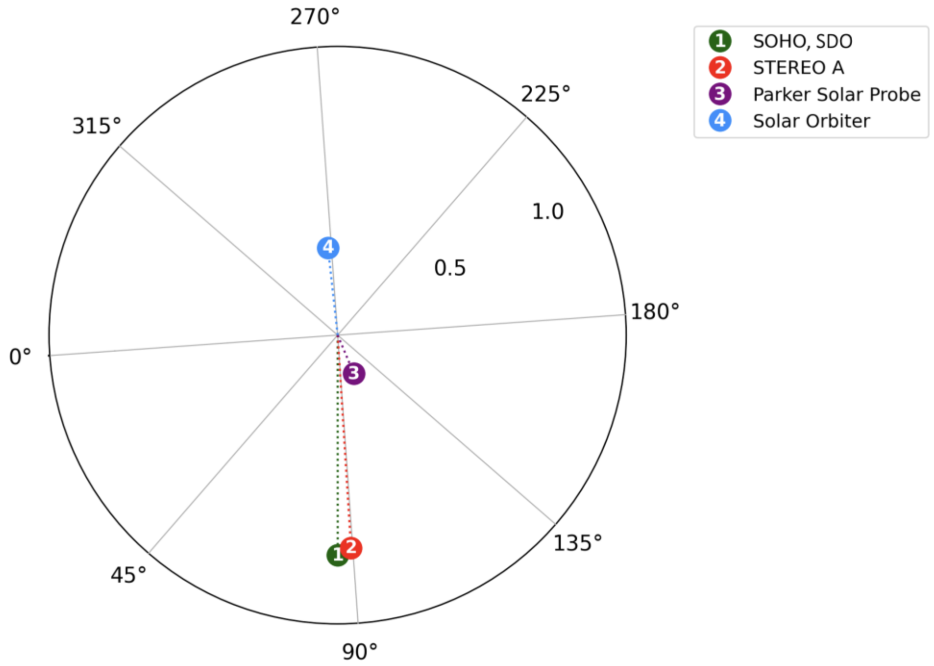

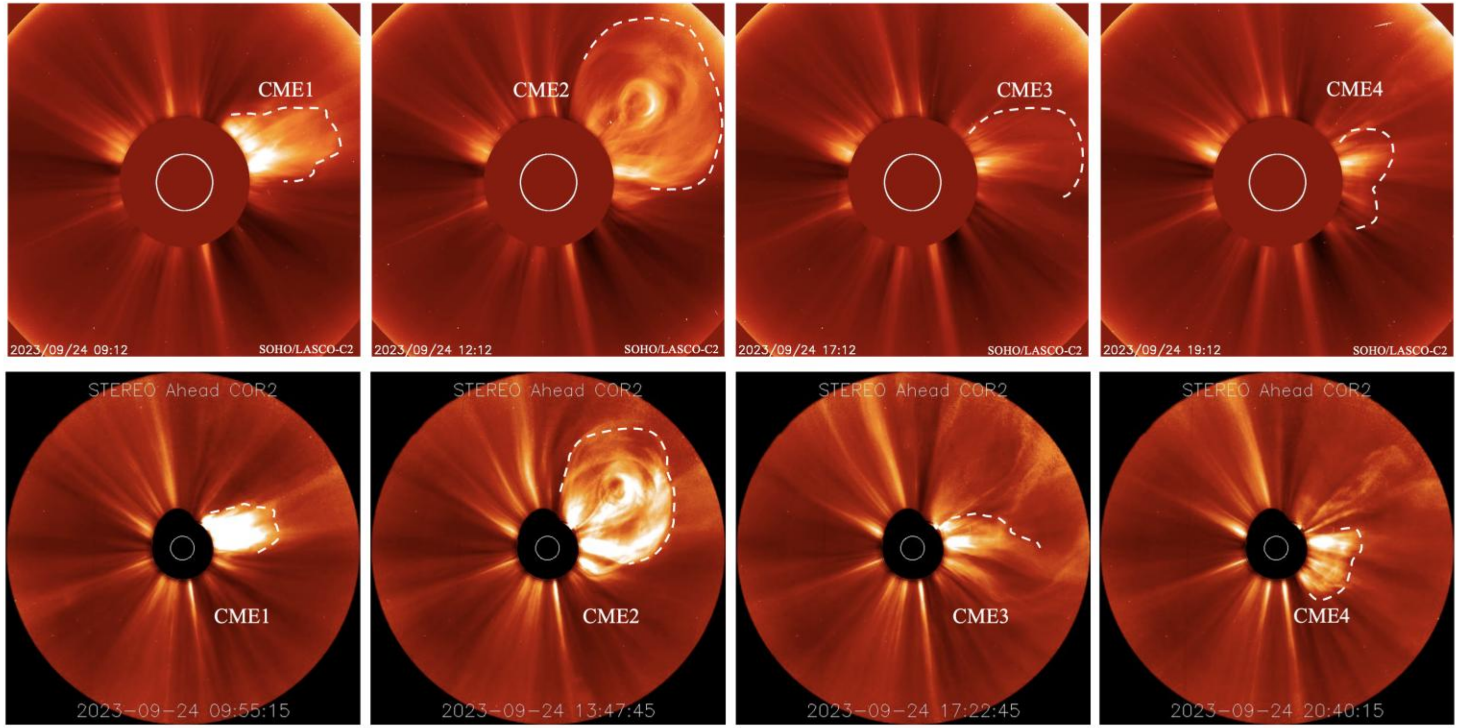

	SOHO	SDO	STEREO-A	Parker Solar Probe	Solar Orbiter
Carrington Longitude [deg]	86.0	85.9	89.5	108.9	272.2
Carrington Latitude [deg]	7.0	7.0	6.9	3.0	-7.9
Heliocentric dist. [AU]	0.99	1.0	0.96	0.19	0.4
Instruments used	• LASCO-C2 • LASCO-C3	• AIA • HMI	• EUVI • Cor1 • Cor2	• WISPR	• EUI • SoloHI • PHI

A. Liberatore (work in progress)

CME/CME interaction – PSP and SolO heliospheric imagers

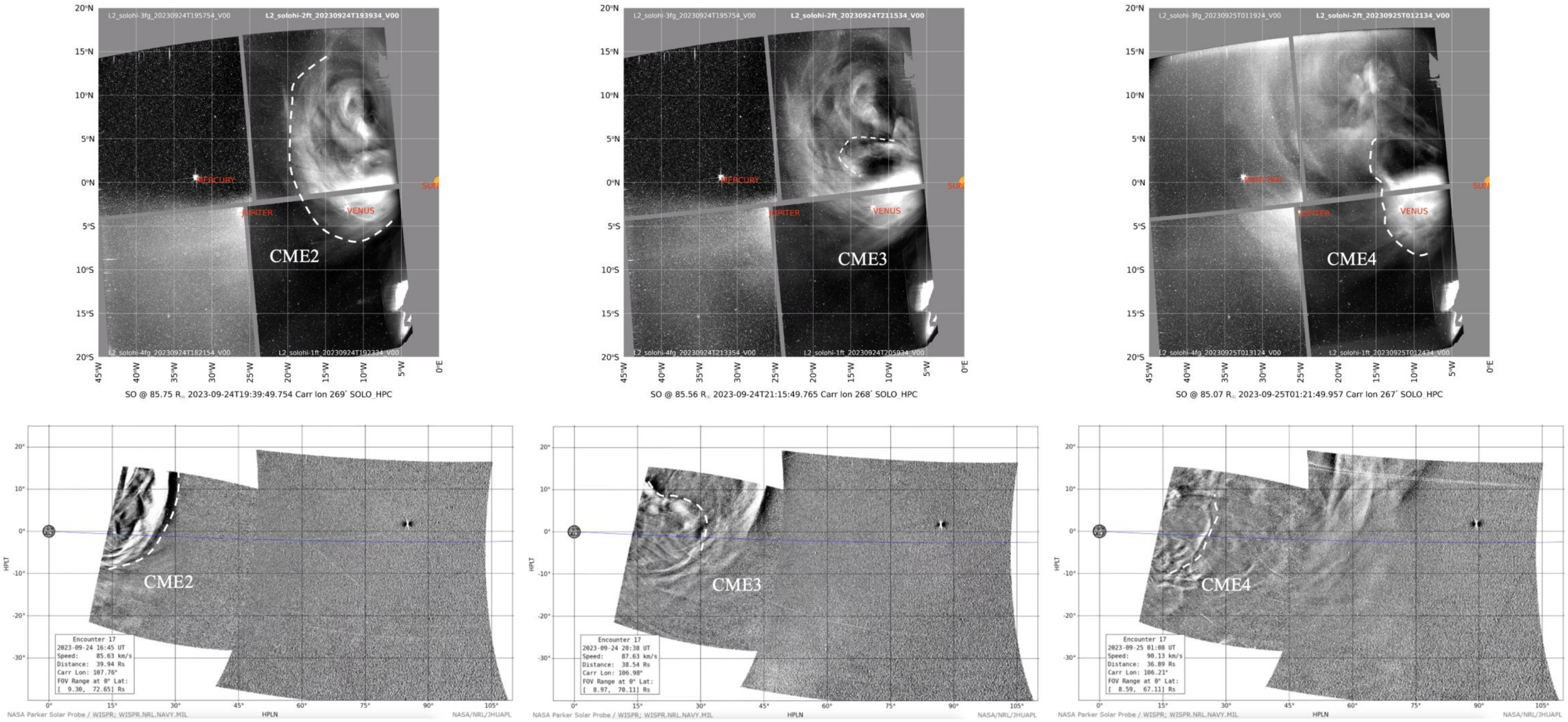

CME/CME interaction – GCS combining SOHO, STEREO, PSP, SolO

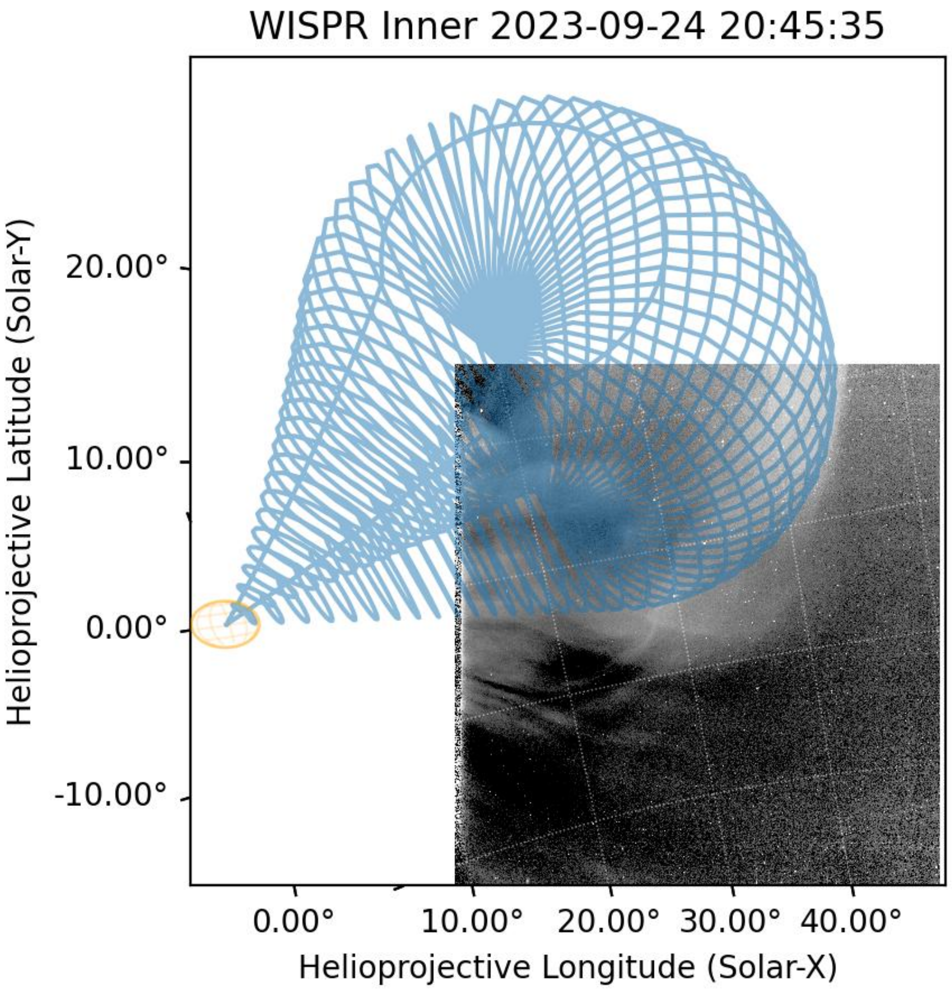

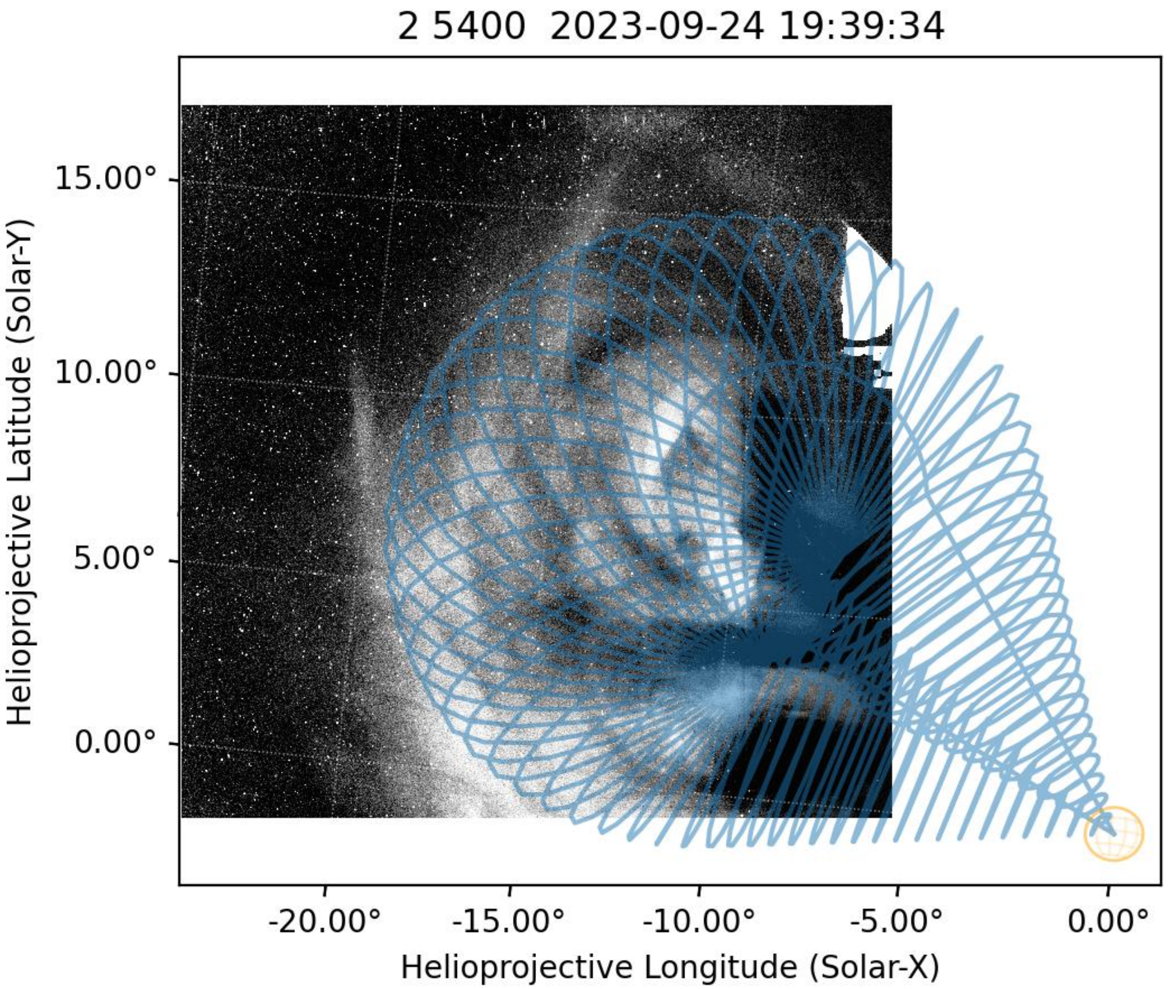

CME/CME interaction – GCS combining SOHO, STEREO, PSP, SolO

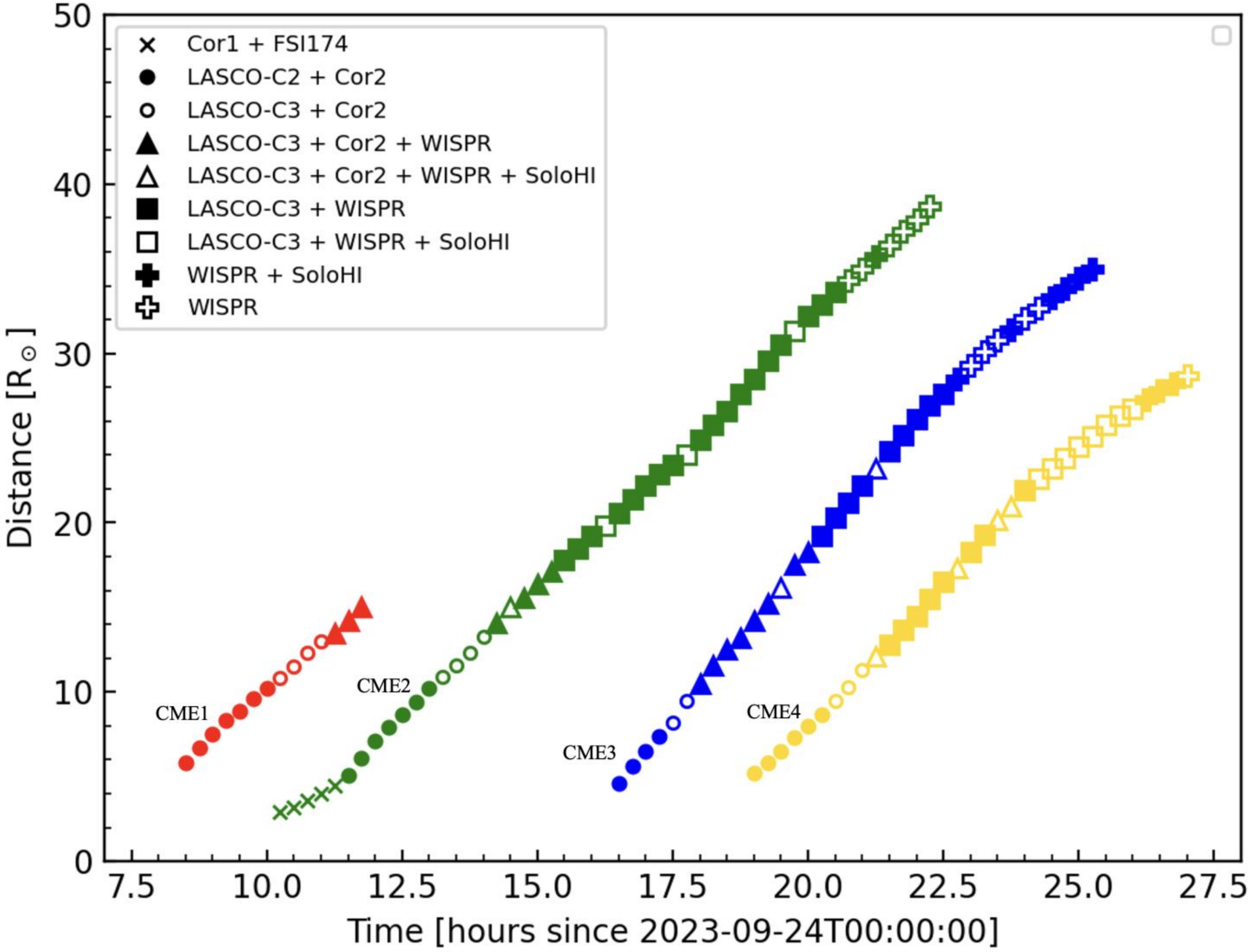

CME/CME interaction – GCS combining SOHO, STEREO, PSP, SolO

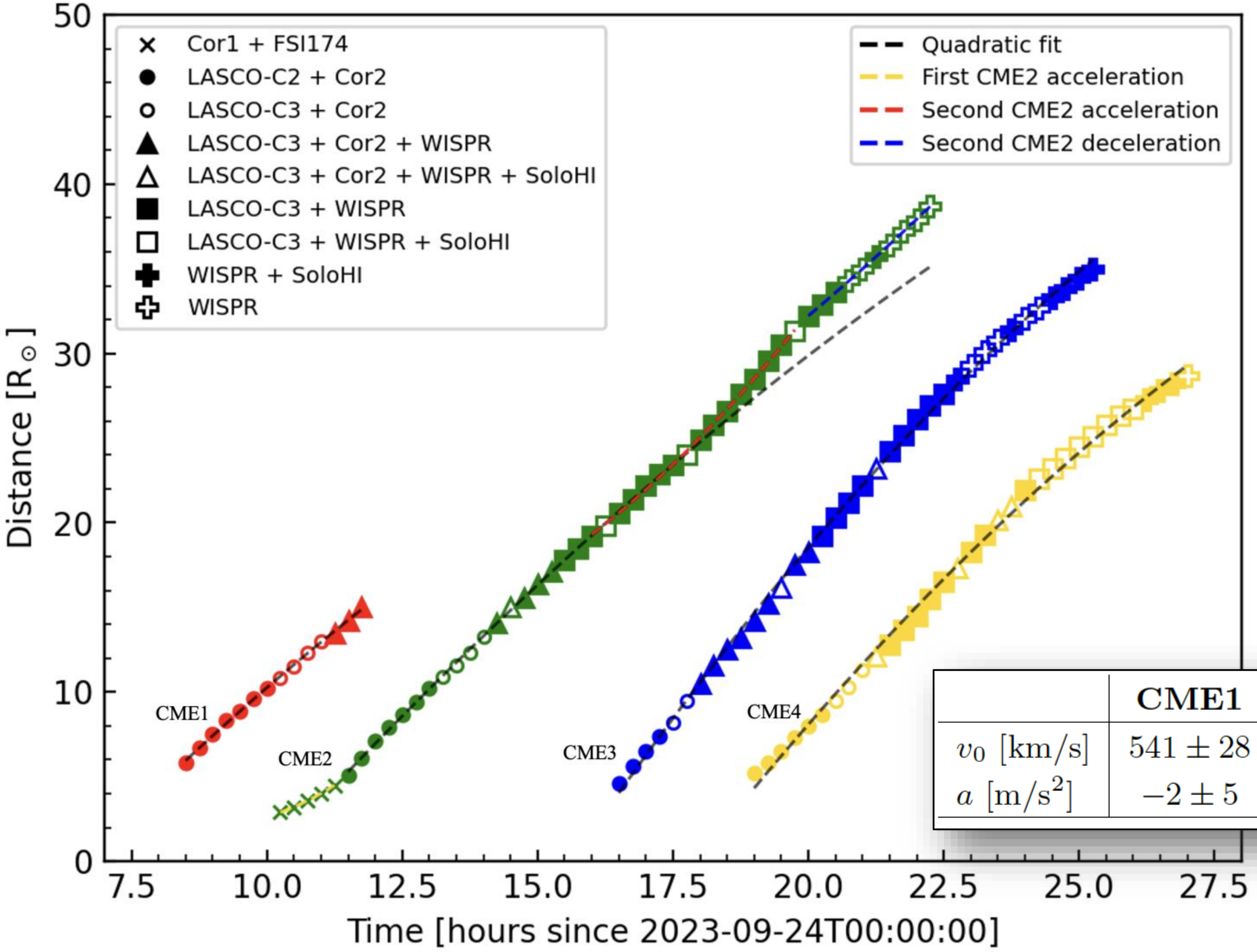

	CME1	CME2	CME3	CME4
v_0 [km/s]	541 ± 28	671 ± 20	859 ± 17	490 ± 16
a [m/s^2]	-2 ± 5	-8 ± 2	-22 ± 2	-10 ± 5

CME/CME interaction – GCS combining SOHO, STEREO, PSP, SolO

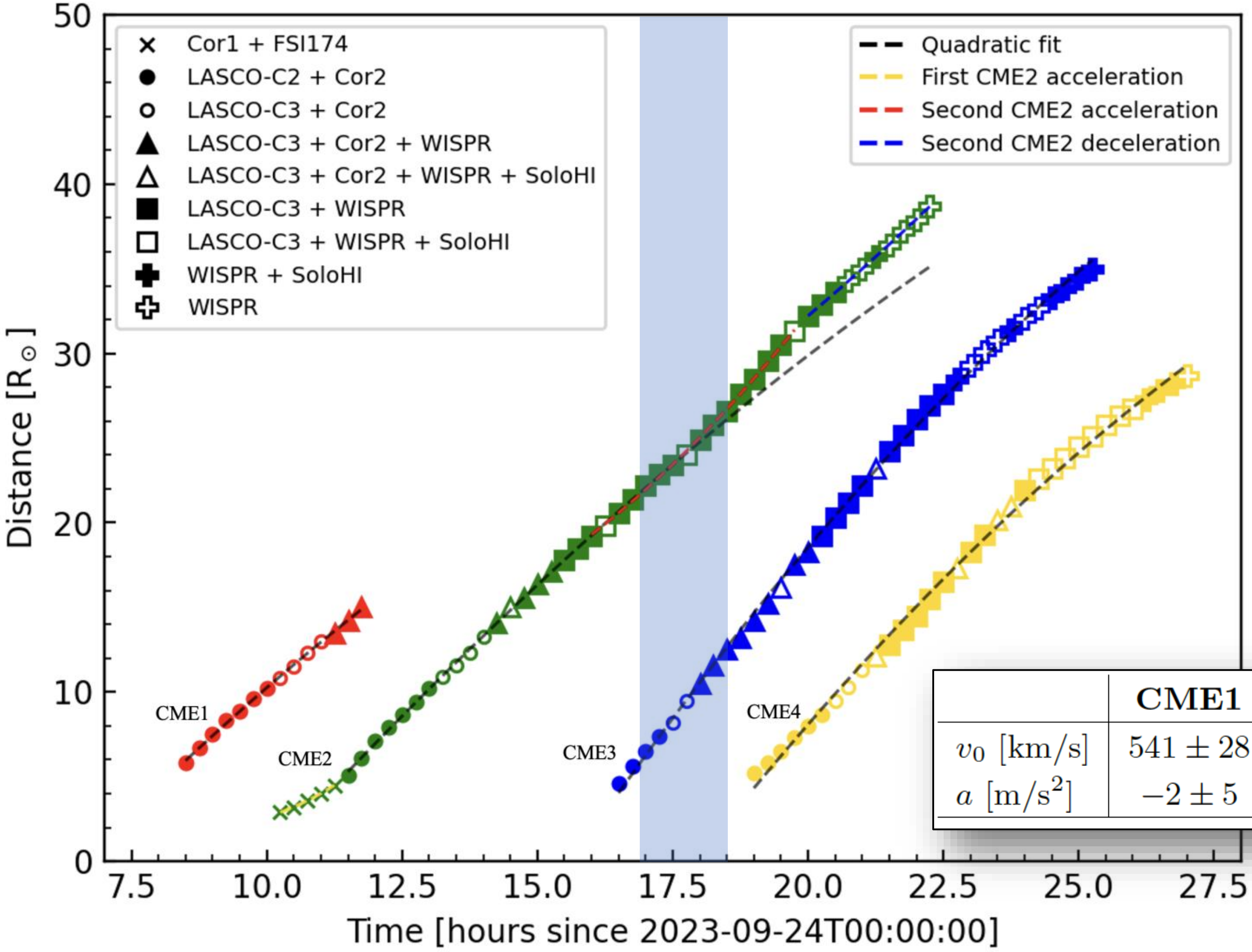

	CME1	CME2	CME3	CME4
v_0 [km/s]	541 ± 28	671 ± 20	859 ± 17	490 ± 16
a [m/s^2]	-2 ± 5	-8 ± 2	-22 ± 2	-10 ± 5

CME/CME interaction – CME deflection

[CME3 interact with CME2]

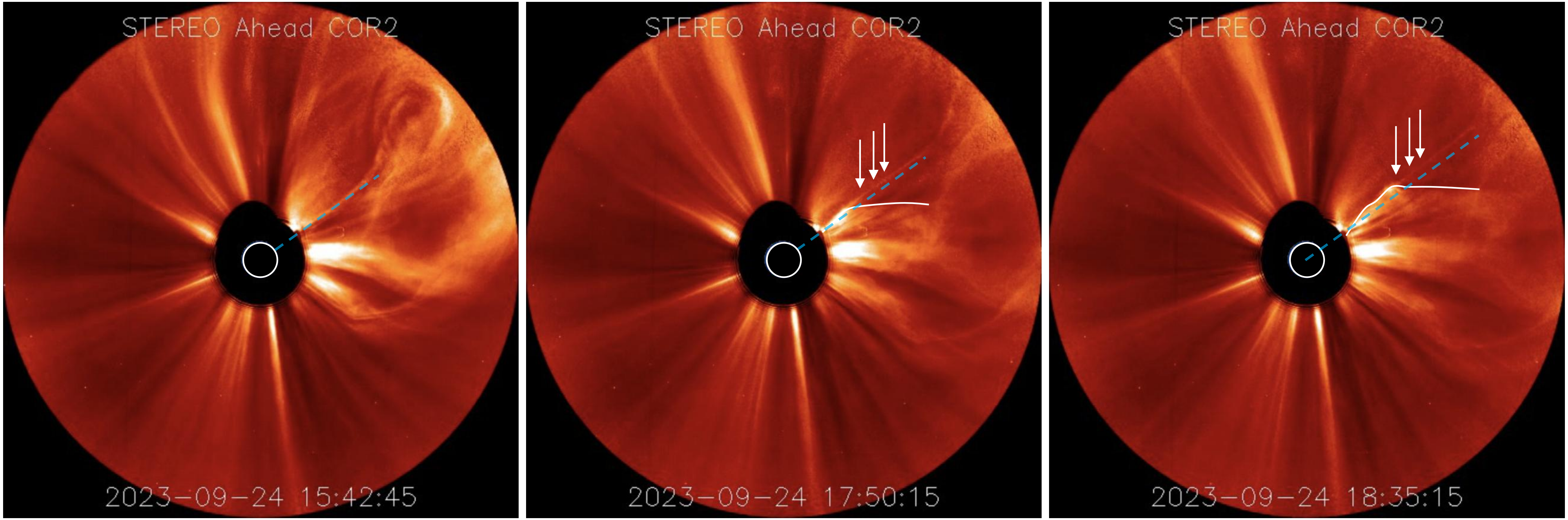

We have CME-CME interaction in their very early phase (1-2 $R_\odot$)

Post-CME current sheet deflection (~6°) and “bouncing effect” on CME3

alessandro.liberatore@inaf.it

Non-radial propagation of CMEs

[CME *vs* magnetic field; see Liewer, 2015]

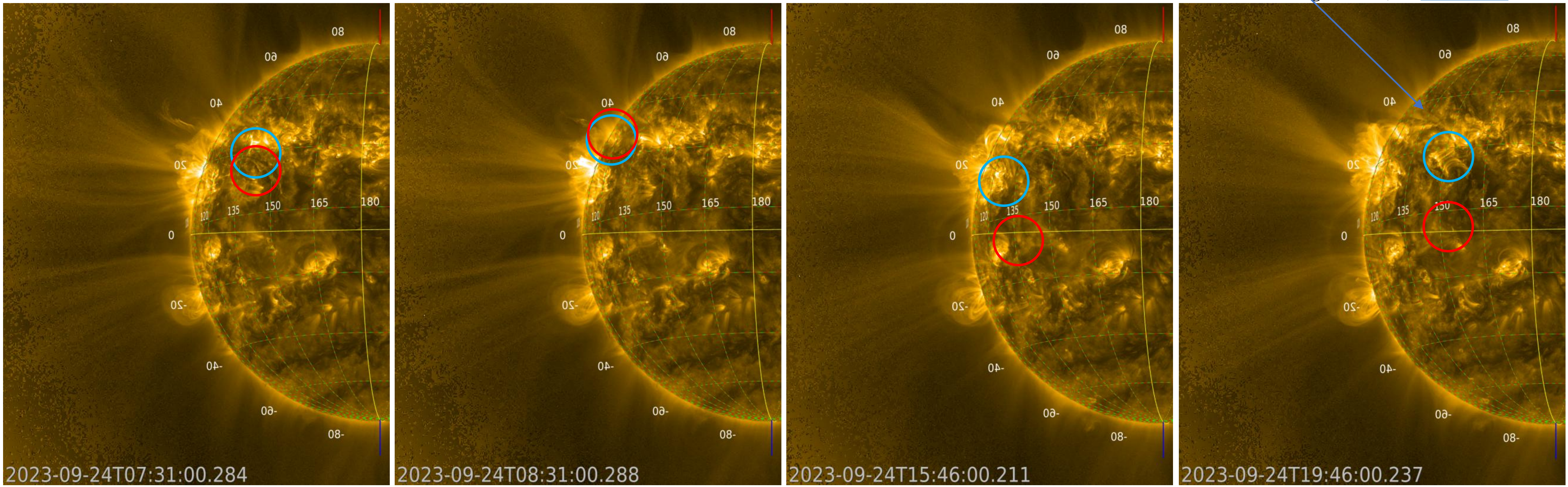

Source Region (LN, LT)	CME1	CME2	CME3	CME4
Observed Carrington	(229, 20)	(205, 27)	(209, 14)	(233, 16)
GCS Carrington	(226, 11)	(205, 28)	(206, 1)	(233, -11)

CME propagation

- What determines the evolution of the CMEs in corona and interplanetary space?
- The role of PSP and SolO in studying the CME evolution (taking into account distortions, deflections, rotations, CME-CME interactions, …)
- How can we improve the ETA forecasting? [To date: ~8-10h error -average-] [e.g., Colaninno et al. 2013; Riley et al. 2018]
- WISPR and SoloHI as fine-tuning tool for GCS parameters and CME evolution models?
- 3D reconstruction with SolO and PSP?
- More viewpoints → more distortions → we need more GCS for a single strongly distorted event?

About high temporal resolution

- Are we missing something because of a too low temporal resolution?

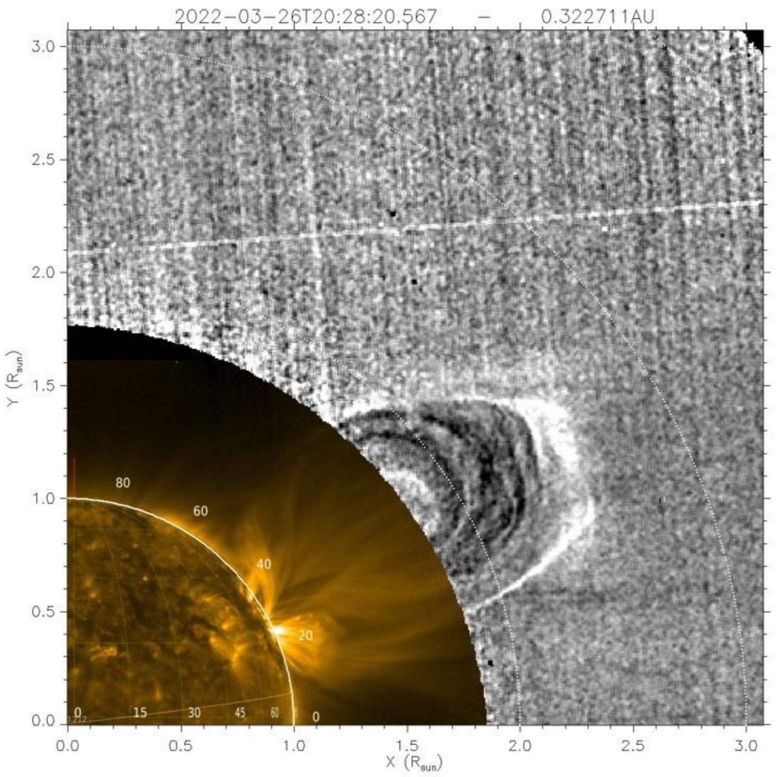

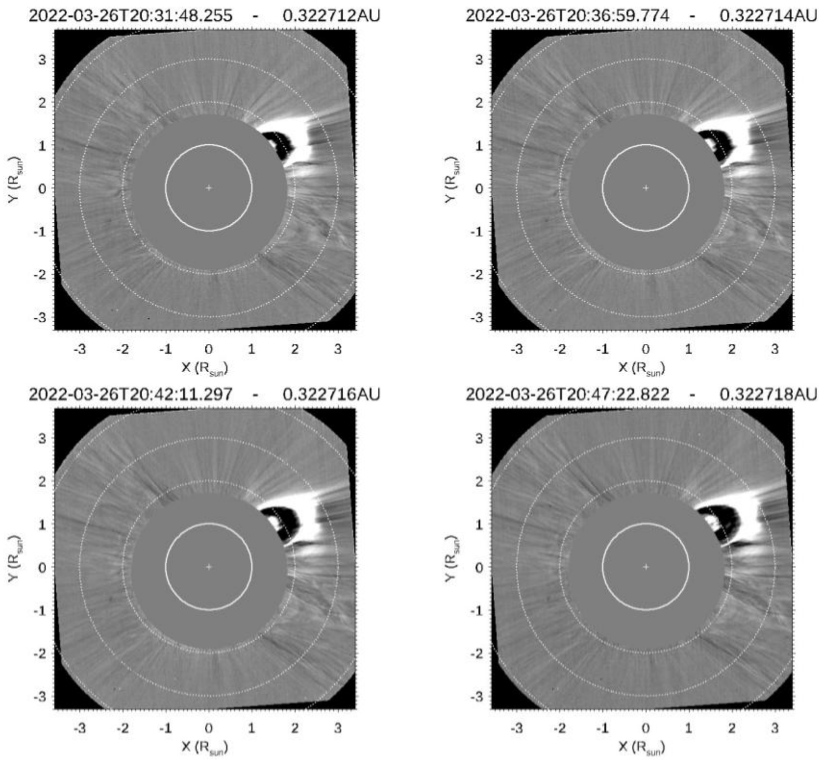

A. Bemporad (work in progress)

LASCO-C2 vs Metis (2022-03-22)

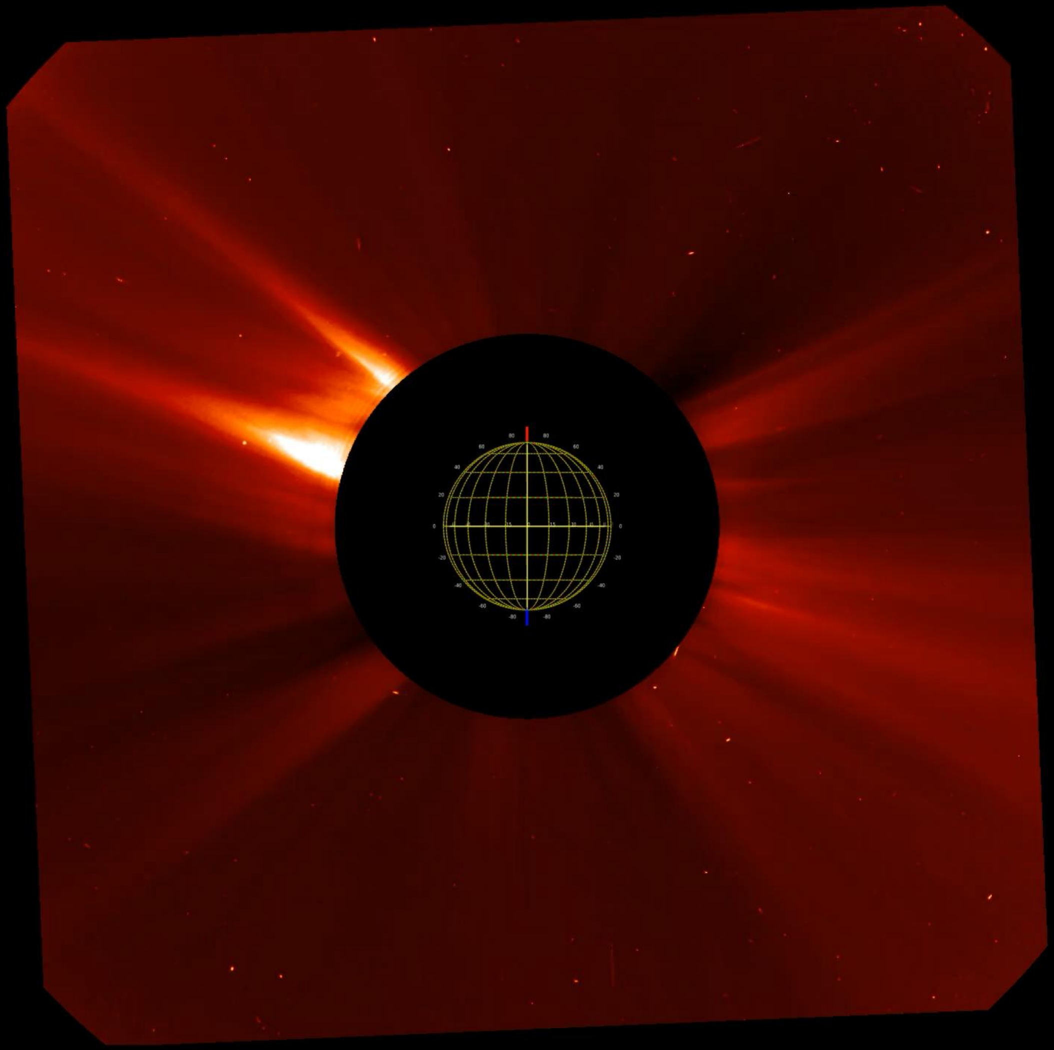

2022-03-22T00:00:07.604

LASCO-C2 vs Metis (2022-03-22)

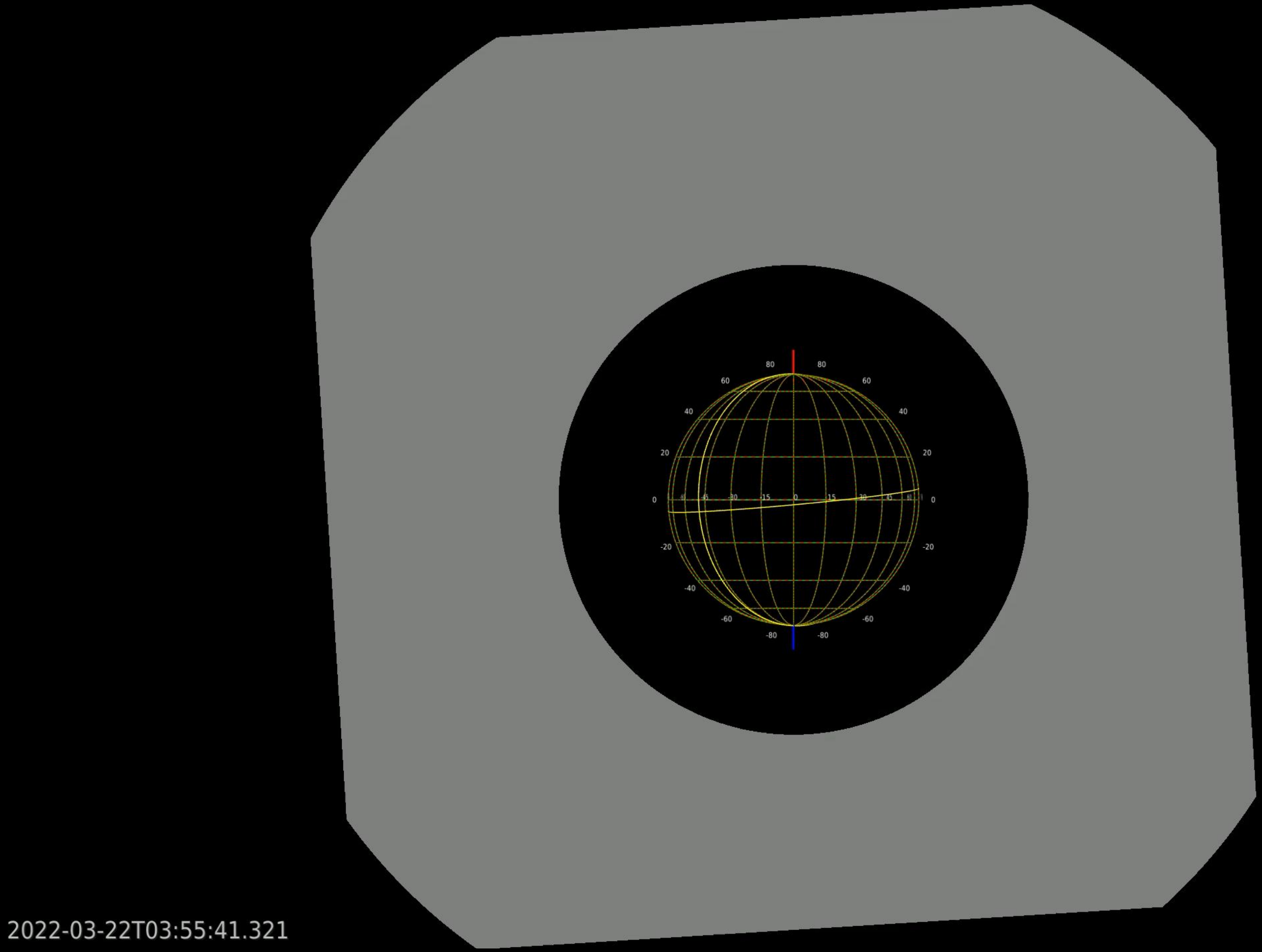

CMEs: Early-phase and lower corona

→ joint use of EUV imagers & coronagraphs

- Several activities in regions correlated with the CME eruptions: flares, filaments, etc…
- It is logical to assume that the effects of violent processes will not remain confined in the in active region area:
  - ➔ EIT/EUV Waves (first obs. in 1997)

CMEs: Early-phase and lower corona

→ joint use of EUV imagers & coronagraphs

- Several activities in regions correlated with the CME eruptions: flares, filaments, etc…
- It is logical to assume that the effects of violent processes will not remain confined in the in active region area:
  - ➔ EIT/EUV Waves (first obs. in 1997)

Open question: What is the nature of EUV waves & Interrelation with CMEs

CMEs: Early-phase and lower corona

→ joint use of EUV imagers & coronagraphs

- Several activities in regions correlated with the CME eruptions: flares, filaments, etc…
- It is logical to assume that the effects of violent processes will not remain confined in the in active region area:
  - ➔ EIT/EUV Waves (first obs. in 1997)

Open question: What is the nature of EUV waves & Interrelation with CMEs

Main interpretations [Wang 2000; Wills-Davey et al., 2007; …]:

- Pseudo-waves ⟶ "[…] EUV waves are the disk projection of the CME's expanding envelope and not a true wave phenomenon."
- Slow/Fast MHD wave ⟶ $v_{f,s}^2 = \frac{1}{2}\left(v_A^2 + c_s^2 \pm \sqrt{(v_A^2 + c_s^2)^2 - 4c_s^2 v_A^2 \cos^2\theta}\right)$ where $v_A^2 = B^2/(4\pi\rho)$
- Hybrid ⟶ A combination of both pseudo-waves and MHD wave.
- Can be interpreted as a phenomenon that starts as a **driven wave** at the flanks of the CME (due to a rapid lateral expansion of the associated CME) **and** then propagates as a **fast-mode MHD wave** (once the CME lateral expansion ceases).

Patsourakos & Vourlidas (2009); Kienreich et al. (2009)

CMEs: Early-phase and lower corona

→ joint use of EUV imagers & coronagraphs

- Several activities in regions correlated with the CME eruptions: flares, filaments, etc…
- It is logical to assume that the effects of violent processes will not remain confined in the in active region area:
  - ➔ EIT/EUV Waves (first obs. in 1997)

Open question: What is the nature of EUV waves & Interrelation with CMEs

Main interpretations [Wang 2000; Wills-Davey et al., 2007; …]:

- Pseudo-waves → "[…] EUV waves are the disk projection of the CME's expanding envelope and not a true wave phenomenon."
- Slow/ … $B^2/(4\pi\rho)$
- Hybrid → A combination of both pseudo-waves and MHD wave.
- Can be interpreted as a phenomenon that starts as a **driven wave** at the flanks of the CME (due to a rapid lateral expansion of the associated CME) **and** then propagates as a **fast-mode MHD wave** (once the CME lateral expansion ceases).

Patsourakos & Vourlidas (2009); Kienreich et al. (2009)

Last ***Living Rev. Solar Phys.*** on Coronal Waves (Warmuth, 2015) still debates on the physical nature of these perturbations going back and forth between the different scenarios.

Interrelation between CMEs and EUV waves

First Solar Orbiter close perihelion (March 2022)

2022 March 25

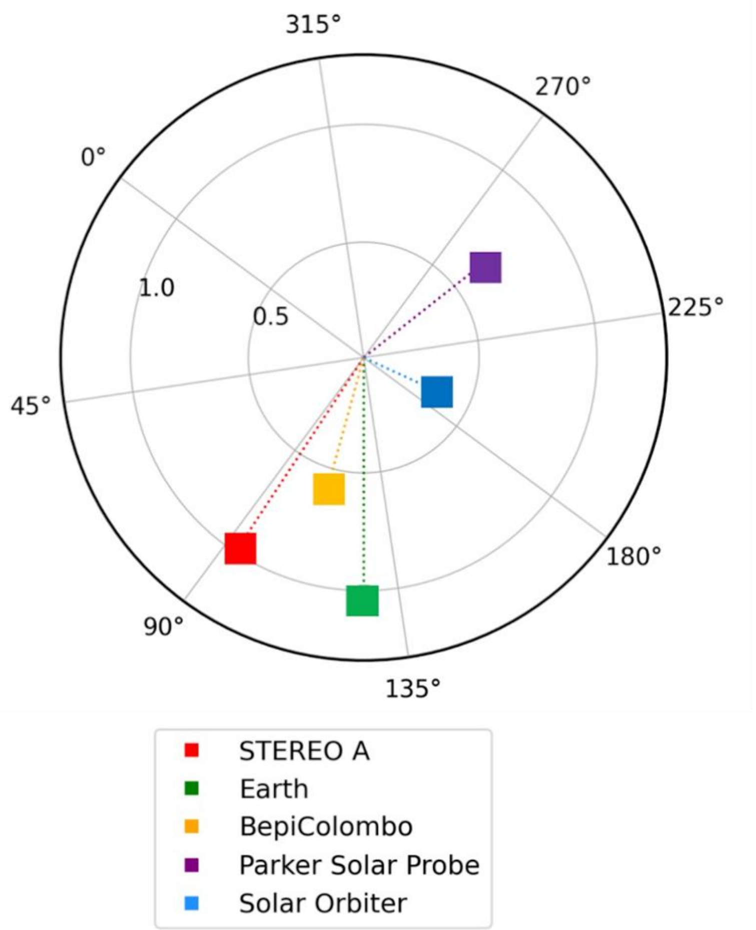

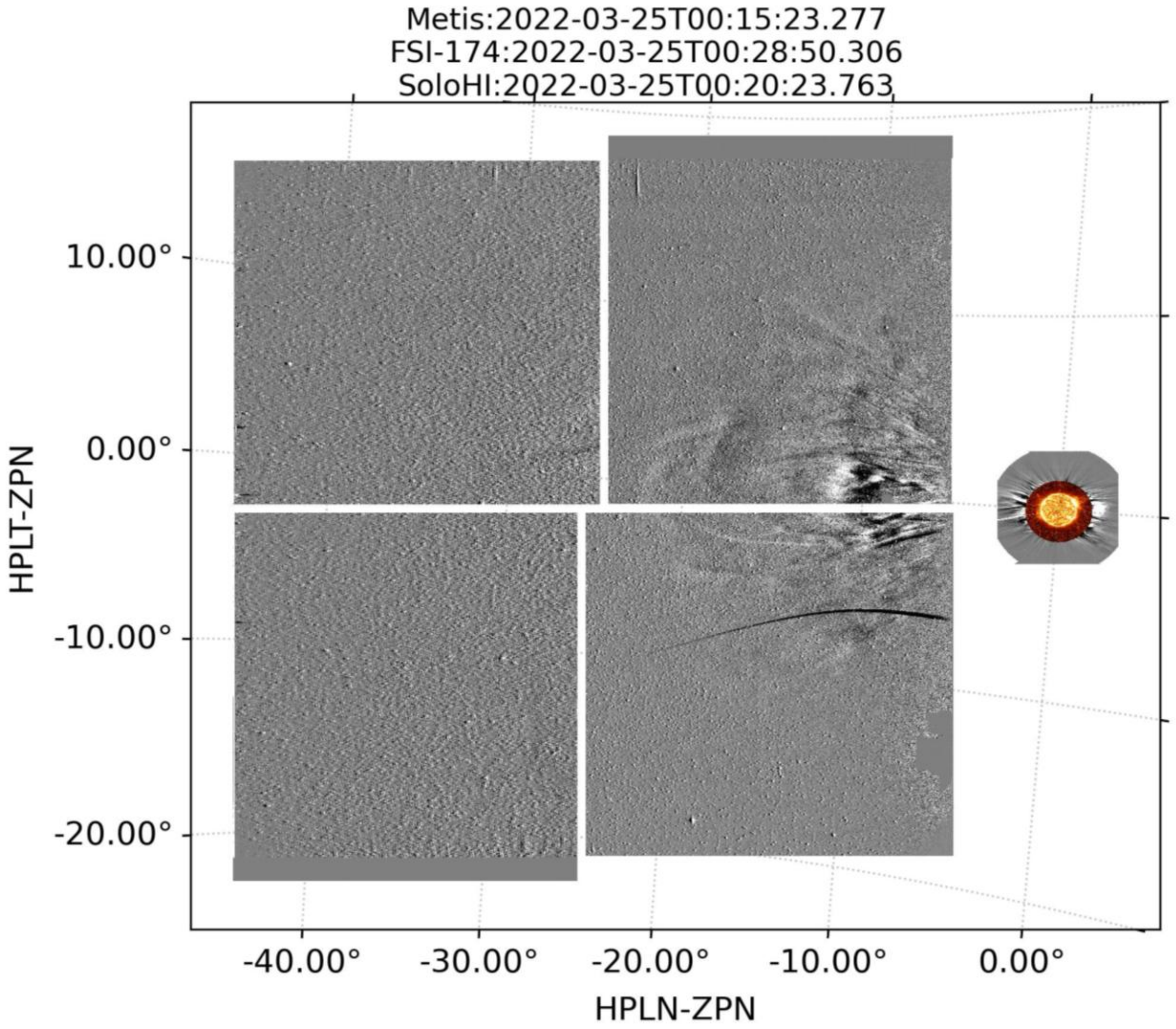

Interrelation between CMEs and EUV waves

→ EUV wave observation

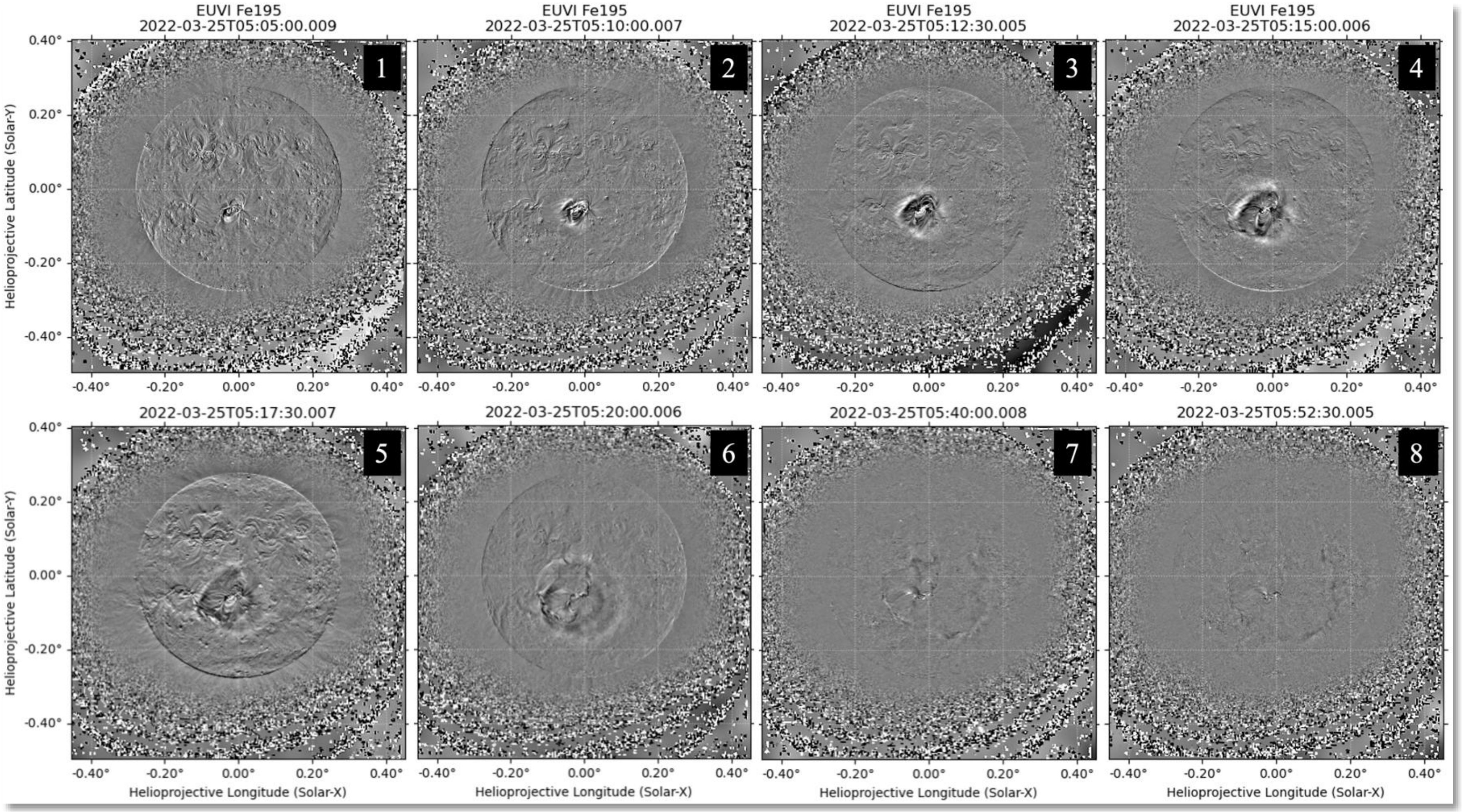

Interrelation between CMEs and EUV waves

→ EUV wave observation

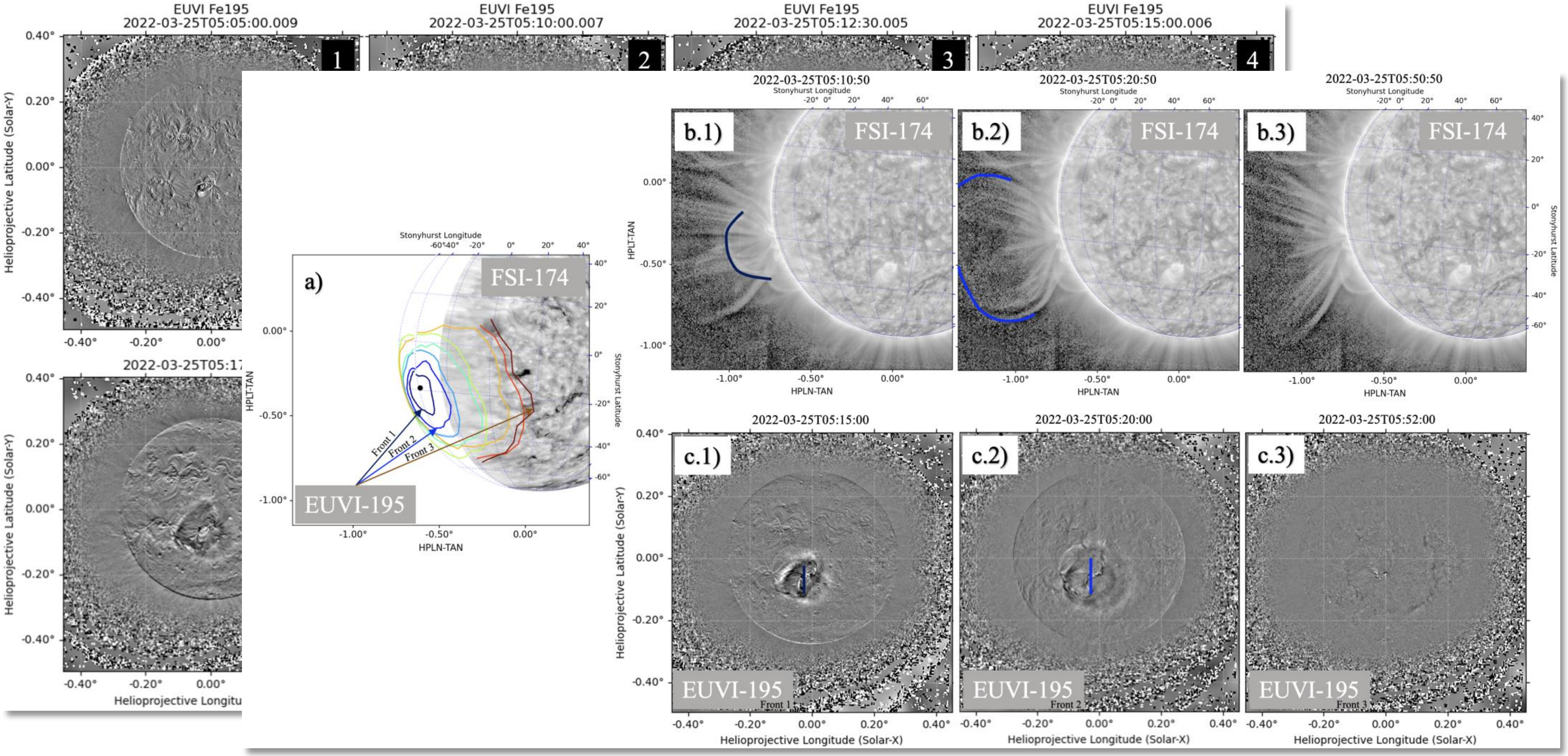

alessandro.liberatore@inaf.it

Interrelation between CMEs and EUV waves → EUV wave observation

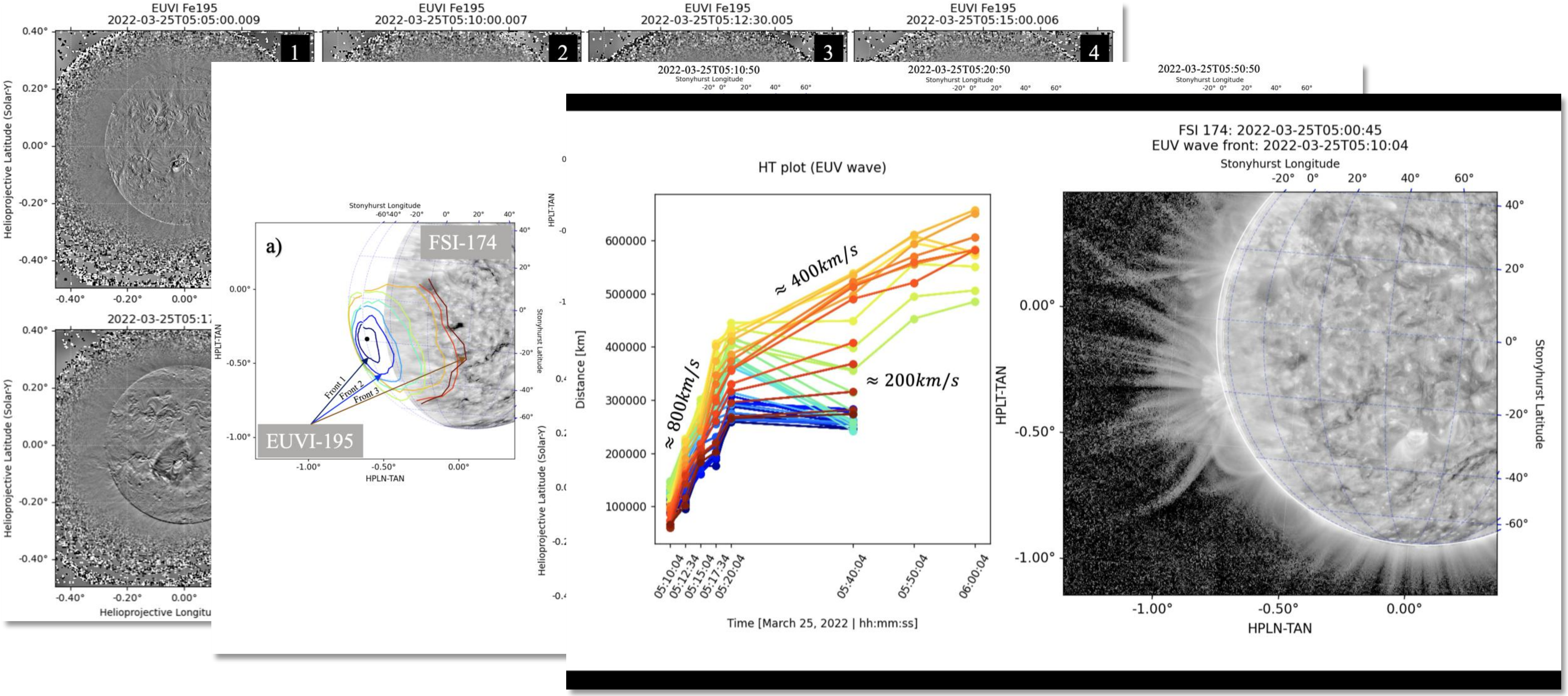

alessandro.liberatore@inaf.it

Interrelation between CMEs and EUV waves → EUV wave observation

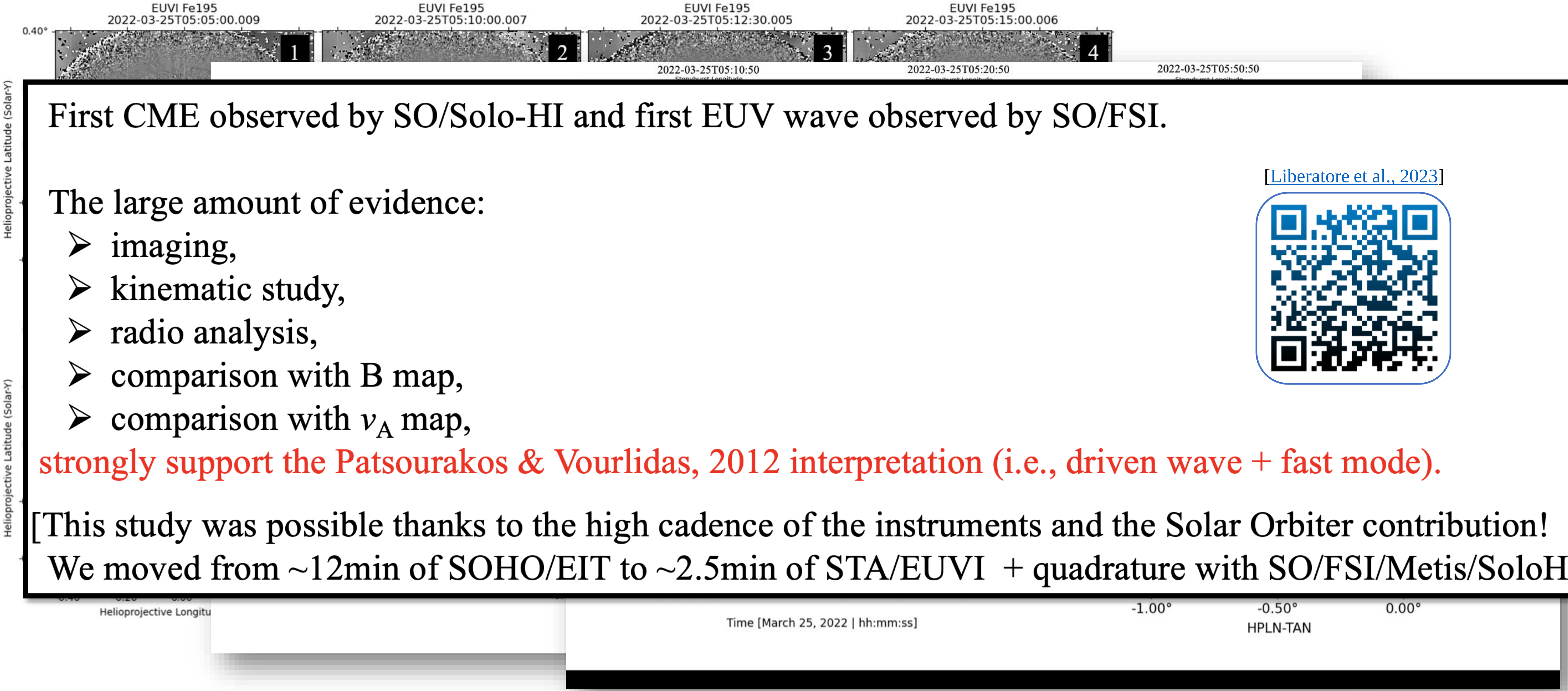

First CME observed by SO/Solo-HI and first EUV wave observed by SO/FSI.

[Liberatore et al., 2023]

The large amount of evidence:

- imaging,
- kinematic study,
- radio analysis,
- comparison with B map,
- comparison with v_A map,

strongly support the Patsourakos & Vourlidas, 2012 interpretation (i.e., driven wave + fast mode).

[This study was possible thanks to the high cadence of the instruments and the Solar Orbiter contribution! We moved from ~12min of SOHO/EIT to ~2.5min of STA/EUVI + quadrature with SO/FSI/Metis/SoloHI]

About high temporal resolution

- Are we missing something because of a too low temporal resolution?

Metis VL RD high cadence (20s)

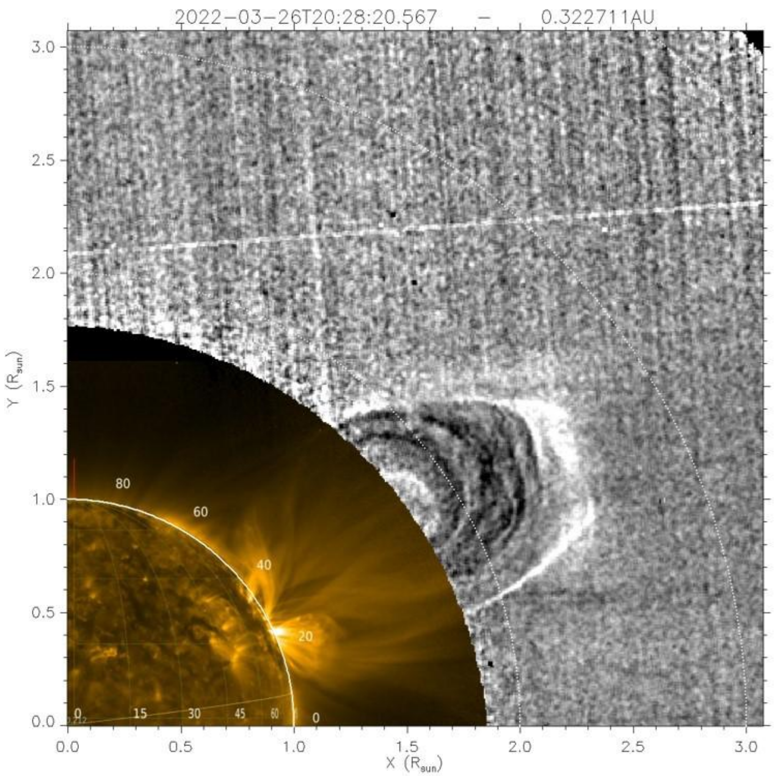

Metis VL RD regular cadence (5min)

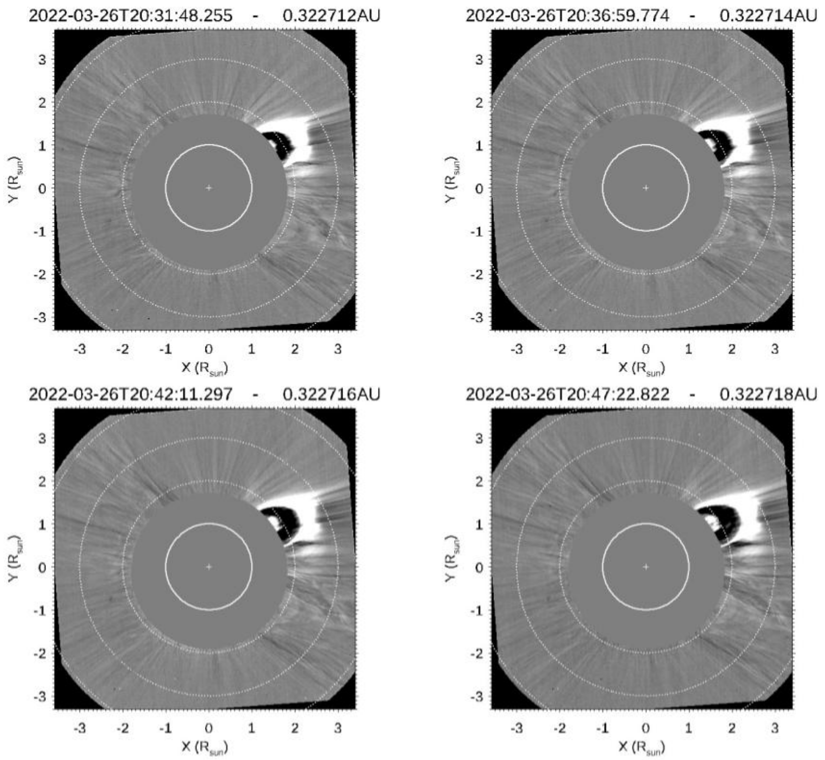

“New present” & Future

- **Additional viewpoints**
  - at different LN, LT, inside 1AU (SolO, PSP)
  - new S/C (PROBA-3? CODEX?)

- **High temporal & spatial resolution** (SolO, PSP)

- **High speed** (PSP)

- **“Observing the Sun in 4π”**
  - leaving the ecliptic plane (SolO)
  - additional viewpoints (Vigil)
  - spacecraft constellations (PUNCH)
  - …

- **Remote measure of CME magnetic fields?**

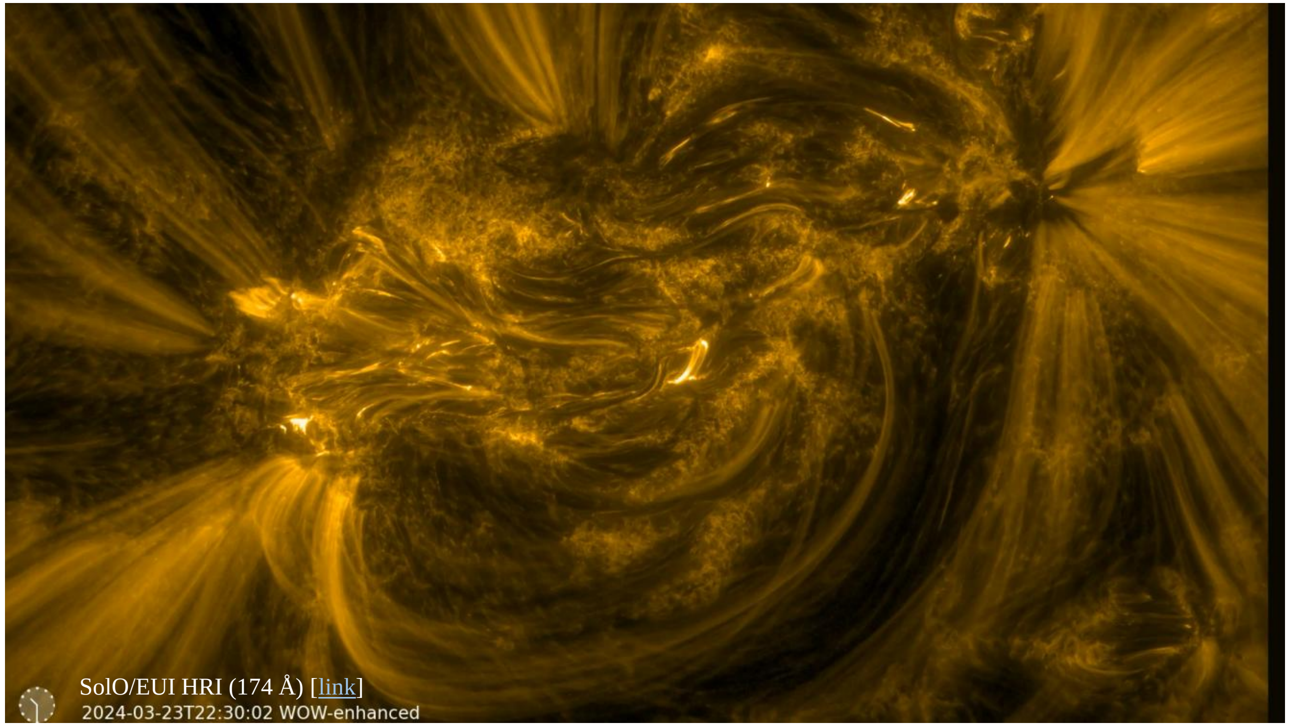

SolO/EUI HRI (174 Å) [link]

CORHI Explorer

Investigating Heliospheric Events Through Multiple Observation Angles and Heliocentric Distances

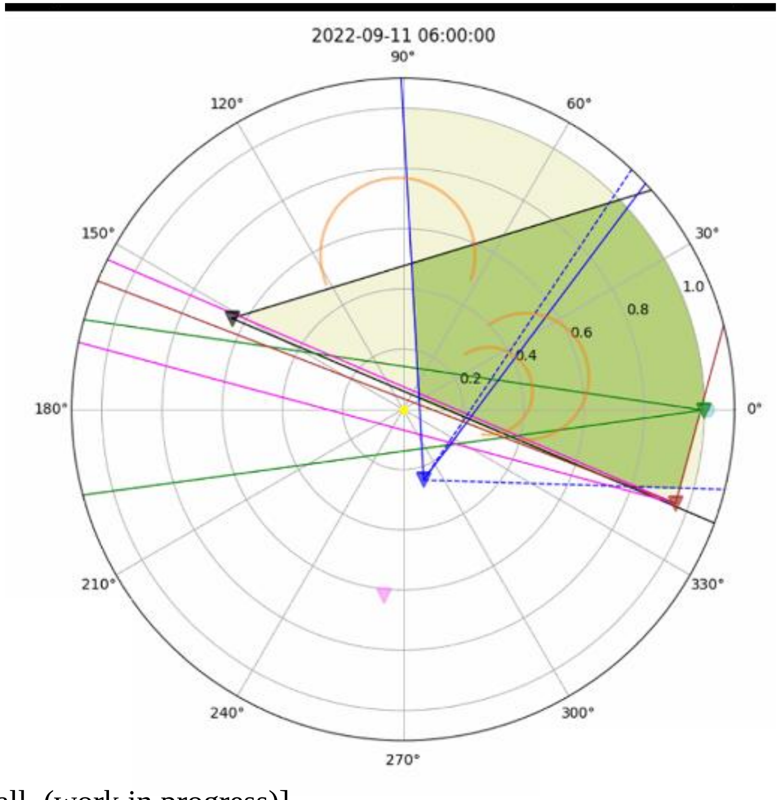

[G. Cappello et all. (work in progress)]

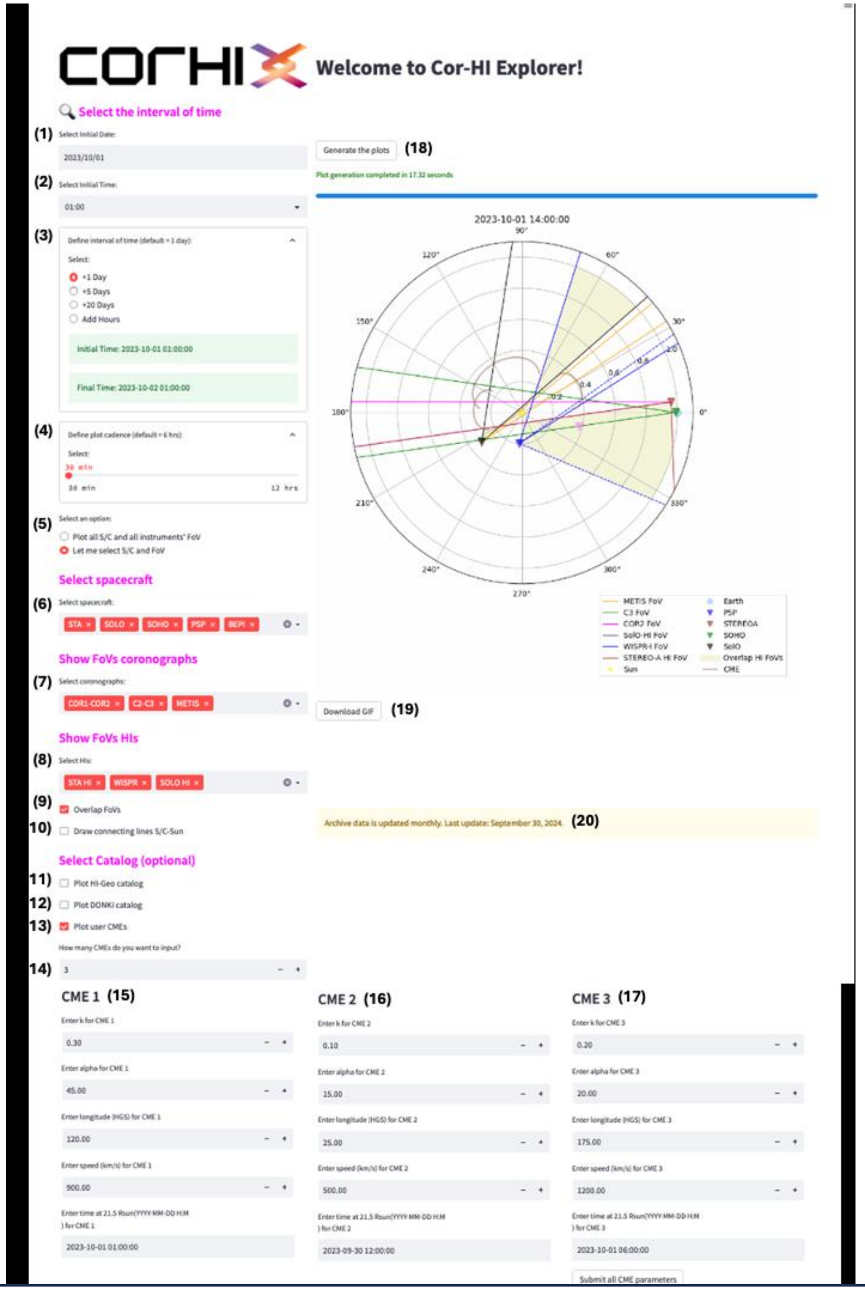

Backup Slides

Polarization in the solar corona

K-corona → Thomson scattering → *linear* polarization → Stokes formalism

$$\begin{cases} I = P_0 + P_{90} \\ Q = P_0 - P_{90} \\ U = P_{45} - P_{135} \\ V = P_{RHC} - P_{LHC} \end{cases}$$

$$pB = \sqrt{Q^2 + U^2}$$

$$I^2 \geq Q^2 + U^2 + V^2$$

$$DoLP = \frac{\sqrt{Q^2 + U^2}}{I}$$

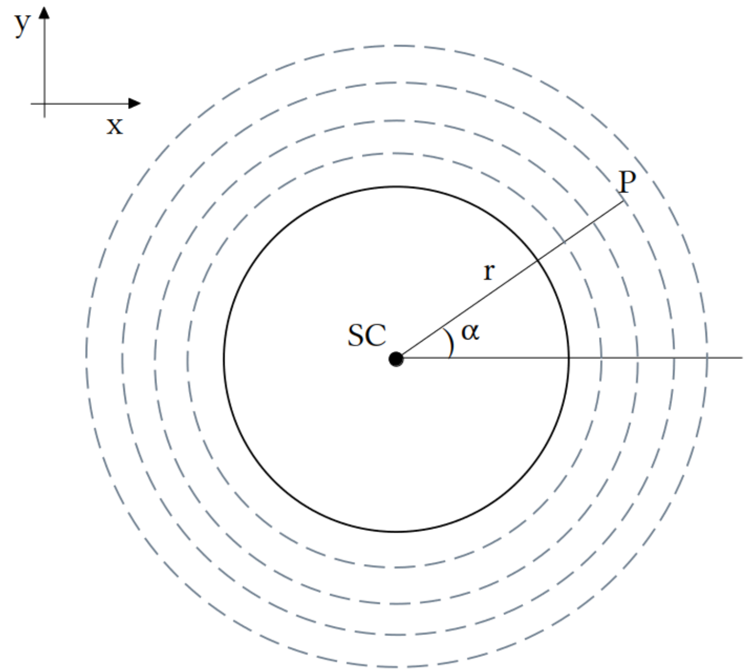

Polarization tangent to the solar limb

CSHKP two-ribbon flare model

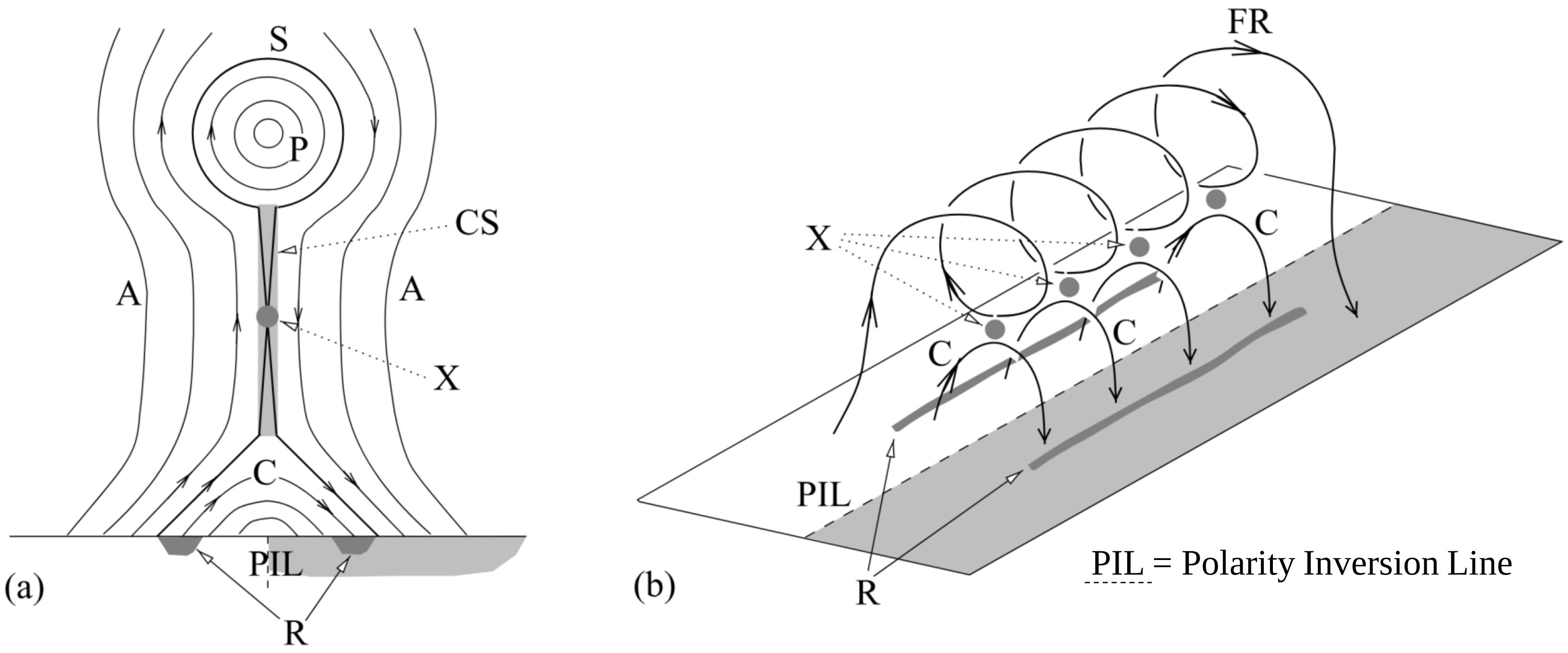

PIL = Polarity Inversion Line

Figure 1 Basic elements of the CSHKP two-ribbon flare model in two (a) and three (b) dimensions. Open field lines (A) are separated by a current sheet (CS). They reconnect at a magnetic X-point (X) to create closed field lines (C) and a plasmoid (P). The energy released by reconnection creates chromospheric flare ribbons (R) on either side of the PIL, just inside the separatrix (S). In the three-dimensional version (b) reconnection occurs at several sites (X) to create closed field lines (C) and a twisted flux rope (FR) instead of the plasmoid.

[Longcope et al., 2007]

Different stages of CME evolution

Based on "the standard CME-flare model" and "the standard magnetic cloud model"

- CMEs are driven by the free magnetic energy stored in the non-potential magnetic fields.
- The erupted structure is twisted, where the most common magnetic structure employed in modeling is a flux rope (i.e., a cylindrical plasma structure with a magnetic field draped around the central axis).
- The eruption of the twisted magnetic structure is interrelated with the magnetic reconnection of the surrounding coronal magnetic field, releasing both thermal and non-thermal energy and producing a number of effects.
- The magnetic dips of the flux rope can support cool plasma, in which case also an eruptive filament can be observed.
- In "the standard magnetic cloud model" the erupting flux rope propagates away from the Sun, expanding at the same time, but stays attached to the Sun, i.e., remains a closed structure.

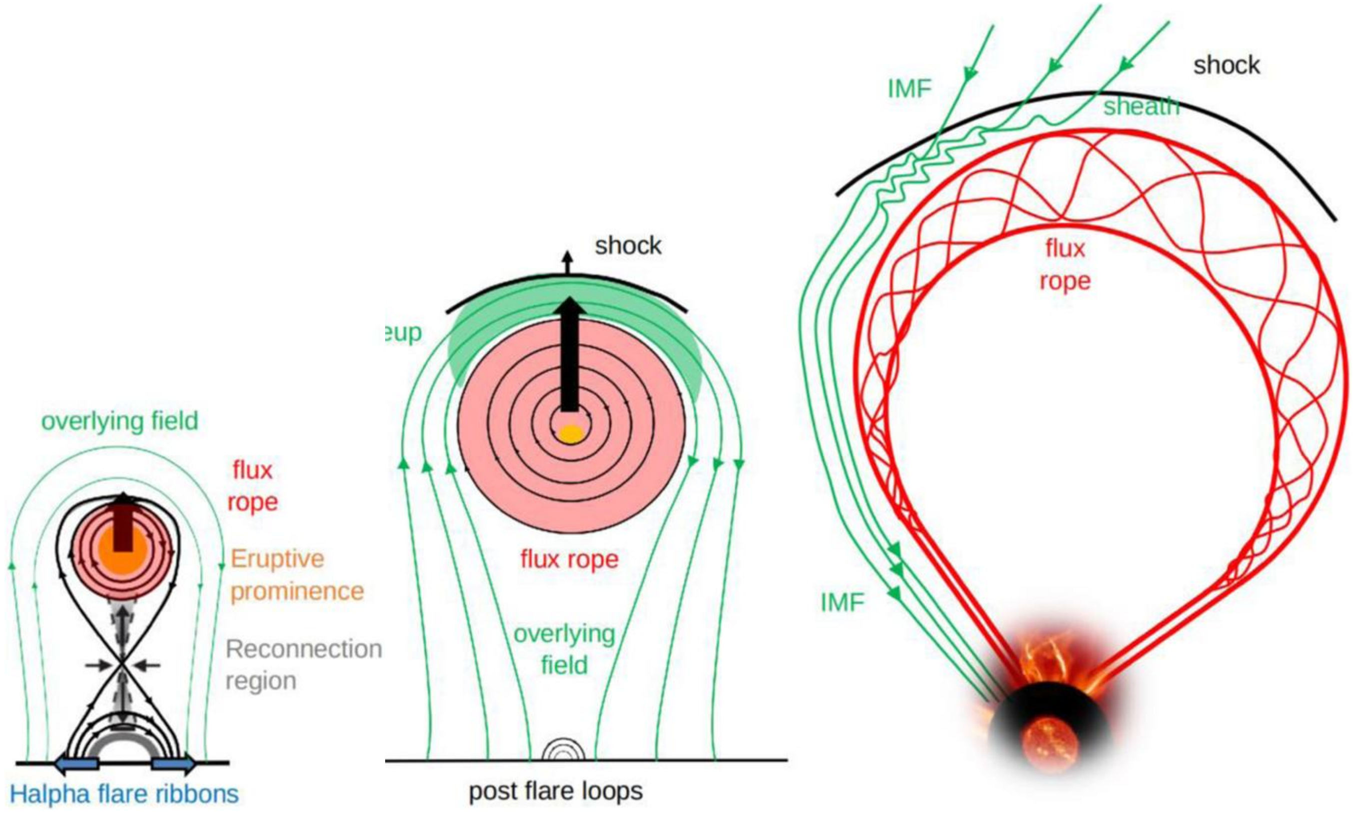

1) onset **2) post-eruption phase** **3) interplanetary propagation**

[Zhang et al., 2021]

Lower atmospheric signatures

Filament eruptions

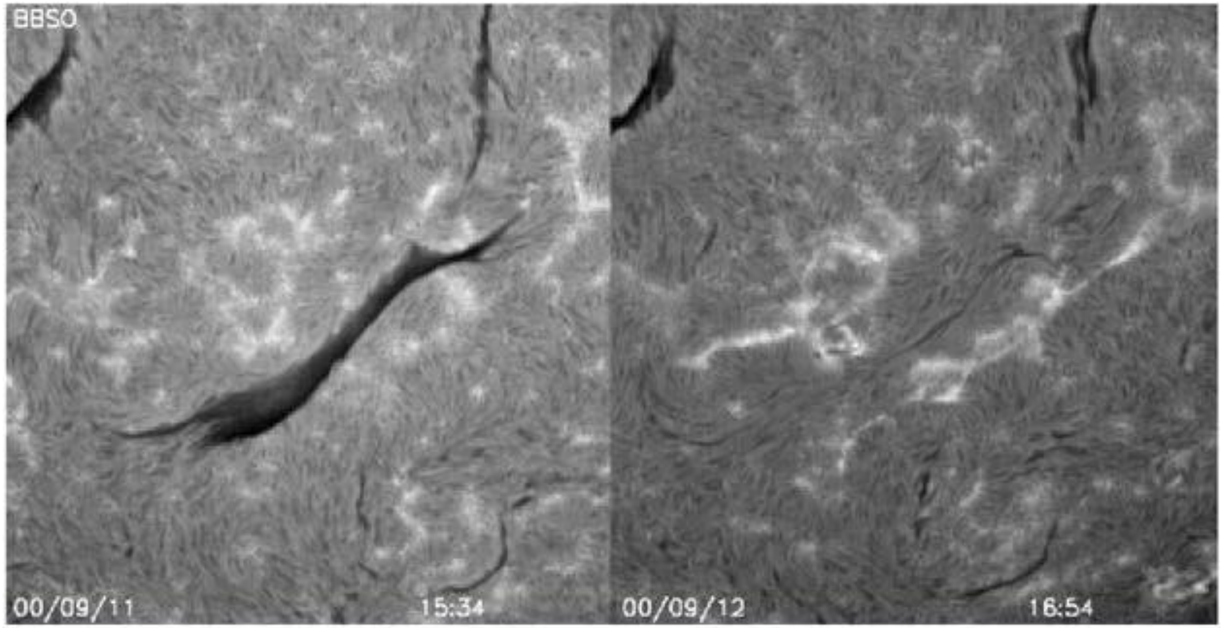

- Hα filament disappears (erupts)
- Two-ribbon flare structure forms after the disappearance

Flares

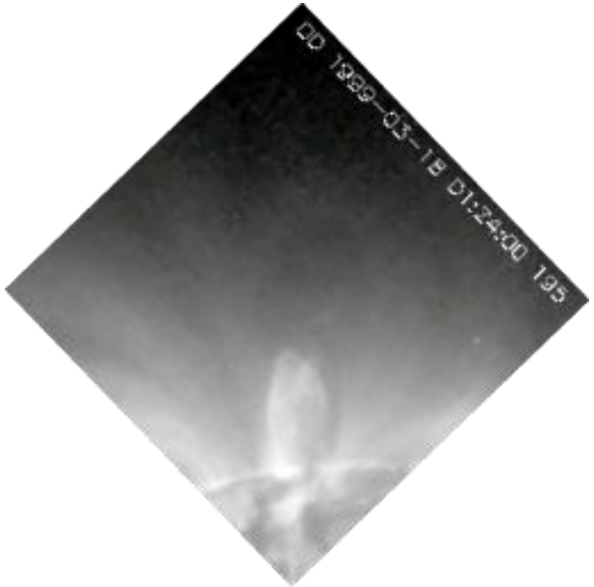

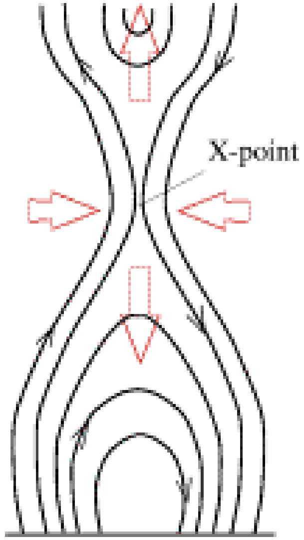

- Magnetic reconnection
- Reconfiguration of coronal field ⇒ liberates stored B energy

Flare loops

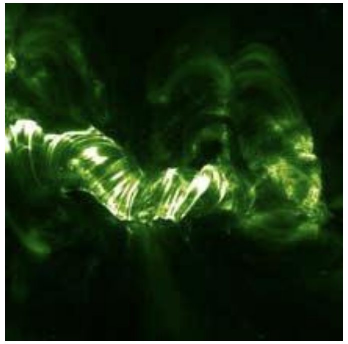

etc…

[Adapted from Lucie Green UCL presentation, 2017]

CME Analysis Tools

- CMEs are highly dynamic events. To analyze them, we need their time-series → movies.

- Most common analysis tasks:
  - Height-time plots (HT-plots) → velocity, acceleration
  - Size & position measurements
  - Mass/energetics → mass, density, kinetic/potential energy
    (pre-event image is subtracted, sum over appropriate features, …)

- Analysis software available in SolarSoft & SunPy.

- Graduated Cylindrical Shell model (GCS), Drag Based Model (DBM), MHD model (e.g., WSA-Enlil).

JHelioviewer

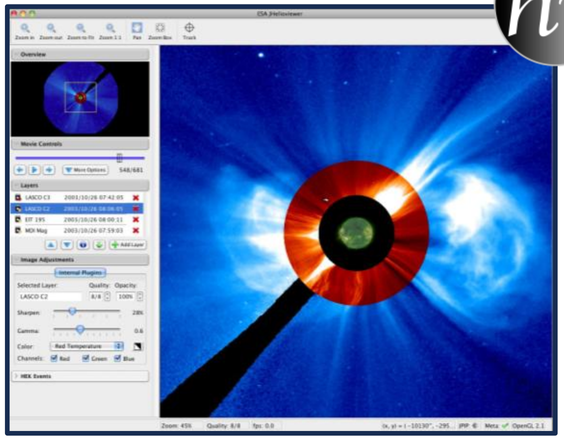

[link]

sunpy

IDL

CME Analysis Tools

GCS [Thernisien 2011]

Geometry: conical legs and a pseudo-circular front (that expands in a self-similar way)

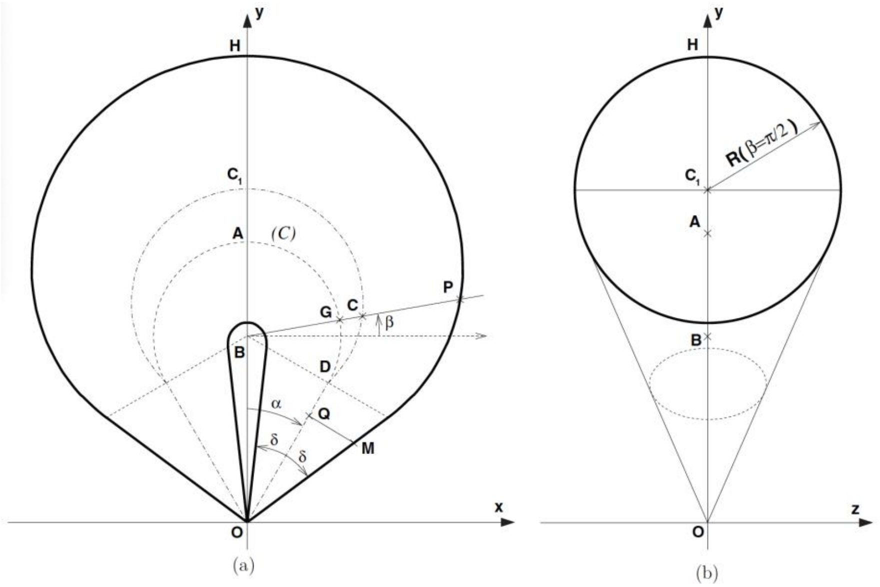

DBM [Vršnak et al., 2011]

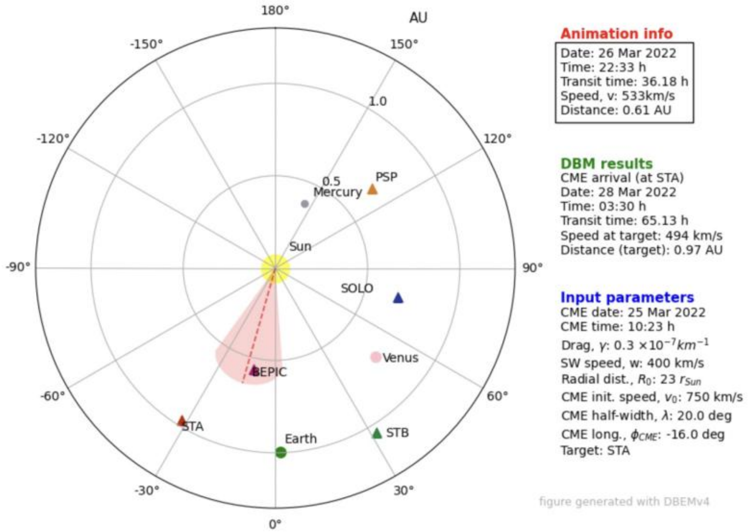

$$a = -\gamma\,(v - w)\,|v - w|$$

Drag parameter: $\gamma = C_d \dfrac{A\,\rho_{SW}}{M}$

WSA-Enlil [Parsons et al., 2011]

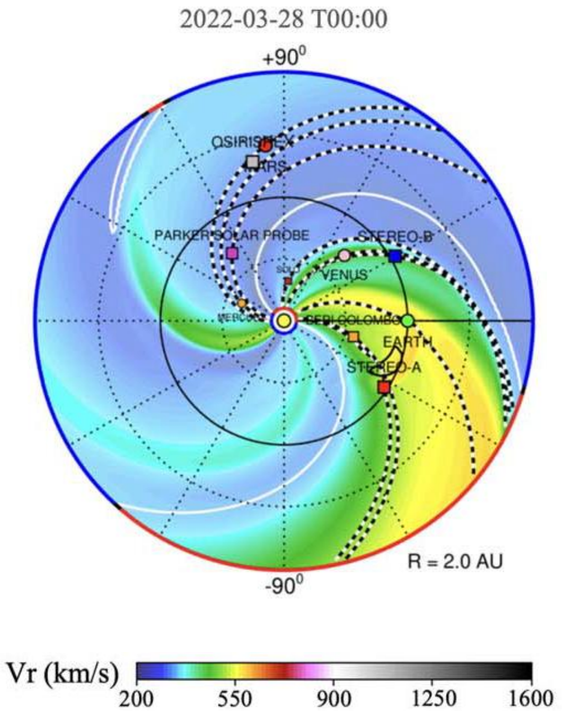

alessandro.liberatore@inaf.it

Interrelation between CMEs and EUV waves → Solar Orbiter and STEREO-A synergy

2022 March 25

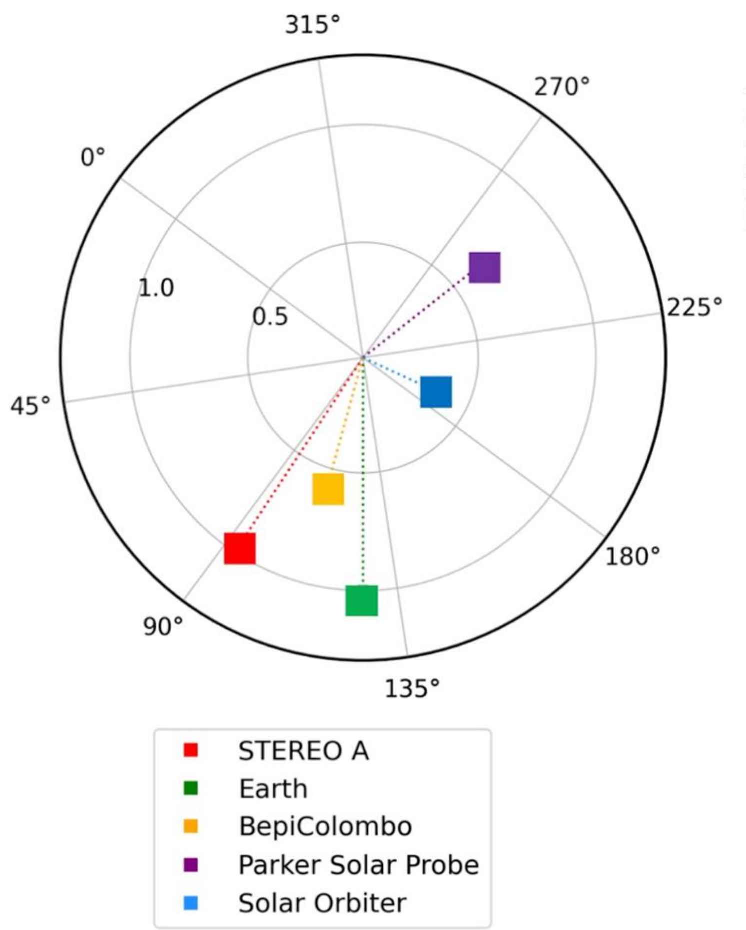

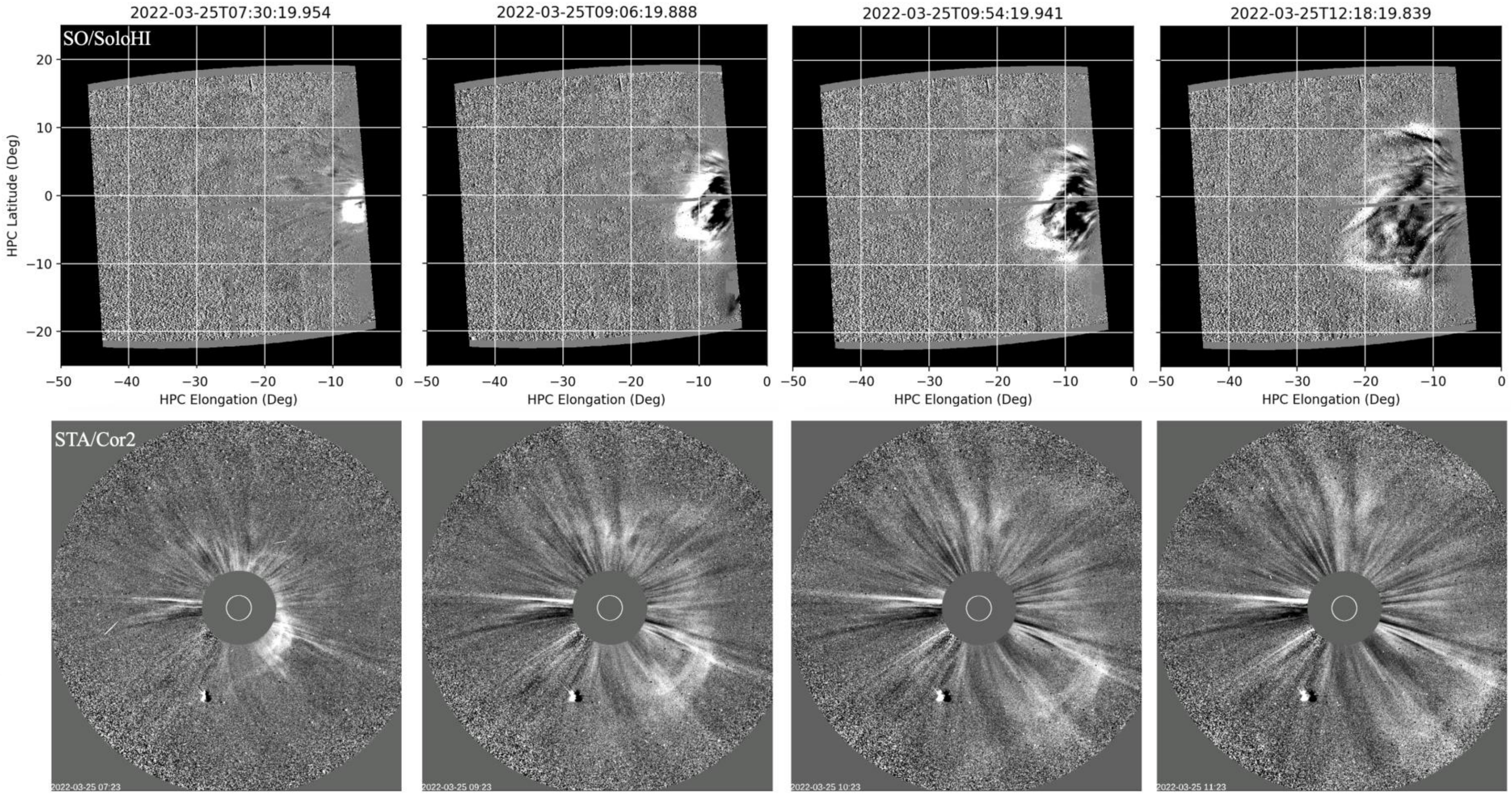

Interrelation between CMEs and EUV waves

→ STA/EUVI-195 & SolO/FSI-174

…and analysis

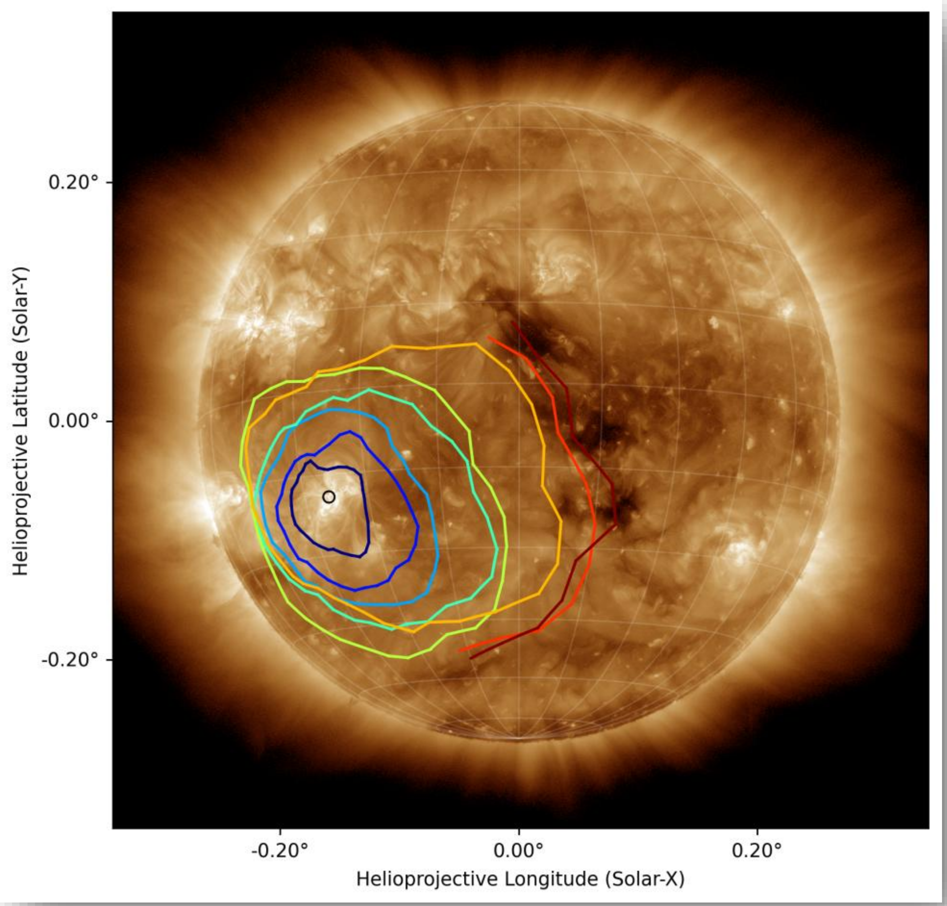

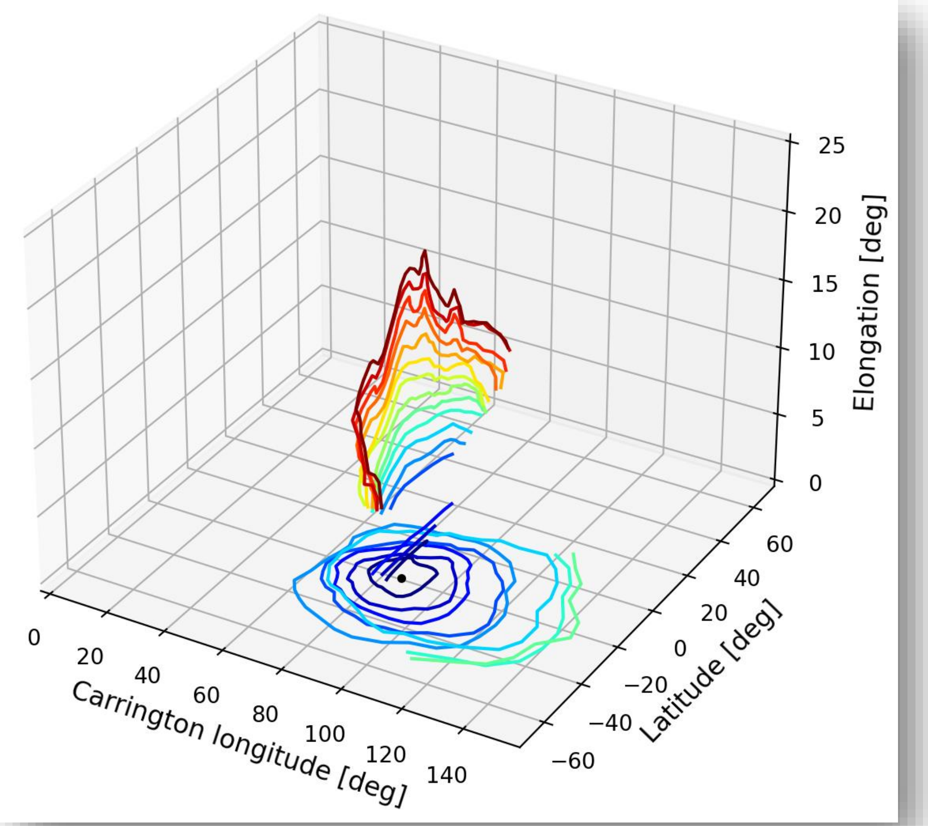

EUV waves 101

-Frequency of occurrence-

→ EUV waves *vs* Hα *vs* CME occurence (Warmuth et al., 2001)

Solar Max

EUV waves: 100/year

Type II: consistent

Solar Min

EUV waves: ~30/year

Type II: consistent

Hα waves:

- Smith and Harvey (1971):
  15 Moreton waves in 8 years (1960 – 1967)
  Considering ground-based solar observation ⟶ 7/year
- Warmuth et al., 2004a: ~ 3-4/year (1997 – 2001)
- Warmuth (2010): 4/year (1997 – 2006)
- Zhang et al. (2011): ~ 7/year (1997 – 2006)

Moreton waves occur at a rate of only ≈ 5% the rate of than coronal EUV waves

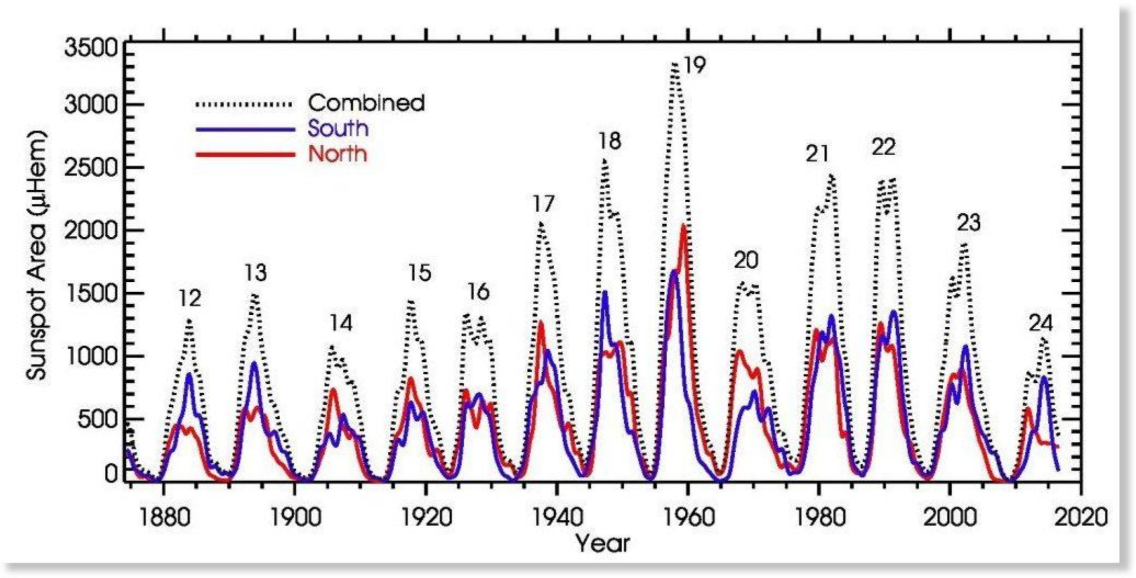

CME: ~180 per year in solar minimum up to ~1500 in solar max (Yashiro et al., 2004) ≈ 6-7% occurrence (?)

Highly detailed observations

From EUI to Metis

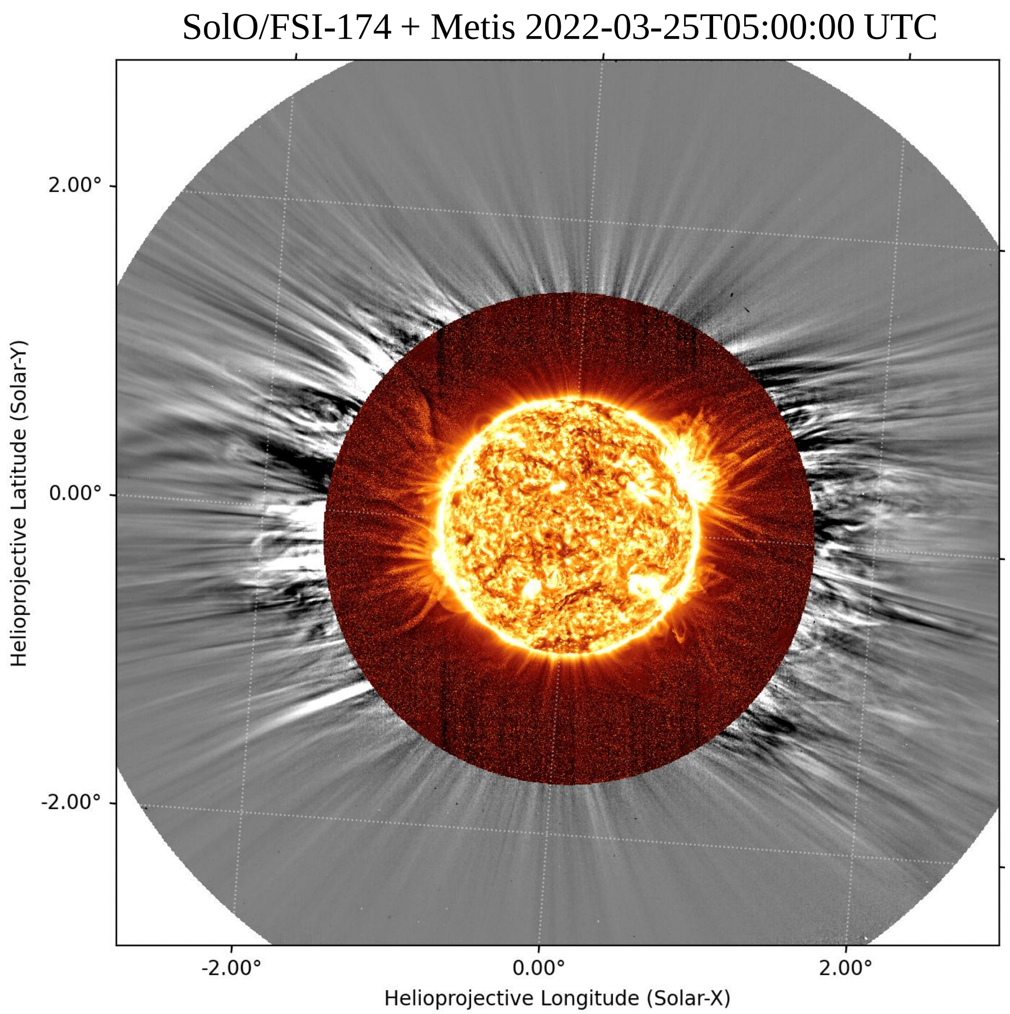

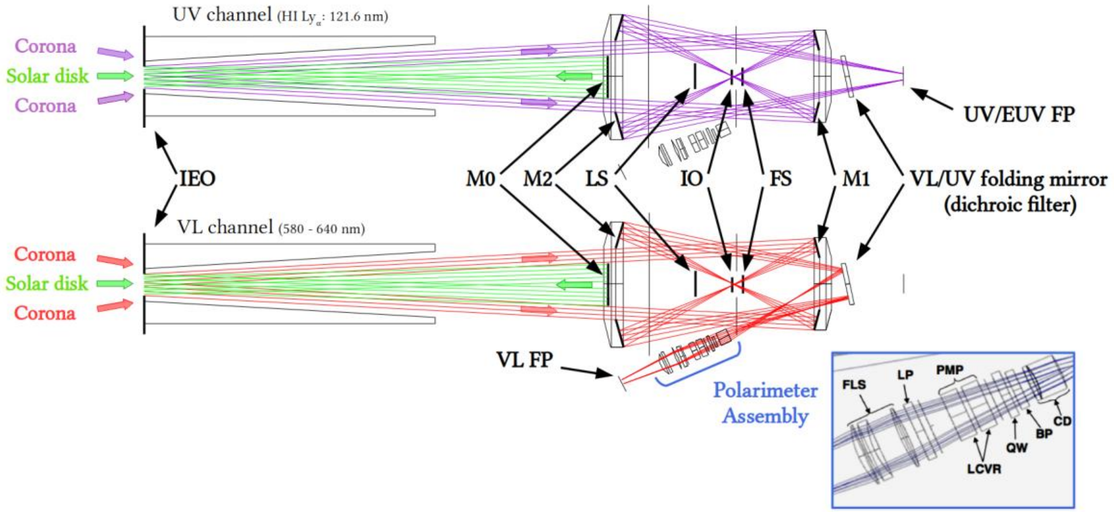

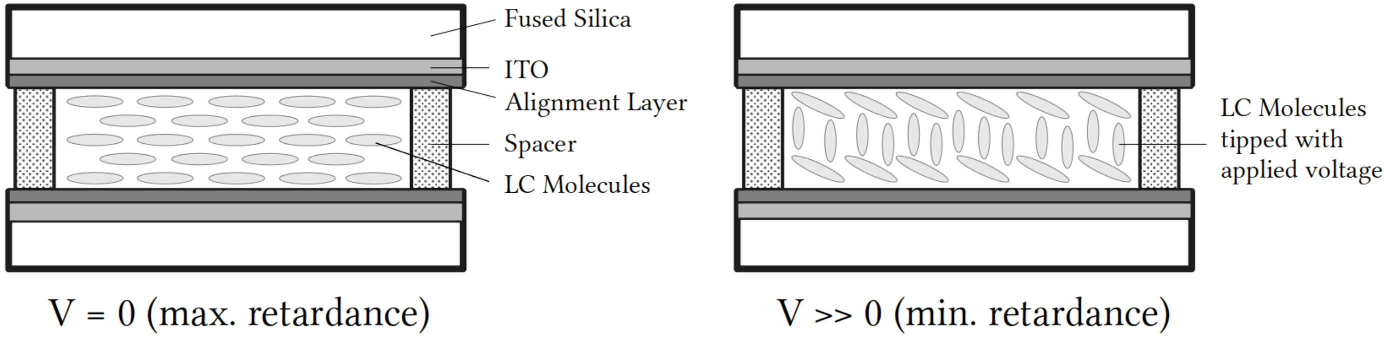

LCVR highest cadence: 1sec + process time (seconds)
- tB every 20sec
- pB every 1min

Metis polarimeter Müller matrix

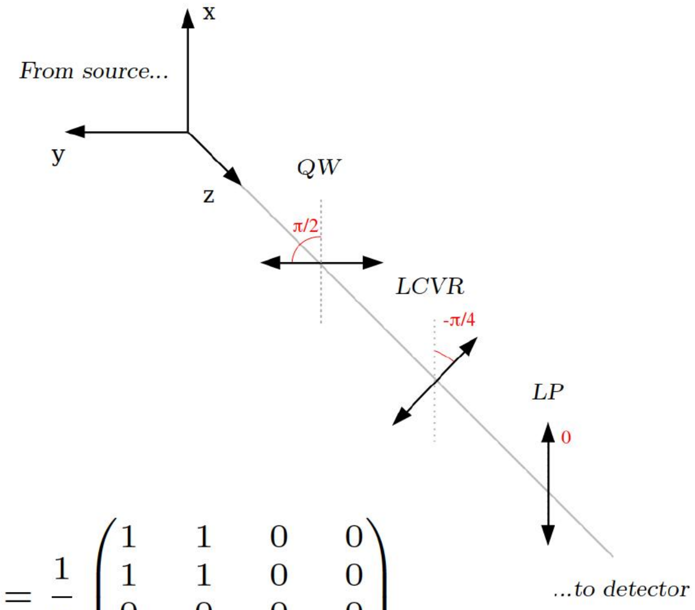

$$M_{POL} = M_{LP} M_{LCVR} M_{QW}$$

$$= \frac{1}{2} \begin{pmatrix} 1 & \cos\delta & \sin\delta & 0 \\ 1 & \cos\delta & \sin\delta & 0 \\ 0 & 0 & 0 & 0 \\ 0 & 0 & 0 & 0 \end{pmatrix}$$

$$\equiv M_{LP} M_{rot}(2\theta = \delta)$$

$$M_{\mathrm{LP}}(0) = \frac{1}{2} \begin{pmatrix} 1 & 1 & 0 & 0 \\ 1 & 1 & 0 & 0 \\ 0 & 0 & 0 & 0 \\ 0 & 0 & 0 & 0 \end{pmatrix}$$

$$M_{\mathrm{LCVR}}(-\frac{\pi}{4}, \delta) = \begin{pmatrix} 1 & 0 & 0 & 0 \\ 0 & \cos\delta & 0 & -\sin\delta \\ 0 & 0 & 1 & 0 \\ 0 & \sin\delta & 0 & \cos\delta \end{pmatrix}$$

Frame rotation:

$$M_{\mathrm{rot}} = \begin{pmatrix} 1 & 0 & 0 & 0 \\ 0 & \cos 2\theta & \sin 2\theta & 0 \\ 0 & -\sin 2\theta & \cos 2\theta & 0 \\ 0 & 0 & 0 & 1 \end{pmatrix}$$

$$M_{\mathrm{QW}}(\frac{\pi}{2}) = \begin{pmatrix} 1 & 0 & 0 & 0 \\ 0 & 1 & 0 & 0 \\ 0 & 0 & 0 & 1 \\ 0 & 0 & -1 & 0 \end{pmatrix}$$

Metis UV detector

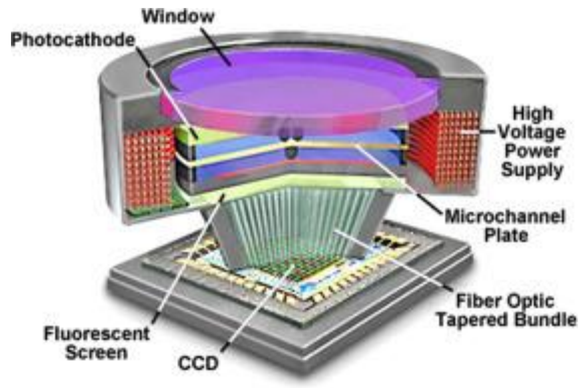

→

UV Micro-channel plate

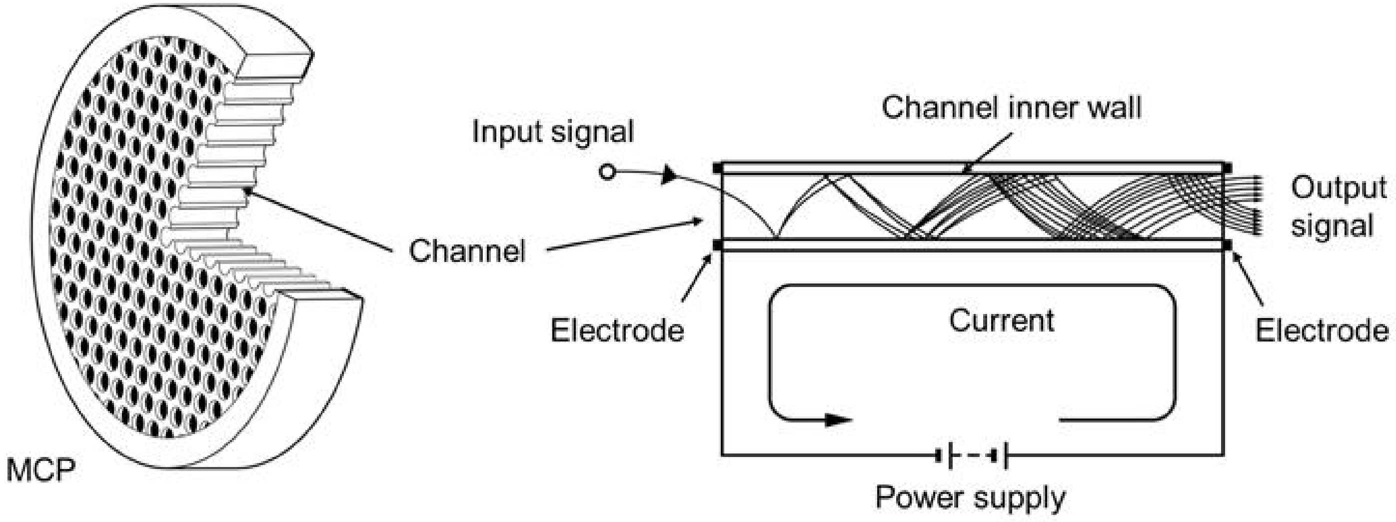

Metis FoV

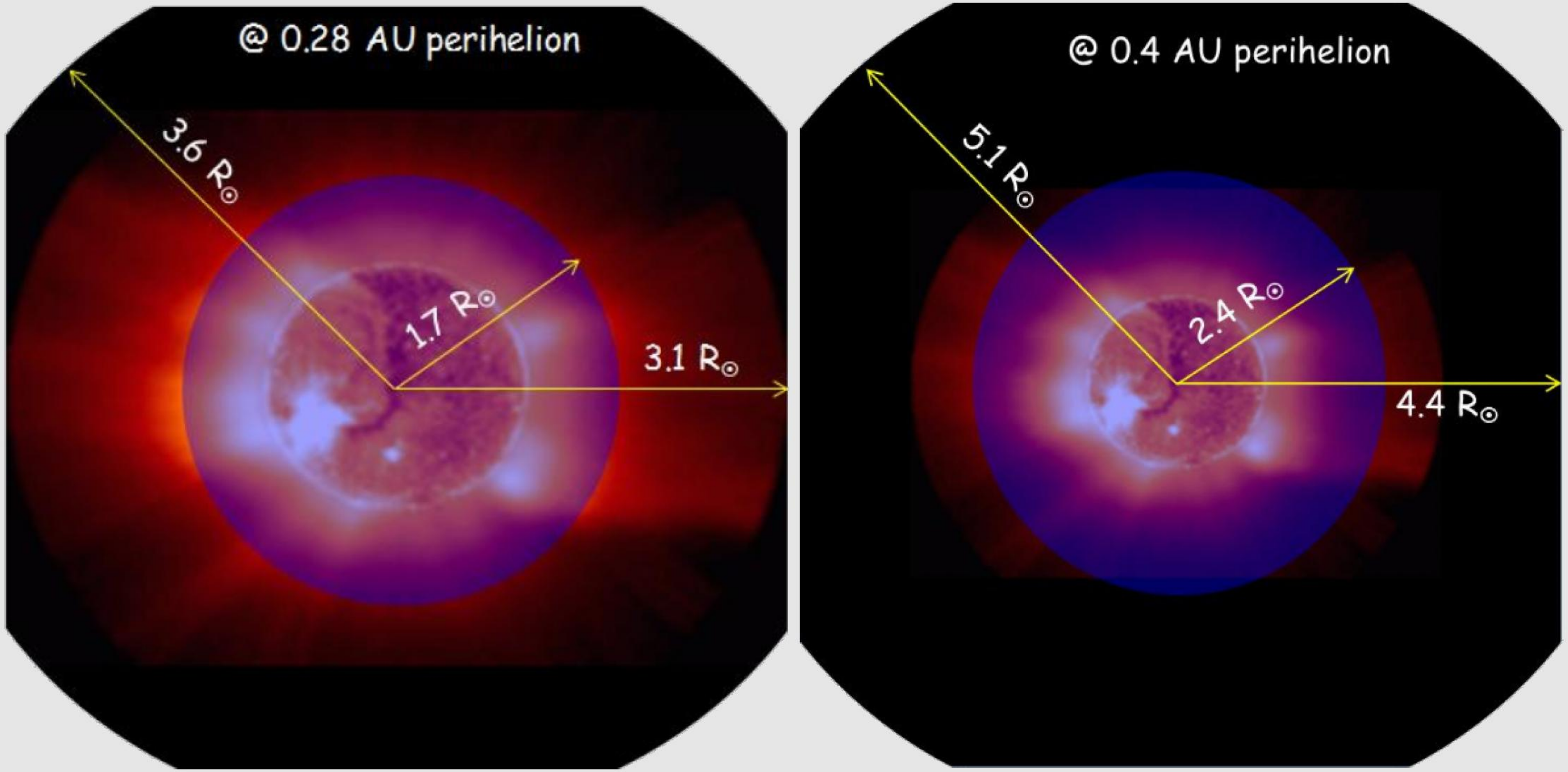

Zoom effect in the field of view due to the orbit eccentricity.

EUI-HRI

Table 2. Optical design parameters of the HRI_{EUV} and HRI_{Lya} channels.

	HRI_{EUV}	HRI_{Lya}
Focal length	4187 mm	5804 mm
Entrance pupil	47.4 mm	30 mm
Field of view	1000 $arcsec^2$	1000 $arcsec^2$
Plate scale	50 arcsec mm^{-1}	31.5 arcsec mm^{-1}
Detector	2048 × 2048, 10 μm pixels	2048 × 2048, 14.1 μm virtual pixel size
Primary mirror (M1)	66 mm ⌀ (54 mm useful) 80 mm off-axis RC = 1518.067 mm CC = −1	42 mm ⌀ (38 mm useful), 80 mm off-axis RC = 1143 mm CC = −1
Secondary mirror (M2)	25 mm ⌀ (12 mm useful), 11.44 mm off-axis RC = 256.774 mm CC = −2.04	20 mm ⌀ (18 mm useful), 7 mm off-axis RC = 91 mm CC = −0.65

SolO/EUI:

EUI FSI 174 Å
EUI FSI 304 Å
EUI HRI 174 Å
EUI HRI 1216 Å

[Rochus et al., 2020]

WISPR

Table 3 WISPR instrument characteristics

Telescope Type	Wide-angle lenses, aperture stop placed in front of lens: Inner: $f = 28$ mm, aperture $= 42$ mm^2, 490–740 nm (bandpass) Outer: $f = 19.8$ mm, aperture $= 51$ mm^2, 475–725 nm (bandpass)
Plate Scale	1.2–1.7 arcmin/pixel (inner-outer)
FOV	95° radial × 58° transverse, inner field limit 13.5° from Sun center
Image Quality	Predicted RMS spot including allowable tolerances at 20° from boresight: Inner: 19.5 microns (2.34 arcmin) Outer: 19.9 microns (3.38 arcmin)
Detector	APS, 10 micron pitch, 2048 × 1920 pixels

Table 1 Comparison of WISPR capabilities to other coronagraphs and imagers

Telescope	Heliocentric Distance (AU)	FOV (R_S, AU_{eq})	Spatial Resolution (arcsec AU_{eq})	Cadence (min)
WISPR	0.25	9.5–83	94	60
	0.1	4.0–41	26	7
	0.044	2.2–20	17	0.05
SoloHI	0.28	5.1–47	25	5
LASCO/C2	1	2.2–6	24	24
SECCHI/COR2	1	2.5–15	30	15
SECCHI/HI1	1	15–90	108	40
SECCHI/HI2	1	74–337	250	120
SMEI	1	74–>337	1440	102

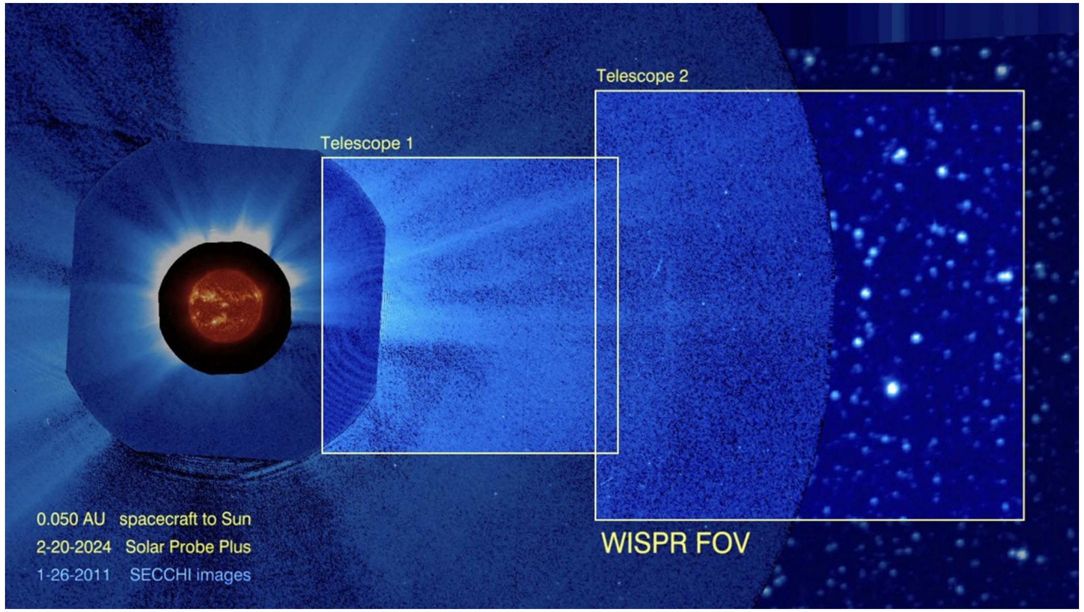

PSP will be a unique mission designed to orbit as close as 7 million km (9.86 solar radii) from Sun center.

- WISPR employs a 95° radial by 58° transverse field of view to image the fine-scale structure of the solar corona.

[Vourlidas et al., 2016]

SoloHI

Table 1. SoloHI instrument parameters.

Parameter	Value (M)easured (C)alculated
SIM mass	15.18 kg (M)
SPS mass	1.38 kg (M)
Volume	66.0 X_{SIM} × 40.5 Z_{SIM} × 29.1 Y_{SIM} (M) (Door Closed) × 50.8 Y_{SIM} (M) (Door Open)
Power	13.5 (w) (average)
Telemetry	53.2 Gbits/Orbit
FOV	40° × 40° square limited to 48° at the detector corners
Image array	3968 × 3968 Pixels (M); Note: Left 10 columns and bottom 10 rows of each die are opaque
Boresight direction	Nominal: 25° from Sun centre Measured: 25° 7′26.3″
Angular range	5°–45° from Sun centre 5.25 $R_\odot$–47.25 $R_\odot$ at 0.28 AU
Angular resolution	36.7 arcsec (Full) 73.5 arcsec (2 × 2 bin); 10.3 arcsec (Full) 20.6 arcsec (2 × 2 bin) equivalent at 0.28 AU
Spectral bandpass	500–850 nm (M)
Exposure time per image	Nominal 30 s (C); Range 0.1–65 s (M)
Number of summed images	Varies from 1–30 (C) depending on observing program, heliocentric distance

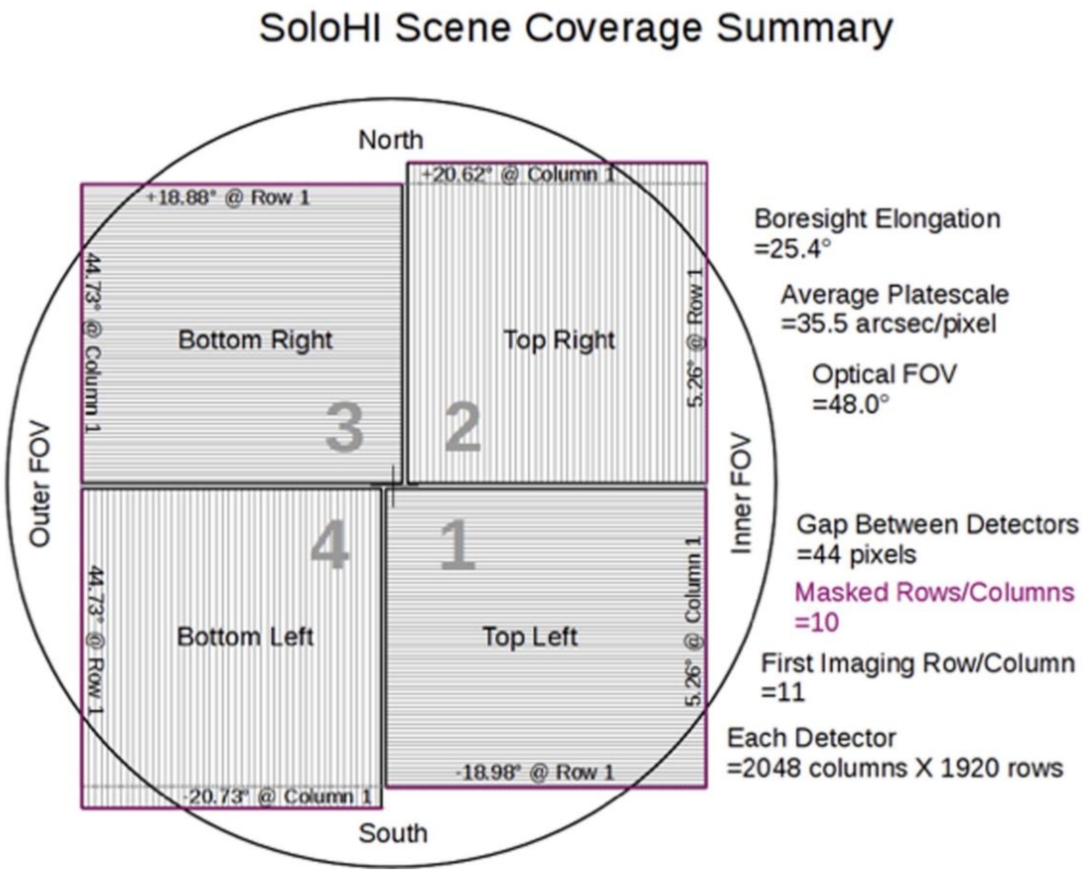

[Howard et al., 2020]

Outflows

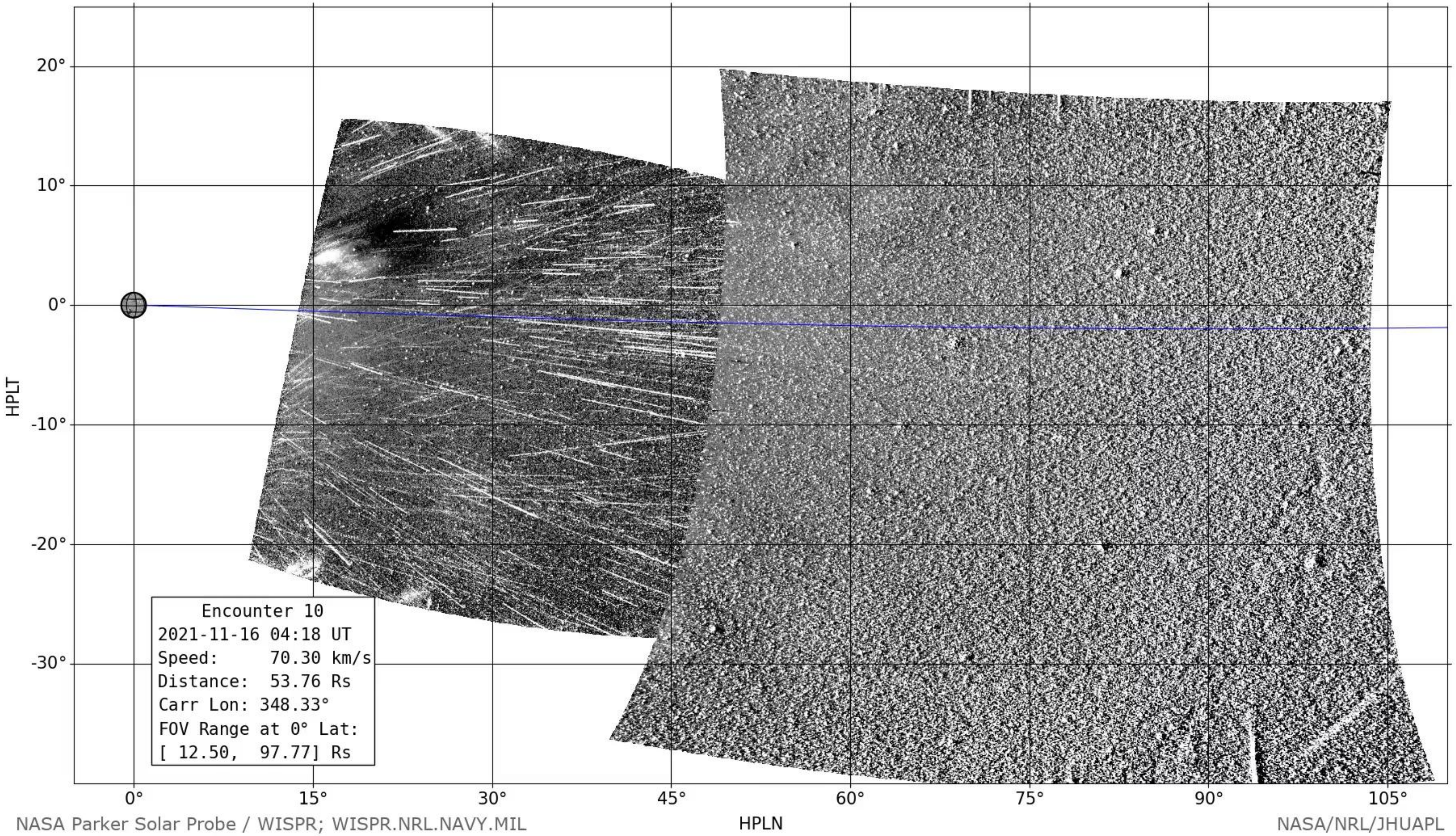

C.Braga, COSPAR 2024

CME/CME interaction – PSP and SolO heliospheric imagers

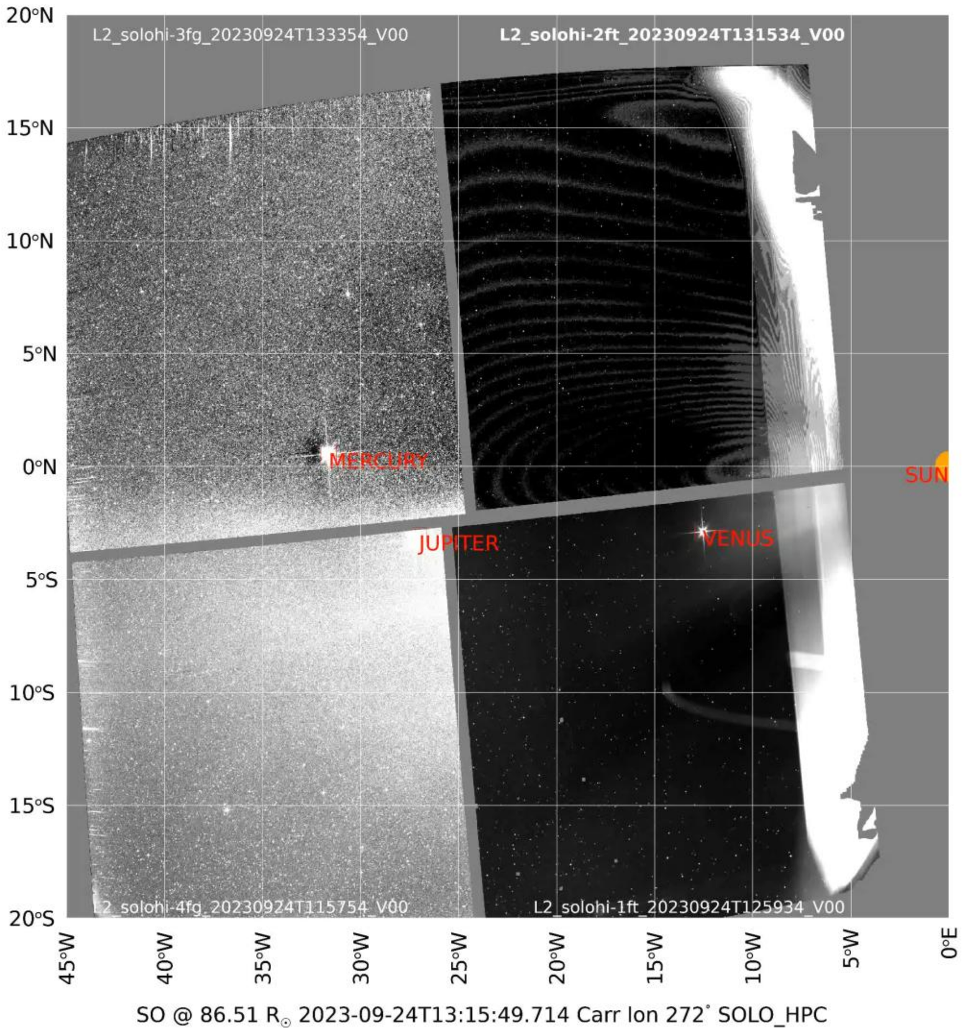

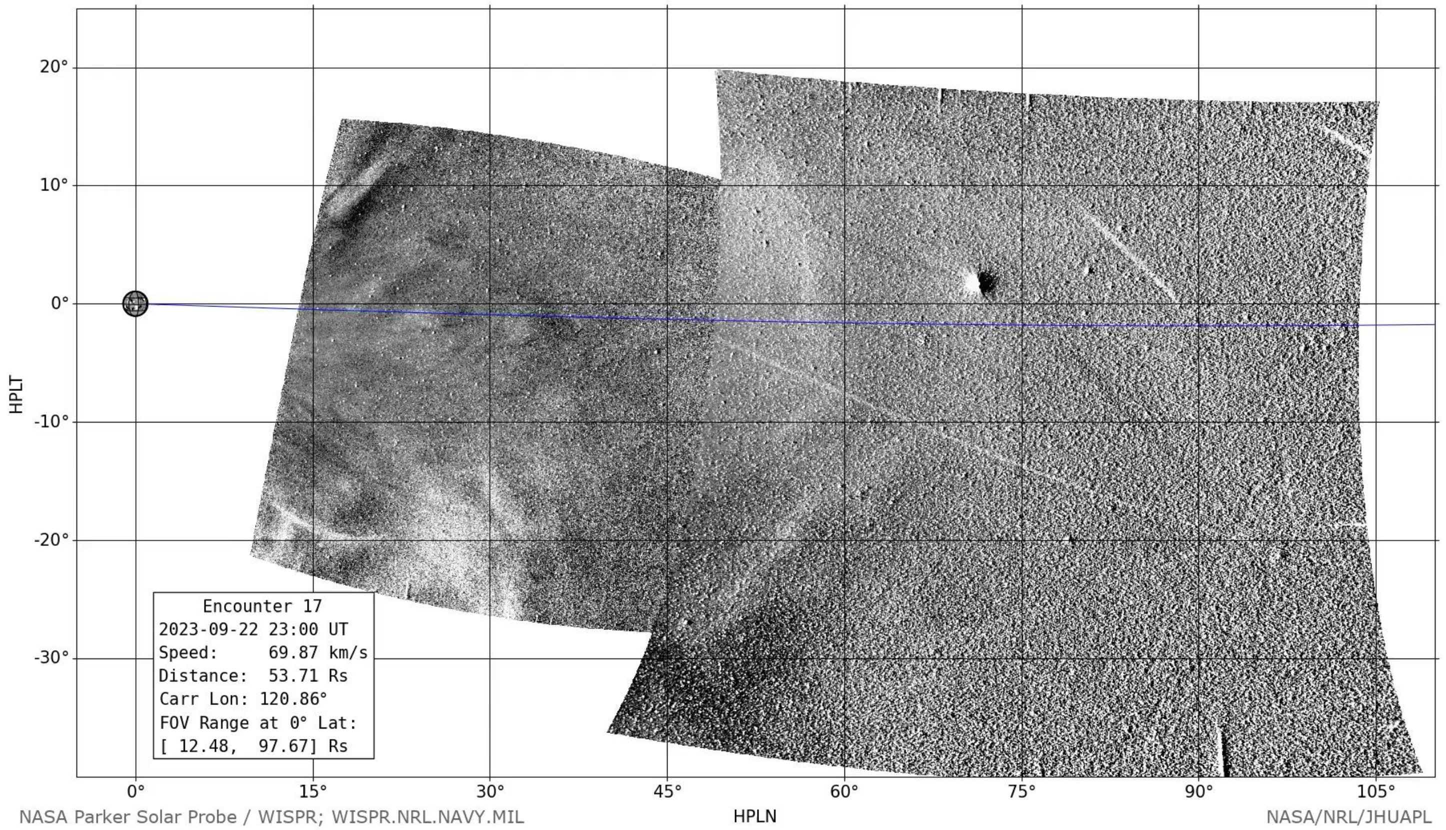

New sunspot observed by SolO/PHI associated with CME2

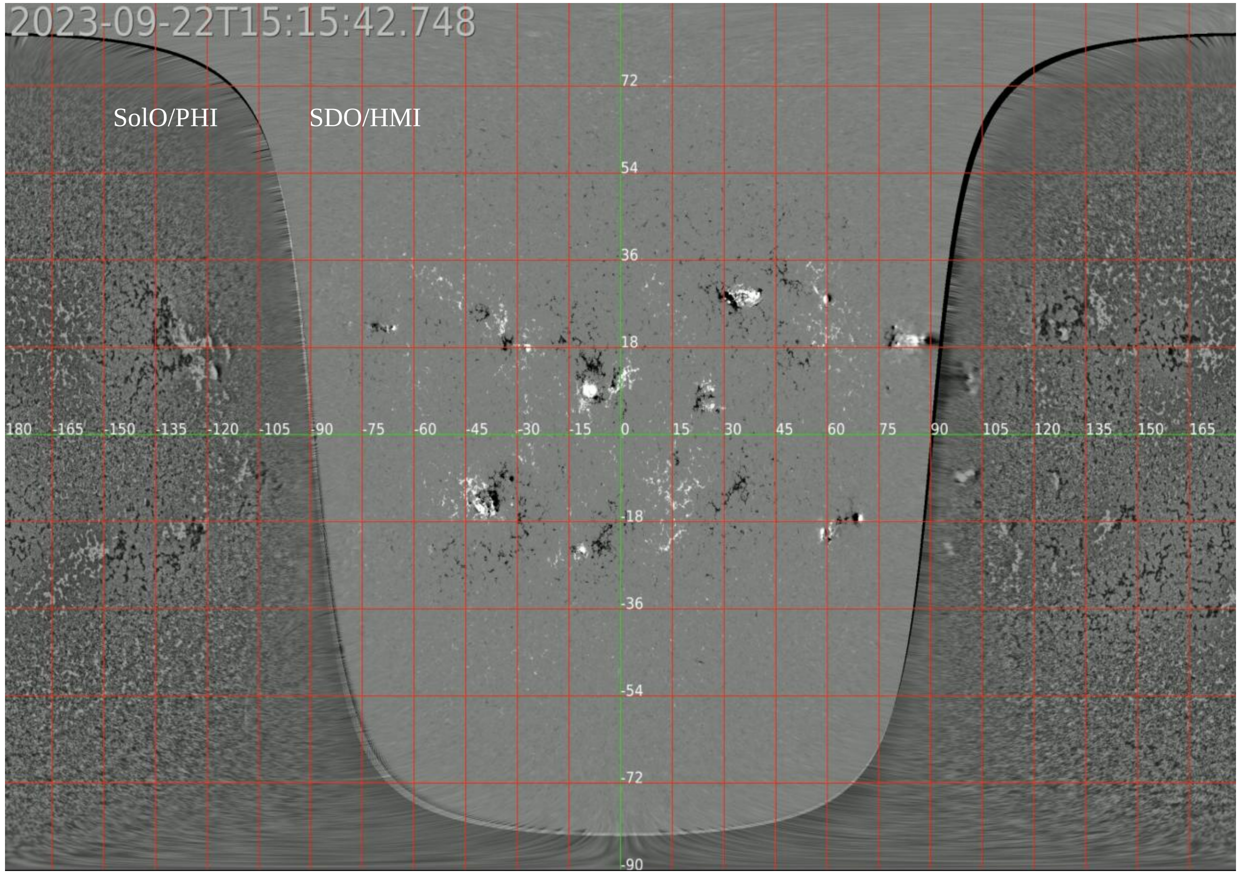

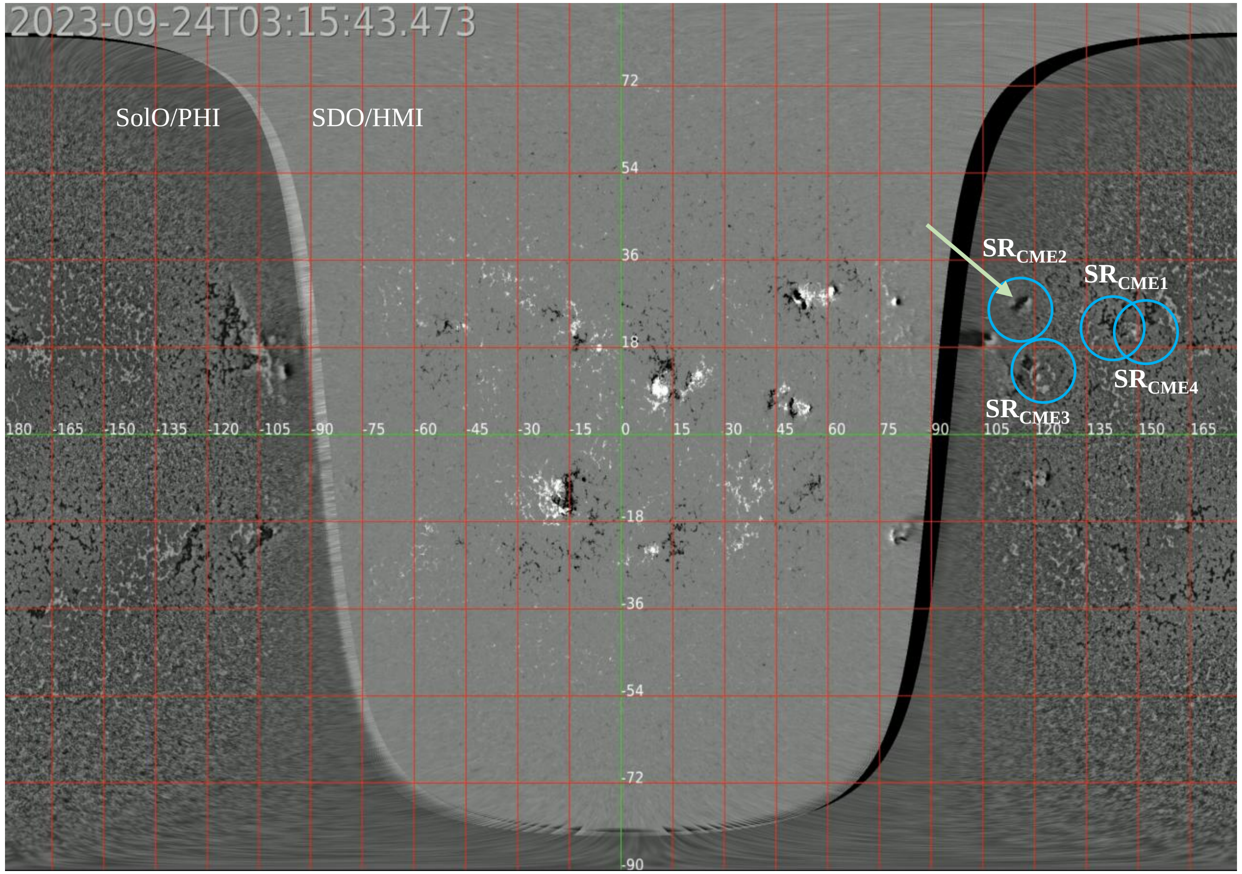

CME/CME interaction – CME deflection

[CME3 interact with CME2]

“Macro-scale” Kelvin-Helmholtz instability?

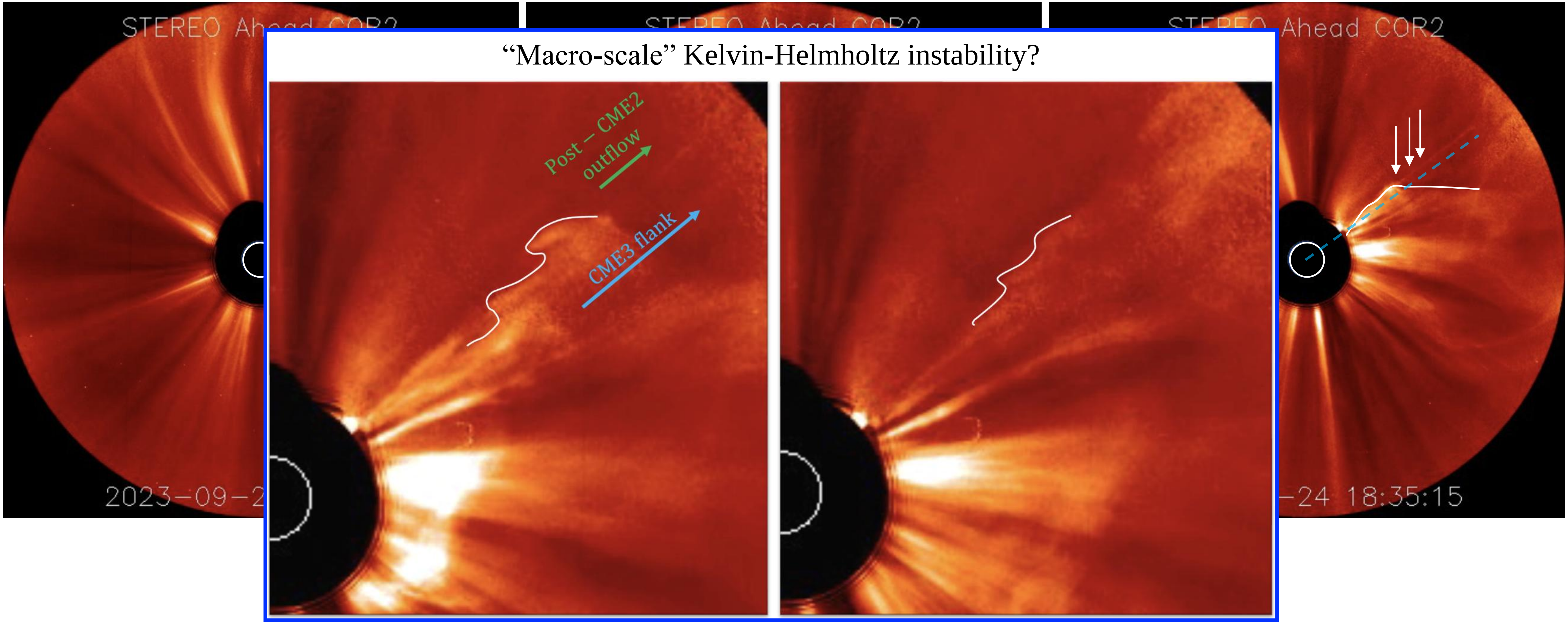

Source regions observed by SolO/EUI (FSI-174)

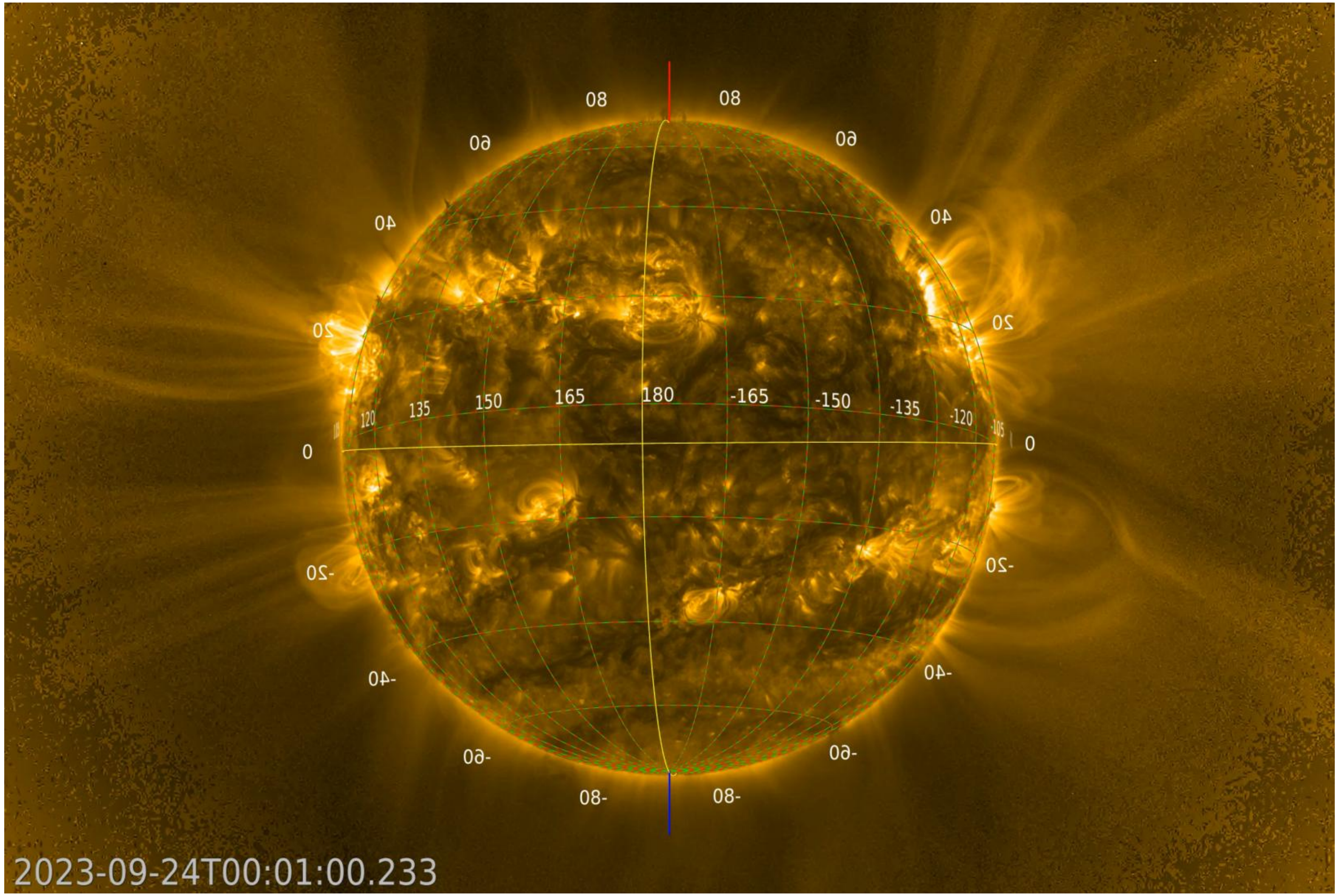

Challenges in Forecasting the Evolution of a Distorted CME

2022 March 25

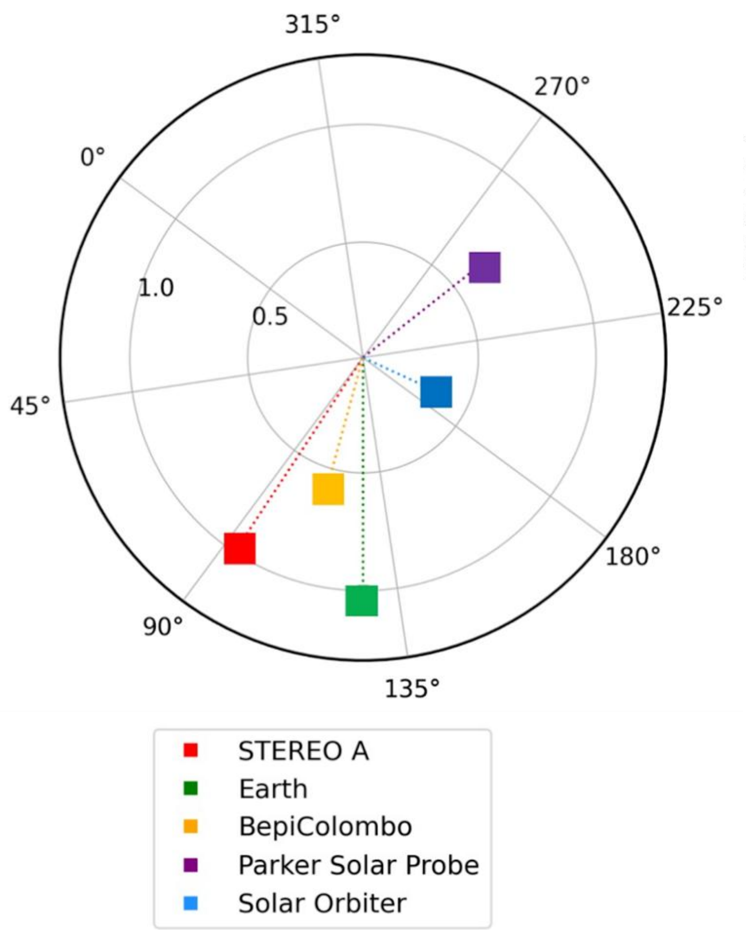

Distortion of the CME in both latitude and longitude

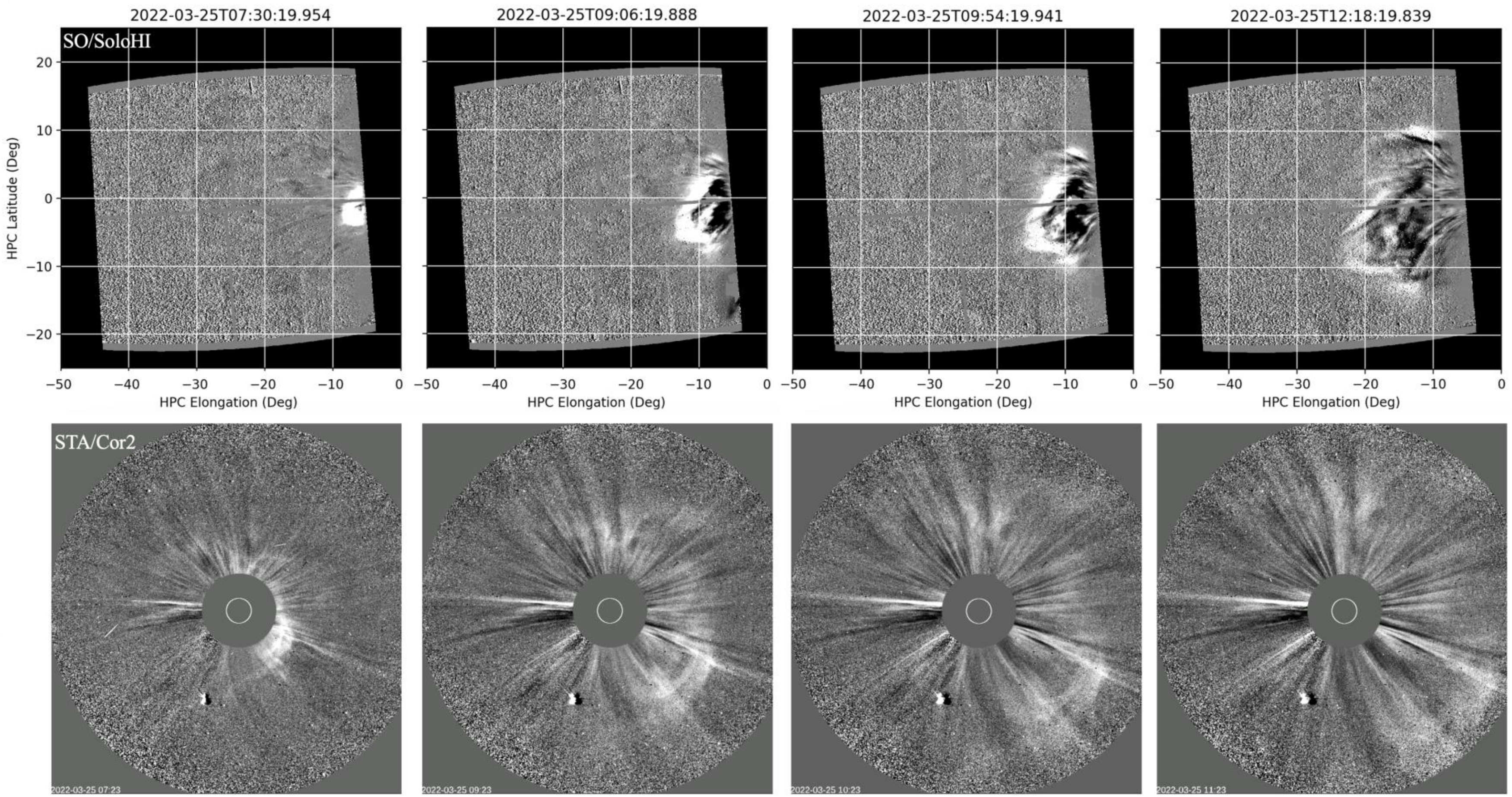

Challenges in Forecasting the Evolution of a Distorted CME

2022 March 25

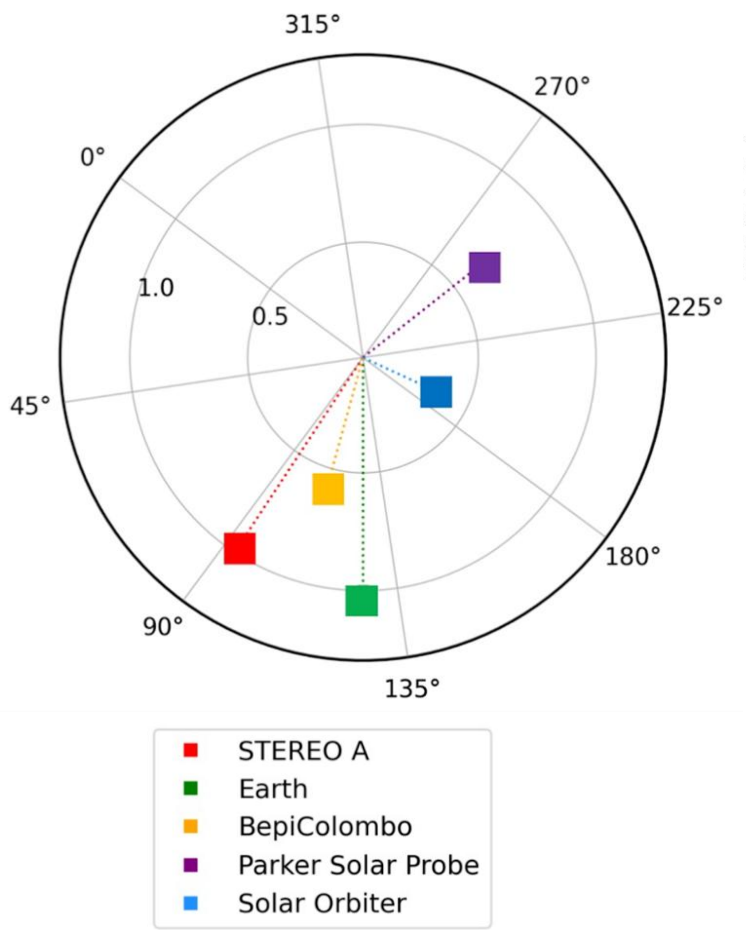

SoloHI

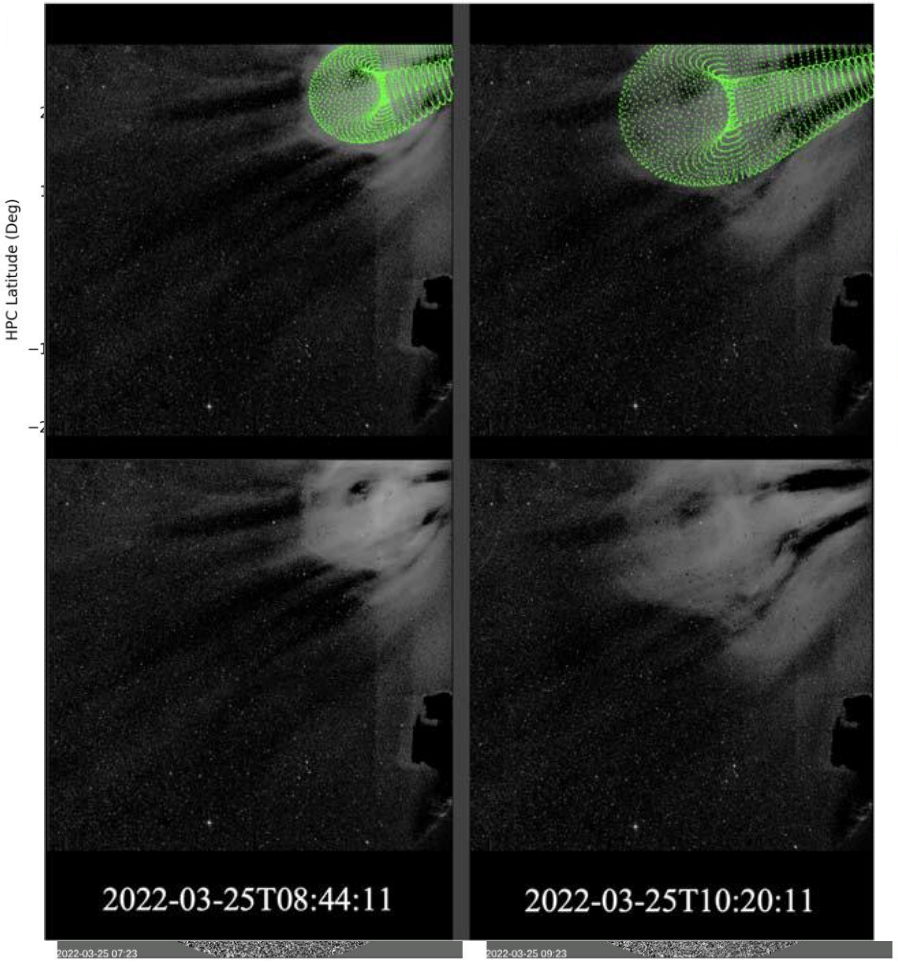

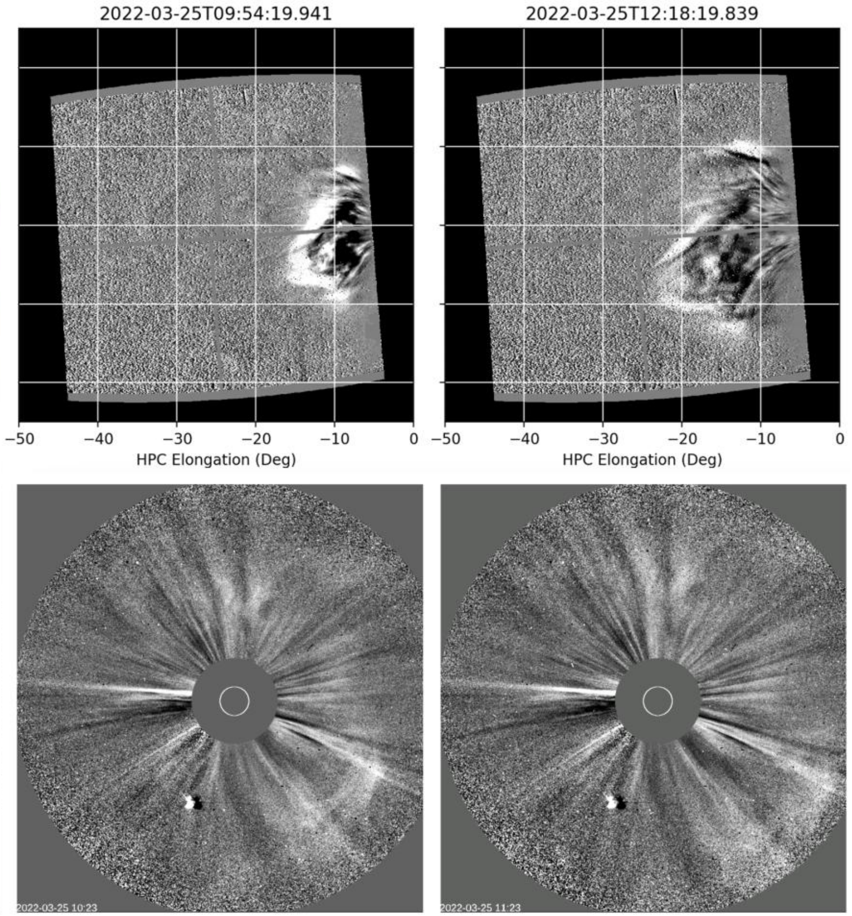

Challenges in Forecasting the Evolution of a Distorted CME

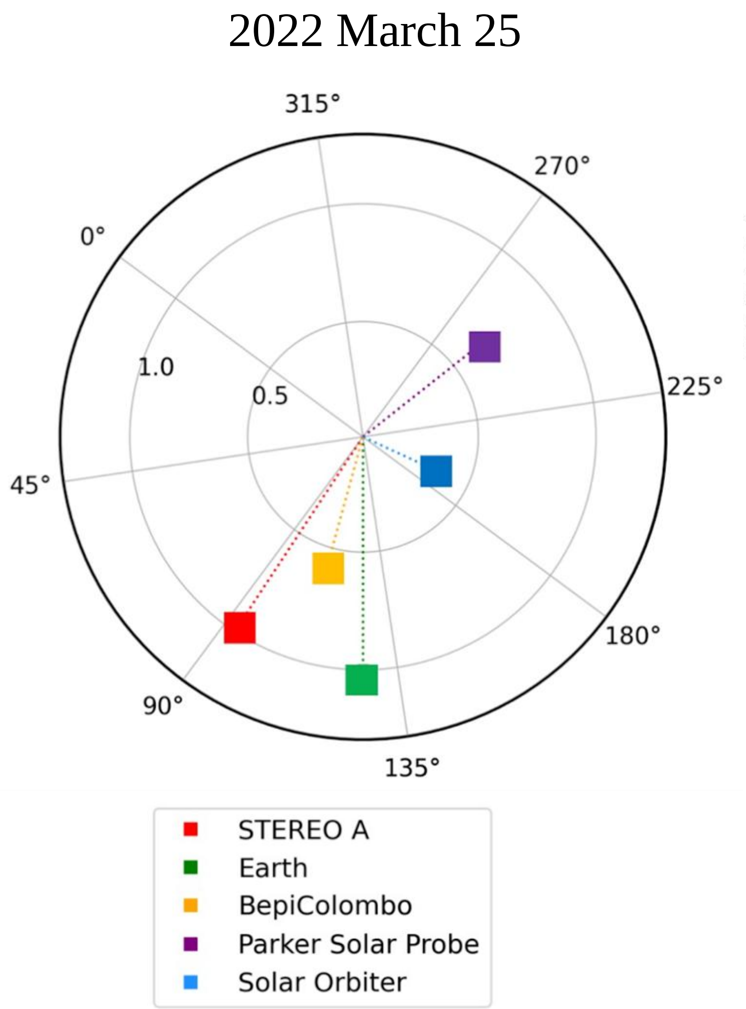

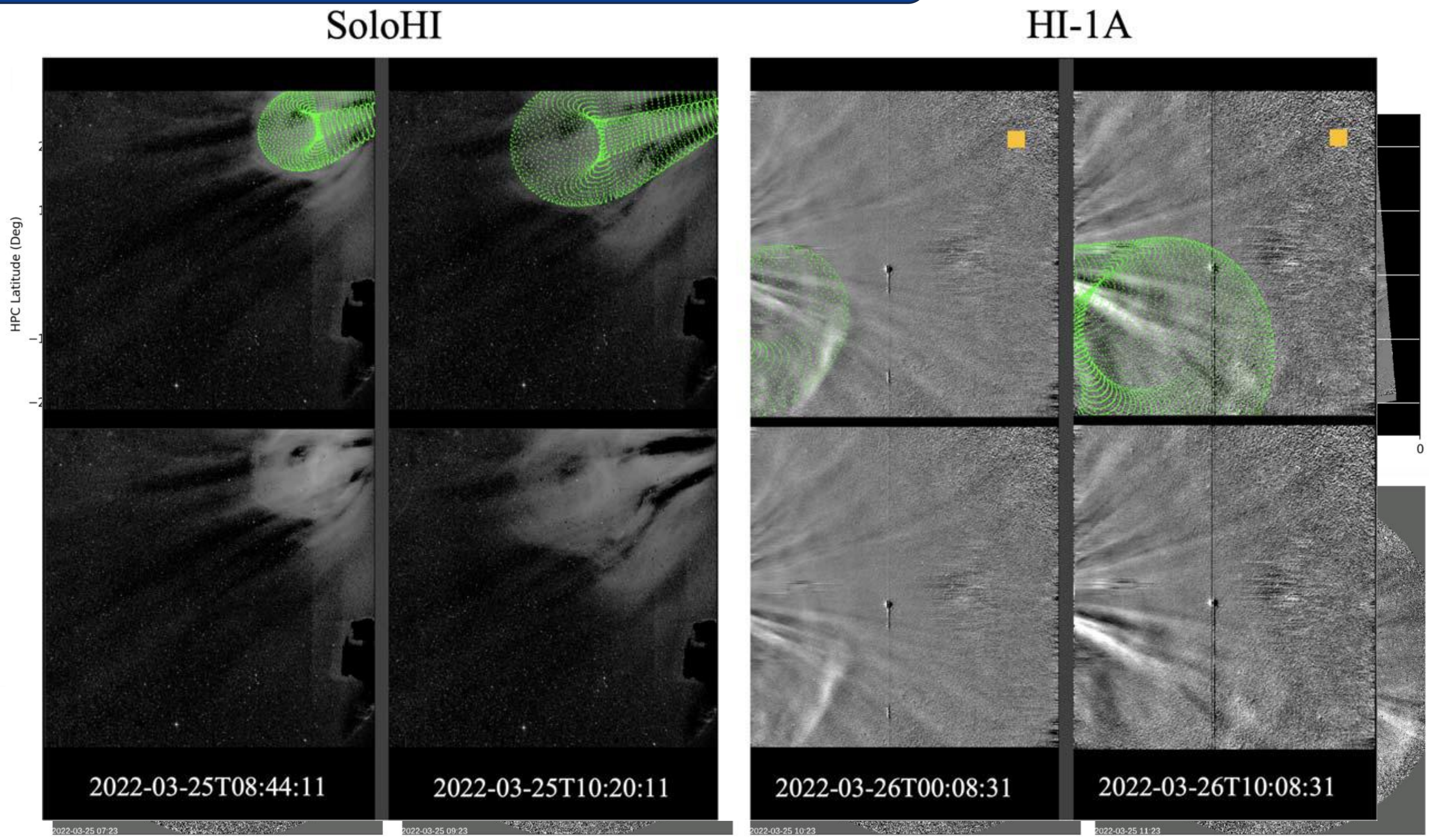

Challenges in Forecasting the Evolution of a Distorted CME

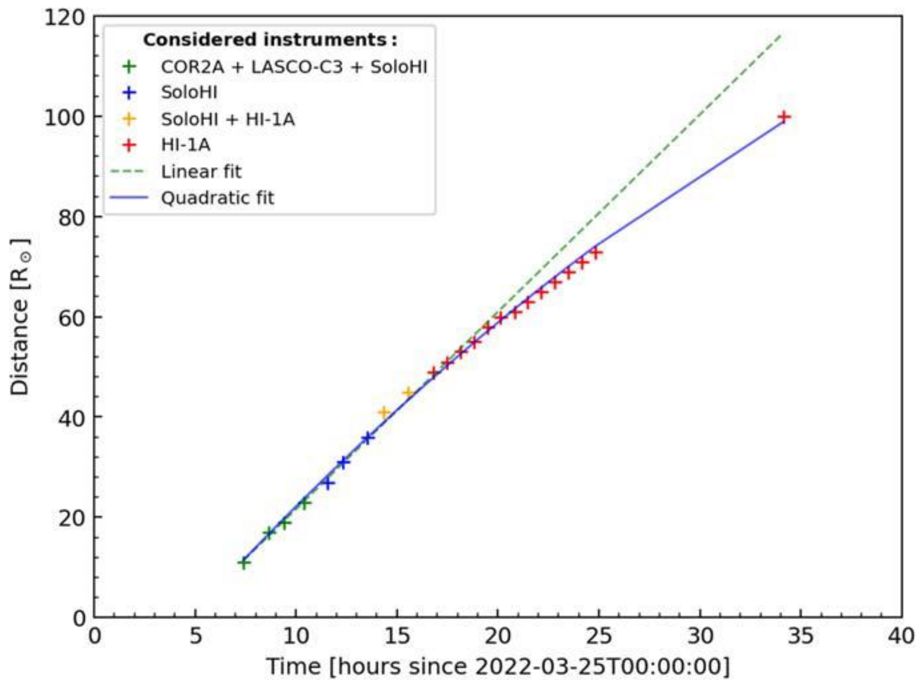

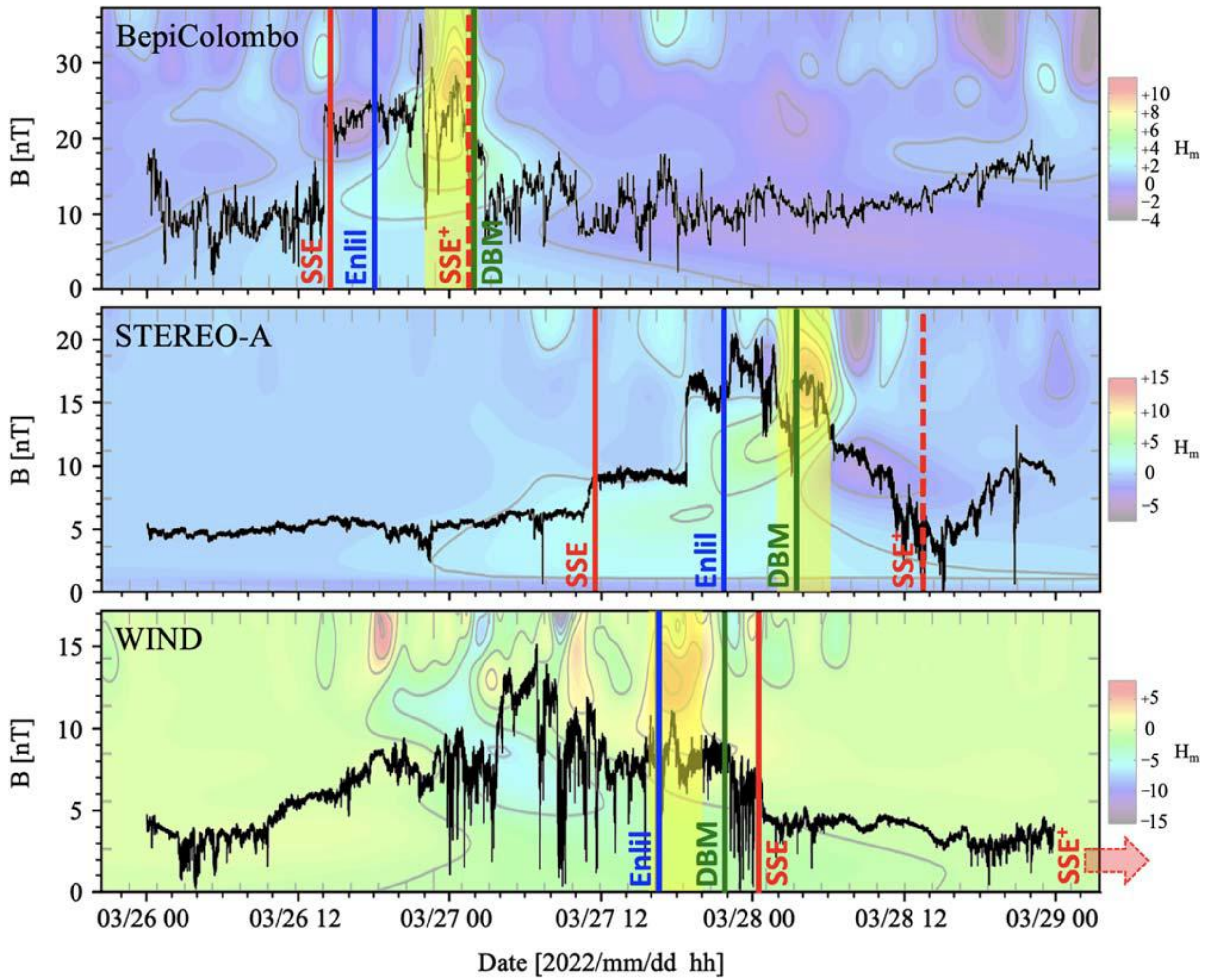

Average error of ≈ 4 hr, much lower than the typical errors in literature (≈ 8–10 hr)

Backup End